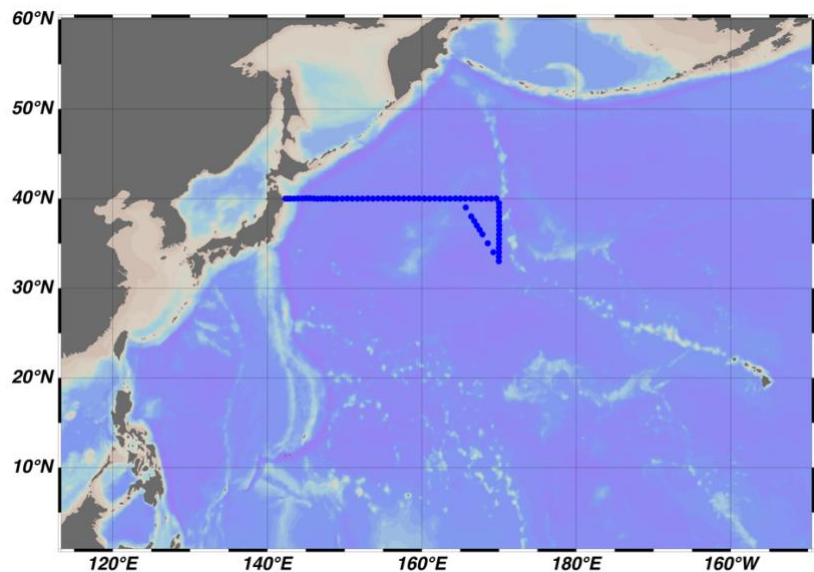


# CRUISE REPORT: RF19-05

Created: December 2024, Updated: June 2025



## Highlights

### Cruise Summary Information

Section Designation	40N
Expedition Designation (ExpoCode)	<b>49UP20190612</b>
Chief Scientist	<b>Shinji MASUDA/ JMA</b>
Dates	Leg 1: 12 June, 2019 – 6 July, 2019 Leg 2: 10 July, 2019 – 3 August, 2019
Ship	R/V Ryofu Maru
Ports of Call	Leg 1: Tokyo, Japan – Hakodate, Japan Leg 2: Hakodate, Japan – Tokyo, Japan
Geographic Boundaries	40° 02''N 142° 33''E 170° 03''E 33° 01''N
Stations	70
Floats and Drifters Deployed	7 floats (5 APEX, 2 DeepAPEX), 1 drifter
Moorings Deployed and Recovered	0

### Contact Information:

#### **Daisuke SASANO**

Global Environment and Marine Department  
Japan Meteorological Agency (JMA)

1-3-4, Otemachi, Chiyoda-ku, Tokyo 100-8122, JAPAN

Phone: +81-3-3212-8341 Ext. 5132

Email: [seadata@met.kishou.go.jp](mailto:seadata@met.kishou.go.jp)

Report assembled by Savannah Lewis

## Contents

### A. Cruise narrative

### B. Underway measurements

1. *Navigation (to be submitted in the next update)*
2. *Bathymetry (to be submitted in the next update)*
3. Maritime Meteorological Observations
4. Thermosalinograph
5. Underway Chlorophyll-a

### C. Hydrographic Measurement Techniques and Calibration

1. CTD/O<sub>2</sub> Measurements
2. Bottle Salinity
3. Bottle Oxygen
4. Nutrients
5. Phytopigment (Chlorophyll-a and phaeopigments)
6. Total Dissolved Inorganic Carbon (DIC)
7. Total Alkalinity (TA)
8. pH

## A. Cruise narrative

### 1. *Highlights*

Cruise designation: RF19-05 (40N revisit)

- a. EXPOCODE: RF19-05 49UP20190612
- b. Chief scientist: Shinji MASUDA  
Marine Division  
Global Environment and Marine Department  
Japan Meteorological Agency (JMA)
- c. Ship name: R/V Ryofu Maru
- d. Ports of call: Leg 1: Tokyo (Japan) – Hakodate (Japan)  
Leg 2: Hakodate (Japan) – Tokyo (Japan)
- e. Cruise dates (JST): Leg 1: 12 June 2019 – 6 July 2019  
Leg 2: 10 July 2019 – 3 August 2019
- f. Floats and drifters deployed: 7 floats  
1 drifter
- g. Principal Investigator (Contact person):  
Daisuke SASANO  
Marine Division  
Global Environment and Marine Department  
Japan Meteorological Agency (JMA)  
1-3-4, Otemachi, Chiyoda-ku, Tokyo 100-8122, JAPAN  
Phone: +81-3-3212-8341 Ext. 5132  
E-mail: seadata@met.kishou.go.jp

## 2. Cruise Summary

RF19-05 cruise was carried out during the period from June 12 to August 3, 2019. The cruise started from the east of Honshu, Japan, and sailed towards east along 40°N. This line was observed by JMA in 2012 as CLIVER (Climate Variability and Predictability Project) / GO-SHIP (Global Ocean Ship-based Hydrographic Investigations Program).

A total of 70 stations were occupied using a Sea-Bird Electronics (SBE) 36 position carousel equipped with 10-liter Niskin water sample bottles, a CTD system (SBE911plus) equipped with SBE35 deep ocean standards thermometer, JFE Advantech oxygen sensor (RINKO III), Teledyne Benthos altimeter (PSA-916D), and Teledyne RD Instruments L-ADCP (300 kHz). To examine consistency of data, we carried out the observation repeatedly twice at stations of 40°N, 160°20'E (Stn.32 and 33) and 40°N, 165°E (Stn.40 and 70). Cruise track and station location are shown in Figure A.1.

At each station, full-depth CTDO<sub>2</sub> (temperature, conductivity (salinity) and dissolved oxygen) profile were taken, and up to 36 water samples were taken and analyzed. Water samples were obtained from 10 dbar to approximately 10 m above the bottom. In addition, surface water was sampled by a stainless steel bucket at each station. Sampling layer is designed as so-called staggered mesh as shown in Table A.1 (Swift, 2010). The bottle depth diagram is shown in Figure A.2.

Water samples were analyzed for salinity, dissolved oxygen, nutrients, dissolved inorganic carbon (DIC), total alkalinity (TA), pH, CFCs (CFC-11, CFC-12, and CFC-113), SF<sub>6</sub> and phytopigments (chlorophyll-*a* and phaeopigment). Underway measurements of partial pressure of carbon dioxide (*p*CO<sub>2</sub>), temperature, salinity, chlorophyll-*a*, subsurface current, bathymetry and meteorological parameters were conducted along the cruise track.

R/V Ryofu Maru departed Tokyo (Japan) on June 12, 2019. Before the observation at the first station, all watch standers were drilled in the method of sample drawing and CTD operations off Boso Peninsula (34°42'N, 139°52'E). The hydrographic cast of CTDO<sub>2</sub> was started at the first station (Stn.1 (40°00'N, 142°20'E; RF6502)) on June 13. Leg 1 consisted of 32 stations from Stn.1 to Stn.32 (40°00'N, 160°20'E; RF6533). The observation at Stn.32 was finished on June 30. She called for Hakodate (Japan) on July 6 (Leg 1). She left Hakodate on July 10, 2019. The hydrographic cast of CTDO<sub>2</sub> was restarted at the last station (Stn.33 (40°00'N, 160°20'E; RF6534)) on July 13. Leg 2 consisted of 38 stations from Stn.33 to Stn.70 (40°00'N, 165°00'E; RF6571). The observation at Stn.70 was finished on July 26. She arrived at Tokyo on August 3, 2019 (Leg 2). Location data of stations is shown in Table A.2.

Seven Argo floats and one drifting ocean data buoy were deployed along the cruise track. The information of deployed the float and the buoy are listed in Table A.3.

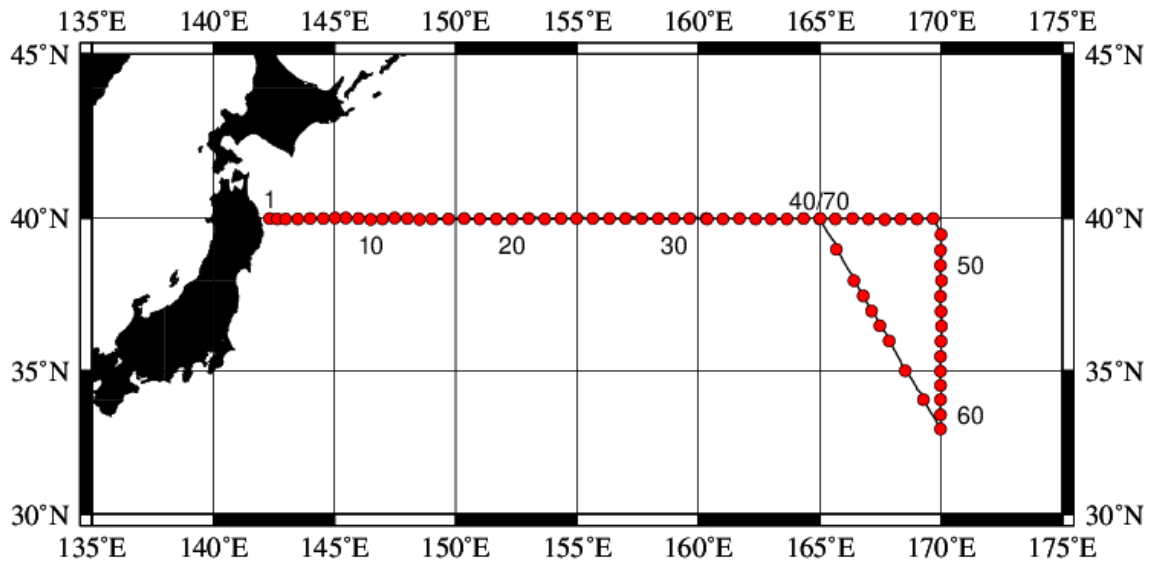


Figure A.1. Location of hydrographic stations of the cruise.

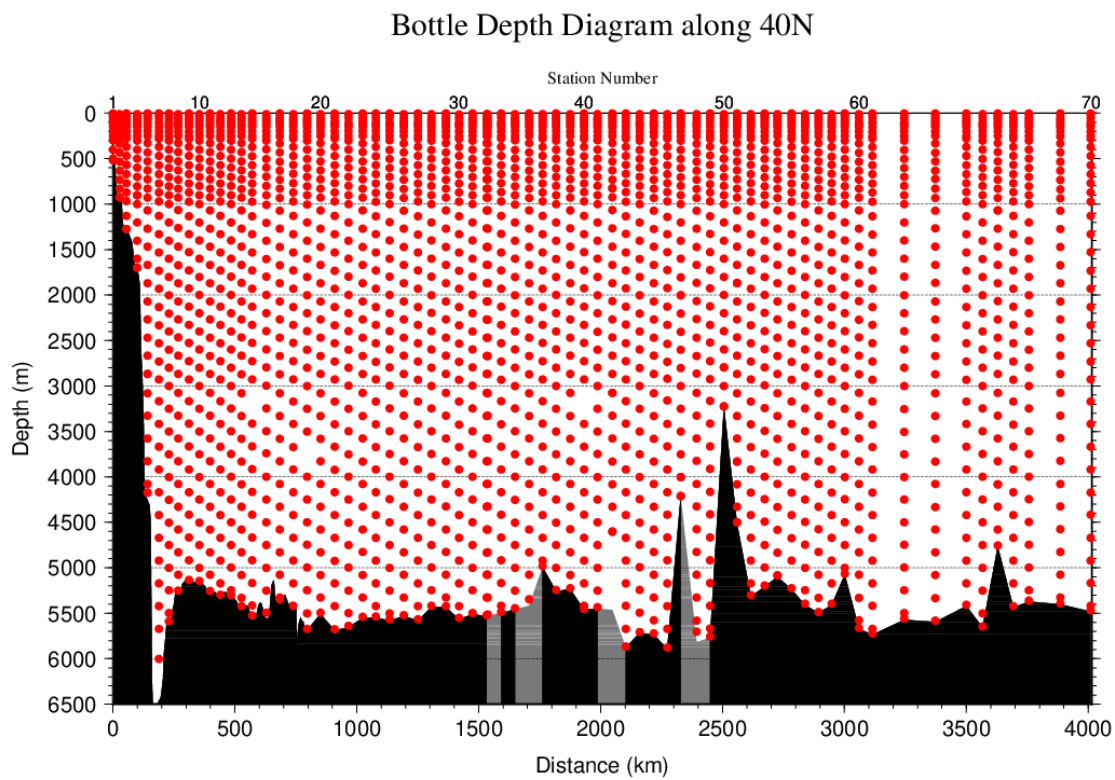


Figure A.2. The bottle depth diagram for the cruise. Seafloor filled with black before RF6520 station indicates data measured continuously by a single beam echo sounder, and after RF6521 station indicates data estimated by CTD observation with altimeter measurement. Seafloor filled with gray indicates data missing station during this cruise and is referred from our previous cruise in 2012.

Table A.1. The schemes of sampling layers in meters.

<i>Bottle count</i>	<i>Scheme 1</i>	<i>Scheme 2</i>	<i>Scheme 3</i>
<i>1</i>	10	10	10
<i>2</i>	25	25	25
<i>3</i>	50	50	50
<i>4</i>	75	75	75
<i>5</i>	100	100	100
<i>6</i>	<i>125</i>	<i>125</i>	<i>125</i>
<i>7</i>	150	150	150
<i>8</i>	200	200	200
<i>9</i>	250	250	250
<i>10</i>	300	330	280
<i>11</i>	400	430	370
<i>12</i>	500	530	470
<i>13</i>	600	630	570
<i>14</i>	700	730	670
<i>15</i>	800	830	770
<i>16</i>	900	930	870
<i>17</i>	1000	1070	970
<i>18</i>	1200	1270	1130
<i>19</i>	1400	1470	1330
<i>20</i>	1600	1670	1530
<i>21</i>	1800	1870	1730
<i>22</i>	2000	2070	1930
<i>23</i>	2200	2270	2130
<i>24</i>	2400	2470	2330
<i>25</i>	2600	2670	2530
<i>26</i>	2800	2870	2730
<i>27</i>	3000	3080	2930
<i>28</i>	<i>3250</i>	<i>3330</i>	<i>3170</i>
<i>29</i>	3500	3580	3420
<i>30</i>	<i>3750</i>	<i>3830</i>	<i>3670</i>
<i>31</i>	4000	4080	3920
<i>32</i>	<i>4250</i>	<i>4330</i>	<i>4170</i>
<i>33</i>	4500	4580	4420
<i>34</i>	<i>4750</i>	<i>4830</i>	<i>4670</i>
<i>35</i>	5000	5080	4920
<i>36</i>	<i>5250</i>	<i>5330</i>	<i>5170</i>
<i>37</i>	5500	5580	5420
<i>38</i>	<i>5750</i>	<i>5830</i>	<i>5670</i>
<i>39</i>	6000	6000	6000

At some deep stations over 36 layers, some layers shown in italic may be skipped.

Table A.2. Station lists of the cruise. The ‘RF’ column indicates original station number of JMA.

<i>Leg</i>	<i>Station</i>		<i>Location</i>		<i>Leg</i>	<i>Station</i>		<i>Location</i>	
	<i>Stn.</i>	<i>RF</i>	<i>Latitude</i>	<i>Longitude</i>		<i>Stn.</i>	<i>RF</i>	<i>Latitude</i>	<i>Longitude</i>
1	1	6502	40-00.03 N	142-19.72 E	2	36	6537	39-59.52 N	162-21.25 E
1	2	6503	39-59.81 N	142-39.05 E	2	37	6538	39-59.62 N	163-00.58 E
1	3	6504	39-59.92 N	142-59.12 E	2	38	6539	39-59.41 N	163-39.70 E
1	4	6505	39-59.78 N	143-29.27 E	2	39	6540	40-00.24 N	164-20.81 E
1	5	6506	40-00.62 N	143-59.99 E	2	40	6541	39-59.71 N	165-00.12 E
1	6	6507	40-00.71 N	144-32.35 E	2	41	6542	39-59.47 N	165-39.57 E
1	7	6508	40-01.67 N	145-01.90 E	2	42	6543	40-00.03 N	166-21.86 E
1	8	6509	40-01.41 N	145-28.85 E	2	43	6544	39-59.69 N	167-01.01 E
1	9	6510	40-00.47 N	145-59.63 E	2	44	6545	39-58.78 N	167-41.05 E
1	10	6511	39-58.13 N	146-29.31 E	2	45	6546	39-59.56 N	168-21.88 E
1	11	6512	39-59.27 N	146-59.91 E	2	46	6547	39-59.84 N	169-00.55 E
1	12	6513	40-01.10 N	147-29.59 E	2	47	6548	40-00.57 N	169-40.17 E
1	13	6514	40-00.95 N	148-00.42 E	2	48	6549	39-29.36 N	170-00.83 E
1	14	6515	39-58.92 N	148-30.32 E	2	49	6550	38-59.54 N	169-59.99 E
1	15	6516	39-59.58 N	149-01.48 E	2	50	6551	38-29.35 N	169-59.95 E
1	16	6517	39-59.68 N	149-42.52 E	2	51	6552	38-00.11 N	170-01.52 E
1	17	6518	40-00.26 N	150-21.58 E	2	52	6553	37-29.68 N	169-59.80 E
1	18	6519	39-59.66 N	150-59.90 E	2	53	6554	36-59.22 N	170-00.92 E
1	19	6520	39-59.82 N	151-40.28 E	2	54	6555	36-30.90 N	170-01.74 E
1	20	6521	39-59.77 N	152-19.58 E	2	55	6556	35-59.41 N	170-00.74 E
1	21	6522	40-00.99 N	153-00.37 E	2	56	6557	35-29.53 N	169-59.85 E
1	22	6523	39-59.98 N	153-40.22 E	2	57	6558	34-59.90 N	169-59.67 E
1	23	6524	40-00.59 N	154-20.51 E	2	58	6559	34-30.47 N	169-59.44 E
1	24	6525	40-00.52 N	154-59.18 E	2	59	6560	34-01.14 N	169-59.72 E
1	25	6526	40-00.24 N	155-38.91 E	2	60	6561	33-30.21 N	169-59.22 E
1	26	6527	40-00.61 N	156-20.11 E	2	61	6562	33-00.50 N	169-59.41 E
1	27	6528	40-00.63 N	157-00.64 E	2	62	6563	34-01.18 N	169-16.89 E
1	28	6529	40-00.97 N	157-39.76 E	2	63	6564	35-00.26 N	168-32.52 E
1	29	6530	40-00.59 N	158-21.28 E	2	64	6565	36-00.60 N	167-52.13 E
1	30	6531	40-00.23 N	158-59.71 E	2	65	6566	36-31.43 N	167-29.23 E
1	31	6532	40-00.51 N	159-38.64 E	2	66	6567	37-00.04 N	167-08.55 E
1	32	6533	40-00.62 N	160-19.65 E	2	67	6568	37-30.20 N	166-47.50 E
2	33	6534	39-59.42 N	160-21.46 E	2	68	6569	38-00.38 N	166-24.97 E
2	34	6535	39-59.39 N	161-00.90 E	2	69	6570	39-01.05 N	165-41.91 E
2	35	6536	40-00.34 N	161-41.08 E	2	70	6571	40-00.74 N	165-01.32 E

Table A.3. Information of deployed float and buoy.

<i><b>Float WMO number</b></i>	<i><b>Date and Time of Deployment (UTC)</b></i>	<i><b>Position of deployment</b></i>		<i><b>PI</b></i>	
		<i><b>Latitude</b></i>	<i><b>Longitude</b></i>		
2903373	2019 June 14 23:23	40-00.09 N	143-59.93 E	JMA	APEX
2903374	2019 June 18 13:19	39-59.96 N	145-28.46 E	JMA	APEX
2903375	2019 June 19 11:58	39-59.94 N	146-58.53 E	JMA	APEX
2903405	2019 July. 17 13:28	40-00.44 N	169-39.01 E	JAMSTEC	APEX
2903407	2019 July. 21 5:47	35-01.11 N	169-59.79 E	JAMSTEC	APEX
2903406	2019 July 17 13:32	40-00.33 N	169-38.81 E	JAMSTEC	DeepAPEX
2903408	2019 July 21 5:55	35-00.94 N	169-59.39 E	JAMSTEC	DeepAPEX
<i><b>Buoy WMO number</b></i>	<i><b>Date and Time of Deployment (UTC)</b></i>	<i><b>Position of deployment</b></i>		<i><b>PI</b></i>	
		<i><b>Latitude</b></i>	<i><b>Longitude</b></i>		
11143	2019 June 18 4:20	40-00.16 N	144-58.61 E	JMA	YTSS-2100

APEX: Teledyne Webb Research (USA)  
YTSS-2100: JVC KENWOOD Co., Japan



### 3. List of Principal Investigators for Measurements

The principal investigators for each parameter are listed in Table A.4.

Table A.4. List of principal investigators for each parameter.

Hydrography	CTDO <sub>2</sub>	Keita KAKUYA
	Salinity	Noriyuki OKUNO
	Dissolve oxygen	Hiroyuki HATAKEYAMA
	Nutrients	Hiroyuki HATAKEYAMA
	Phytopigments	Hiroyuki HATAKEYAMA
	DIC	Kazutaka ENYO
	TA	Kazutaka ENYO
	pH	Kazutaka ENYO
	CFCs	Kazutaka ENYO
	LADCP	Keita KAKUYA
Underway	Meteorology	Shinji MASUDA
	Thermo-Salinograph	Kazutaka ENYO
	<i>p</i> CO <sub>2</sub>	Kazutaka ENYO
	Chlorophyll <i>a</i>	Hiroyuki HATAKEYAMA
	ADCP	Keita KAKUYA
	Bathymetry	Keita KAKUYA
Float	JMA	Tetsuya NAKAMURA
	JAMSTEC APEX	Shigeki HOSODA
	JAMSTEC DeepAPEX	Shigeki HOSODA
Buoy	JMA	Shoji SHIRAISHI

### 4. Major Problems

The Precision Depth Recorder (Kongsberg Maritime EA600) was broken down on the way from Stn.19 (RF6520) to Stn.20 (RF6521) at June 26. After this failure, bathymetry cannot be measured.

### ***Reference***

Swift, J. H. (2010): Reference-quality water sample data: Notes on acquisition, record keeping, and evaluation. *IOCCP Report No.14, ICPO Pub. 134, 2010 ver.1*

## B. Underway Data

### 5. *Underway chlorophyll-a*

10 June 2021

#### (1) Personnel

Hiroyuki HATAKEYAMA (GEMD/JMA)  
Kei KONDOU (GEMD/JMA)  
Rie SANAI (GEMD/JMA)  
Masakazu TAKAMI (GEMD/JMA)  
(Leg 1) Kouichi WADA (GEMD/JMA)  
(Leg 2) Tomohiro UEHARA (GEMD/JMA)

#### (2) Method

The Continuous Sea Surface Water Monitoring System of fluorescence (Nippon Kaiyo, Japan) automatically had been continuously measured seawater which is pumped from a depth of about 4.5 m below the maximum load line to the laboratory. The flow rate of the surface seawater was controlled by several valves and adjusted to about 0.6 L min<sup>-1</sup>. The sensor in this system is a fluorometer 10-AU (S/N: 7062, Turner Designs, United States).

#### (3) Observation log

The chlorophyll-*a* continuous measurements were conducted during the entire cruise; from 12 Jun. to 3 Jul., 2019 in Leg 1, and from 10 Jul. to 2 Aug., 2019 in Leg 2.

#### (4) Water sampling

Surface seawater was corrected from outlet of water line of the system at nominally 1 day intervals. The seawater sample was measured in the same procedure as hydrographic samples of chlorophyll-*a* (see Chapter C5 “Phytopigments”).

#### (5) Calibration

At the beginning and the end of legs, a raw fluorescence value of sensor was adjusted in sensitivity of the sensor using deionized water and a rhodamine 0.1ppm solution measured. After the cruise, the fluorescence value was converted to chlorophyll-*a* concentration by programs in the system based on nearby water sampling data (chlorophyll-*a* concentration and distance from location of sensor data).

#### (6) Data

Underway fluorescence and chlorophyll-*a* data is distributed in JMA format in “49UP20190612\_40N\_underway\_chl.csv”. The record structure of the format is as follows;

Column1 DATE: Date (YYYYMMDD) [JST]  
Column2 TIME: Time (HHMM) [JST] (= UTC + 9h)  
Column3 LATITUDE: Latitude

Column4 LONGITUDE: Longitude

Column5 FLUOR: Fluorescence value (RFU)

Column6 CHLORA: Chlorophyll-*a* concentration ( $\mu\text{g L}^{-1}$ )

Column7 BTLCHL: Chlorophyll-*a* concentration of water sampling ( $\mu\text{g L}^{-1}$ ).

### 3. Maritime Meteorological Observations

Jan 17, 2025

#### (1) Personnel

MASUDA Shinji (JMA)

#### (2) Data Period

09:00, 12 Jun. 2019 to 03:00, 21 Jun. 2019 (UTC).

02:00, 22 Jun. 2019 to 00:00, 04 Jul. 2019 (UTC).

07:00, 10 Jul. 2019 to 03:00, 30 Jul. 2019 (UTC).

06:00, 31 Jul. 2019 to 21:00, 01 Aug. 2019 (UTC).

#### (3) Methods

The maritime meteorological observation system on R/V Ryofu Maru is Ryofu Maru maritime meteorological measurement station (RMET). Instruments of RMET are listed in Table B.3.1. All RMET data were collected and processed by KOAC-7800 weather data processor made by KOSHIN DENKI KOGYO CO., LTD., Japan. The result of Maritime meteorological observation data were shown in Figures B.3.1 and B.3.2.

Table B.3.1. Instruments and locations of RMET.

Sensor	Parameter	Type (Manufacture)	Location (Height from maximum load line)
Thermometer	Air Temperature	R005-341 (CHINO CORPORATION)	Compass deck (13.3 m)
Hygrometer	Relative humidity	HMT3303JM (Vaisala)	Compass deck (13.3 m)
Thermometer	Sea surface temperature	RFN1-0 (CHINO CORPORATION)	Engine Room (-4.7 m)
Aerovane	Wind Speed	KVS-400-J	Mast top
	Wind Direction	(KOSHIN DENKI KOGYO CO., LTD.)	(19.8 m)
Wave gauge	Wave Height	Micro Wave WM-2	Ship front
	Wave period	(Tsurumi-Seiki Co., Ltd.)	(6.5 m)
Barometer	Air pressure	PTB-220 (Vaisala)	Observation room (2.8 m)

Note that there are two sets of a thermometer and a hygrometer at the starboard and the port sides.

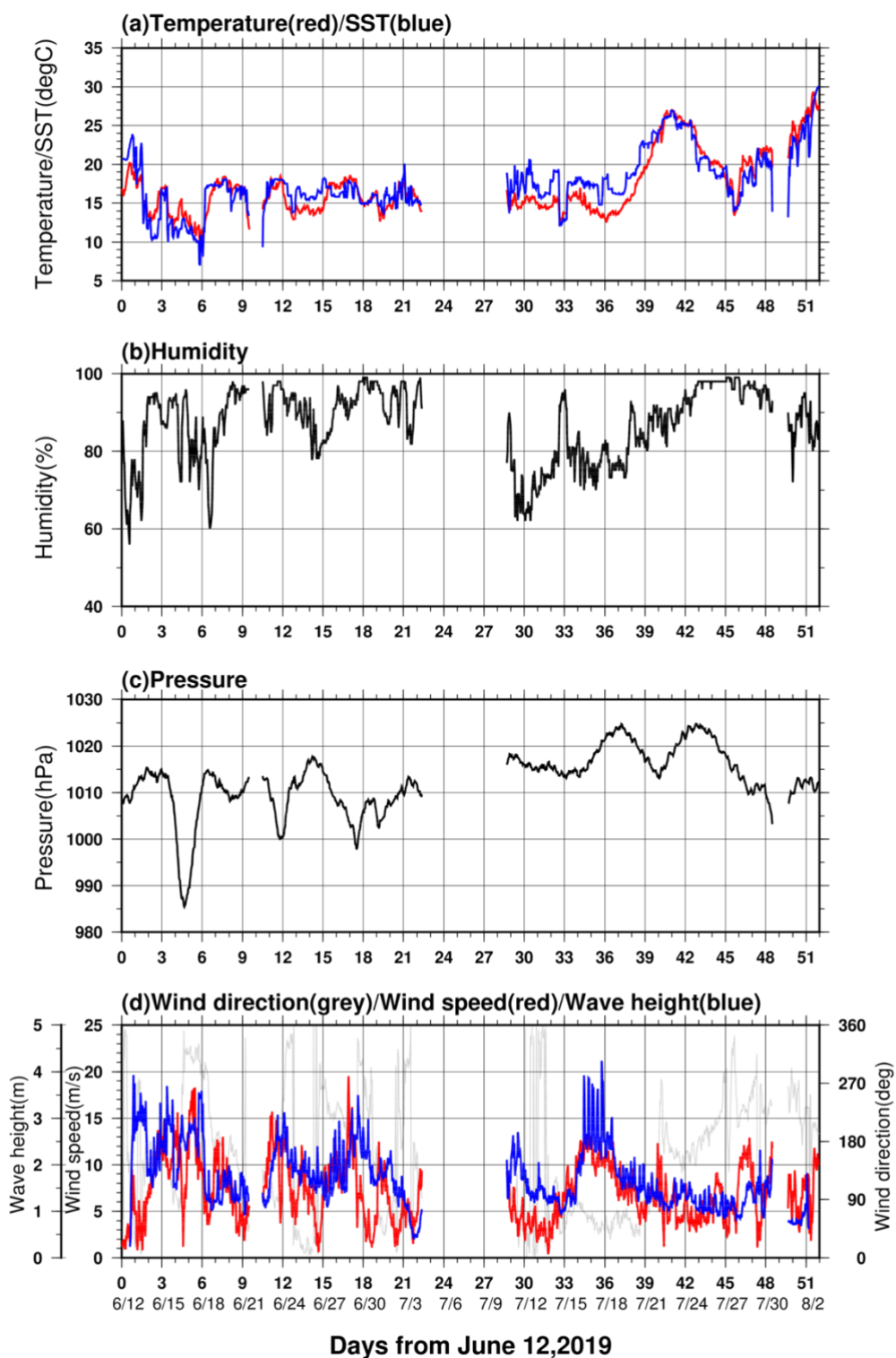


Figure B.3.1. Time series of (a) air temperature and sea surface temperature (SST), (b) relative humidity, (c) sea-level pressure, and (d) wind direction, wind speed and wave height. The light blue line in (d) panel shows the instrumental observation of wave height. Day 0 corresponds to June 12, 2019 (JST).

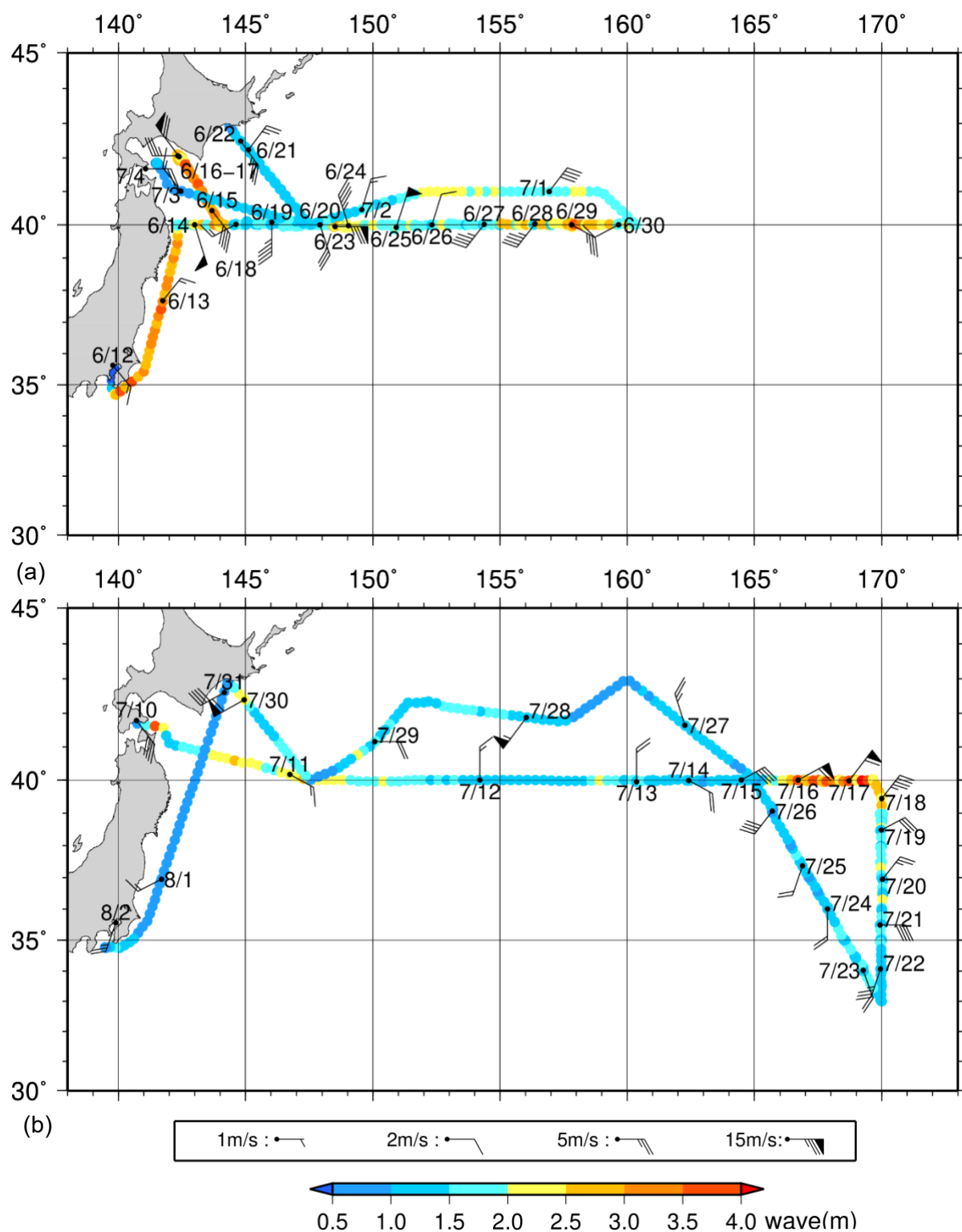


Figure B.3.2 Cruise tracks with wave height (a) from June 12 to July 4, 2019 (JST) and (b) from July 10 to August 2, 2019 (JST). Wind barbs are shown at all noon positions (JST) along the cruise track.

#### **(4) Data processing and Data format**

All raw data were recorded in every 6 seconds. The values of 1-minute and 10-minute data were averaged from 6-second raw data. The 10-minute data in every three hours are available from JMA web site ([https://www.data.jma.go.jp/kaiyou/db/vessel\\_obs/data-report/html/ship/cruisedata\\_e.php?id=RF1905](https://www.data.jma.go.jp/kaiyou/db/vessel_obs/data-report/html/ship/cruisedata_e.php?id=RF1905)) .

Because the thermometers and the hygrometers are equipped on the both starboard/port sides on the compass deck, we used air temperature/relative humidity data taken at upwind side at difference time. Dew point temperature was calculated from relative humidity and air temperature.

Pressure data was corrected to sea level pressure. During the cruise, fixed value +0.5 hPa (for the height of the observation room) was used for the correction. Data were stored in ASCII format and representative parameters are as follows; time in UTC, longitude (E), latitude (N), ship speed (knot), ship direction (degrees), sea-level pressure (hPa), air temperature (degrees Celsius), dew point temperature (degrees Celsius), relative humidity (%), sea surface temperature (degrees Celsius), wind direction (degrees) and wind speed (m/sec).

Wave height and period were observed twice in an hour. The measurement period was 20 minutes and each measurement started at 5 minutes and 35 minutes after the hour. In addition to those data, ship's position and observation time were recorded in ASCII format.

#### **(5) Data quality**

To confirm the data quality, each sensor was checked as follows.

##### ***Temperature/Relative humidity sensor:***

The temperature and relative humidity (T/RH) sensors on the both sides of the ship were checked by the manufacturer before delivering and, they were also checked by the calibrated Assmann psychrometer before and after the cruise. The discrepancy between T/RH sensors and Assmann psychrometer were within  $\pm 0.4$  degrees Celsius and  $\pm 4$  %, respectively.

##### ***Thermometer (Sea surface temperature):***

The sea temperature sensor was calibrated once a year by the manufacturer. Certificated accuracy of the sensor is better than  $\pm 0.4$  degrees Celsius. At the start of the cruise, the values are also compared with temperature of water, taken from sea surface using a bucket, which was measured by a calibrated mercury thermometer (Yoshino Keisoku S-441, accuracy is better than  $\pm 0.1$  degrees Celsius).

##### ***Pressure sensor:***

Using calibrated portable barometer (Vaisala 765-16B, certificated accuracy is better than  $\pm 0.1$  hPa), pressure sensor was checked before the cruise. Mean difference of RMET pressure sensor and portable sensor is less than 0.7 hPa.



***Aerovane:***

Aerovane was checked once per year by the manufacturer, and once per five years by the Meteorological Instrument Center, JMA.

**(6) Ship's weather observation**

Non-instrumental observations such as weather, cloud, visibility, wave direction and wave height were made by the ship crews every three hours. We sent those data together with the RMET data to the Global Collecting Centre for Marine Climatological Data in IMMT (International Maritime Meteorological Tape) -V format. The RMET data are available from JMA web site.

([https://www.data.jma.go.jp/kaiyou/db/vessel\\_obs/data-report/html/ship/cruisedata\\_e.php?id=RF1905](https://www.data.jma.go.jp/kaiyou/db/vessel_obs/data-report/html/ship/cruisedata_e.php?id=RF1905))

## 6. *Thermo-Salinograph (TSG)*

Nov 30, 2024

### (1) Personnel

ENYO Kazutaka  
OKA Takahiro  
ONO Etsuro  
INAMI Haruna (Leg 1)  
USHIO Nobuyasu (Leg 1)  
AKIEDA Chikako (Leg 2)  
TANIZAKI Chiho (Leg 2)

### (2) Instrument

#### (2.1) Overview

The Thermo-Salinograph (TSG) measurement system (EMS, Co., Ltd., Japan) consists of the SBE 38 (Digital oceanographic thermometer) and the SBE 45 (MicroTSG). The system was used for measuring temperature and salinity of surface seawater continuously along the cruise line.

The SBE 38 was used for measuring temperature of surface seawater and was placed near the seawater intake at the bottom of the vessel. The SBE 45 was used for calculating salinity, measuring temperature and conductivity of surface seawater in the laboratory of the vessel. The S/N and pre-cruise calibration date for these instruments were described in Table B.4.1. The pre-cruise calibration was performed at SBE, Inc., USA.

**Table B.4.1** S/N and calibration date for the TSG system.

Instrument	S/N	Latest calibration date
SBE 38	3856783-0512	Nov 1, 2018
SBE 45	4556783-0301	Dec 2, 2018

#### (2.2) Temperature calculation

The temperature( $T$  [°C]) for each instrument was calculated from the instrument output( $n$ ) and the coefficients (obtained at the pre-cruise calibration) with below formula:

$$T = 1/\{a_0 + a_1[\ln(n)] + a_2[\ln^2(n)] + a_3[\ln^3(n)]\} - 273.15$$

$n$  :instrument output [counts]

The coefficients for each instrument were described in Table B.4.2:

**Table B.4.2** The coefficients for temperature calculation.

	SBE 38	SBE 45
$a_0$	5.775648e-05	3.460761e-05
$a_1$	2.706480e-04	2.719845e-04
$a_2$	-2.219593e-06	-2.273192e-06
$a_3$	1.448739e-07	1.461784e-07

**(2.3) Conductivity calculation**

The conductivity( $C$  [S/m]) was calculated from the instrument output( $f$ ) of the SBE 45 and the coefficients (obtained at the pre-cruise calibration) with below formula:

$$C = (g + h \times F^2 + i \times F^3 + j \times F^4) / \{10 \times (1 + CT_{cor} \times t + CP_{cor} \times p)\}$$

$$F = f \times \sqrt{(1.0 + WBOTC \times t) / 1000}$$

$f$ : instrument output [Hz]

$t$ : temperature [°C] obtained at SBE 45 measurement

$p$ : pressure [dbar] (=0)

$WBOTC$ : 4.9027e-07

Other coefficients for calculating conductivity were described as Table B.4.3.

**Table B.4.3** The coefficients for conductivity calculation.

	SBE 45
$CT_{cor}$	3.2500e-06
$CP_{cor}$	-9.5700e-08
$g$	-9.826667e-01
$h$	1.181806e-01
$i$	-2.954452e-04
$j$	3.516859e-05

**(3) Measurement and calibration**

Surface seawater was pumped up from the water intake at approximately 4 meters below the water level. First, the temperature of the seawater sample was measured by the SBE 38 and the data was collected every minute. Next, the seawater sample from the same line was de-bubbled and transferred to the laboratory, where the temperature and the conductivity were measured by the SBE 45 at a flow rate of approximately 1.2 L minute<sup>-1</sup>. The data was collected at the same frequency.

For further on-board correction of the conductivity measurement by the SBE 45, the seawater samples were collected and stored from the same line in the 250 ml colorless bottle with a screw cap at least once a day. The salinity measurement of the collected samples was performed in the same method as the hydrographic salinity measurement, details of which are described in section ‘C-2 Bottle Salinity’. The coefficients( $A$ : slope,  $B$ : offset) for the conductivity correction were determined using linear regression between the conductivity(calculated from the bottled samples salinity and the SBE45

temperature) and the SBE 45 conductivity, expressed as:

$$C_{corrected} = A \times C_{SBE45} + B$$

The determined coefficients are  $A = 1.00059$  and  $B = -0.000390$ .

Finally, salinity was calculated from pressure, the corrected conductivity and the SBE45 temperature by PSS78 (Practical Salinity Scale, UNESCO).

#### **(4) Data and Results**

The data is distributed in “49UP20190612\_40N\_TSG.CSV”. The record structure of JMA format is shown below.

Column1 DATE: Date (YYYYMMDD) [JST]

Column2 TIME: Time (HHMM) [JST] (= UTC + 9h)

Column3 LATITUDE: Latitude

Column4 LONGITUDE: Longitude

Column5 TEMP: Sea Surface Temperature (ITS-90) [°C]

Column6 COND: Corrected Conductivity [S/m]

Column7 ONTEMP: Onboard Sea Temperature (ITS-90) [°C]

Column8 SAL: Salinity (PSS78)

#### **Reference**

UNESCO (1981): Tenth report of the Joint Panel on Oceanographic Tables and Standards. *UNESCO Tech. Papers in Mar. Sci.*, 36, 25 pp.

## C. Hydrographic Measurement Techniques and Calibration

### 1. CTDO<sub>2</sub> Measurements

8 June 2020

#### (5) Personnel

Keita KAKUYA (GEMD/JMA)

Kiyoshi TANAKA (GEMD/JMA)

Noriyuki OKUNO (GEMD/JMA)

Togo IDA (GEMD/JMA)

(Leg 1) Yoshikazu HIGASHI (GEMD/JMA)

(Leg 2) Yuma KAWAKAMI (GEMD/JMA)

#### (6) CTDO<sub>2</sub> measurement system

(Software: SEASAVEwin32 ver7.23.2)

<i>Deck unit</i>	<i>Serial number</i>	<i>Station</i>
SBE 11plus (SBE)	11P35251 – 0683	RF6502 – 6571
<i>Under-water unit</i>	<i>Serial number</i>	<i>Station</i>
SBE 9plus (SBE)	09P31345 – 0722 (Pressure : 90574)	RF6502 – 6571
<i>Temperature</i>	<i>Serial number</i>	<i>Station</i>
SBE 3plus (SBE)	03P4436 (primary)	RF6502 – 6571
SBE 3plus (SBE)	03P5184 (secondary)	RF6502 – 6571
SBE 35 (SBE)	0093	RF6502 – 6571
<i>Conductivity</i>	<i>Serial number</i>	<i>Station</i>
SBE 4C (SBE)	043697 (primary)	RF6502 – 6571
	042987 (secondary)	RF6502 – 6571
<i>Pump</i>	<i>Serial number</i>	<i>Station</i>
SBE 5T (SBE)	056552 (primary)	RF6502 – 6571
	055501 (secondary)	RF6502 – 6571
<i>Oxygen</i>	<i>Serial number</i>	<i>Station</i>
RINKO III (JFE)	007 (foil number:141304A)	RF6502 – 6571
	284 (foil number:164313A)	RF6502 – 6571
<i>Water sampler (36 position)</i>	<i>Serial number</i>	<i>Station</i>
SBE 32 (SBE)	32 – 1270	RF6502 – 6571
<i>Altimeter</i>	<i>Serial number</i>	<i>Station</i>
PSA-916D (TB)	40850	RF6502 – 6571
<i>Water sampling bottle</i>	<i>Station</i>	
Niskin Bottle (GO)	RF6502 – 6571	

SBE: Sea- Bird Electronics, Inc., USA

JFE: JFE Advantech Co., Ltd., Japan

TB: Teledyne Benthos, Inc., USA

GO: General Oceanics, Inc., USA

## (7) Pre-cruise calibration

### (3.1) Pressure

*S/N 09P31345 - 0722, 16 Oct. 2018*

$$\begin{array}{ll} c_1 = -4.802766 \times 10^4 & t_1 = 3.012930 \times 10 \\ c_2 = -2.656902 \times 10^{-1} & t_2 = -3.769891 \times 10^{-4} \\ c_3 = 1.418260 \times 10^{-2} & t_3 = 4.208190 \times 10^{-6} \\ d_1 = 3.830200 \times 10^{-2} & t_4 = 1.503050 \times 10^{-9} \\ d_2 = 0.000000 & t_5 = 0.000000 \end{array}$$

Formula:

$$c = c_1 + c_2 \times U + c_3 \times U^2$$

$$d = d_1 + d_2 \times U$$

$$t_0 = t_1 + t_2 \times U + t_3 \times U^2 + t_4 \times U^3 + t_5 \times U^4$$

$$U (\text{degrees Celsius}) = M \times (12\text{-bit pressure temperature compensation word}) + B$$

*U*: temperature in degrees Celsius

*S/N 0722 coefficients in SEASOFT (configuration sheet dated on 16 Oct. 2018)*

$$M = 1.29410 \times 10^{-2}, B = -9.10099$$

Finally, pressure is computed as

$$P(\text{psi}) = c \times (1 - t_0^2/t^2) \times \{1 - d \times (1 - t_0^2/t^2)\}$$

*t*: pressure period (μsec)

The drift-corrected pressure is computed as

$$\text{Drift corrected pressure(dbar)} = \text{slope} \times (\text{computed pressure in dbar}) + \text{offset}$$

$$\text{Slope} = 1.00006, \text{Offset} = -0.1142$$

### (3.2) Temperature (ITS-90): SBE 3plus

*S/N 03P4436 (primary), 30 Aug. 2018*

$$\begin{aligned} g &= 4.33647067 \times 10^{-3} & j &= 1.75059815 \times 10^{-6} \\ h &= 6.37628029 \times 10^{-4} & f_0 &= 1000.0 \\ i &= 2.08841605 \times 10^{-5} \end{aligned}$$

*S/N 03P5184 (secondary), 30 Aug. 2018*

$$\begin{aligned} g &= 4.34777201 \times 10^{-3} & j &= 1.89805716 \times 10^{-6} \\ h &= 6.36464492 \times 10^{-4} & f_0 &= 1000.0 \\ i &= 2.14978512 \times 10^{-5} \end{aligned}$$

Formula:

$$Temperature(ITS-90) = \frac{1}{g + h \times \ln(f_0/f) + i \times \ln^2(f_0/f) + j \times \ln^3(f_0/f)} - 273.15$$

$f$ : Instrument freq.[Hz]

### (3.3) Deep Ocean Standards Thermometer Temperature (ITS-90): SBE 35

*S/N 0093, 27 Jun. 2014*

$$\begin{aligned} a_0 &= 4.06873596 \times 10^{-3} & a_3 &= -9.25907373 \times 10^{-6} \\ a_1 &= -1.06370821 \times 10^{-3} & a_4 &= 1.99023461 \times 10^{-7} \\ a_2 &= 1.65409501 \times 10^{-4} \end{aligned}$$

Formula:

$$Linearizedtemperature(ITS-90) = 1/\{a_0 + a_1 \times \ln(n) + a_2 \times \ln^2(n) + a_3 \times \ln^3(n) + a_4 \times \ln^4(n)\} - 273.15$$

$n$ : instrument output

The slow time drift of the SBE 35

*S/N 0093, 25 Feb. 2019 (2nd step: fixed point calibration)*

$$Slope = 0.999989, Offset = 0.000196$$

Formula:

$$Temperature(ITS-90) = slope \times (Linearized\ temperature) + offset$$

### (3.4) Conductivity: SBE 4C

*S/N 043697 (primary), 26 Oct. 2018*

$$\begin{array}{llll} g & = & -9.73127203 & j & = & 5.76368338 \times 10^{-5} \\ h & = & 1.24473240 & CP_{cor} & = & -9.5700 \times 10^{-8} \\ i & = & -4.11024108 \times 10^{-5} & CT_{cor} & = & 3.2500 \times 10^{-6} \end{array}$$

*S/N 042987 (secondary), 16 Aug. 2018*

$$\begin{array}{llll} g & = & -9.92052697 & j & = & 4.72212263 \times 10^{-5} \\ h & = & 1.36213626 & CP_{cor} & = & -9.5700 \times 10^{-8} \\ i & = & 5.27078448 \times 10^{-4} & CT_{cor} & = & 3.2500 \times 10^{-6} \end{array}$$

Conductivity of a fluid in the cell is expressed as:

$$C(S/m) = (g + h \times f^2 + i \times f^3 + j \times f^4) / \{10 \times (1 + CT_{cor} \times t + CP_{cor} \times p)\}$$

*f*: instrument frequency (kHz)

*t*: water temperature (degrees Celsius)

*p*: water pressure (dbar).

### (3.5) Oxygen (RINKO III)

The RINKO III (JFE Advantech Co., Ltd., Japan) sensor is based on the ability of a selected substance to act as a dynamic fluorescence quencher. The RINKO III model is designed to be used with a CTD system that accepts an auxiliary analog sensor, and it is designed to operate down to 7000 m. The RINKO III output is expressed in voltage from 0 to 5 V.



## (8) Quality control and data correction during the cruise

### (4.1) Temporal change of deck pressure

The post-cruise drift corrected pressure was computed as follows:

$$\text{Drift corrected pressure(dbar)} = \text{slope} \times (\text{computed pressure in dbar}) + \text{offset}$$

*S/N 09P31345 - 0722, 26 Sep. 2019*

*Slope = 0.99998, Offset = -0.3016*

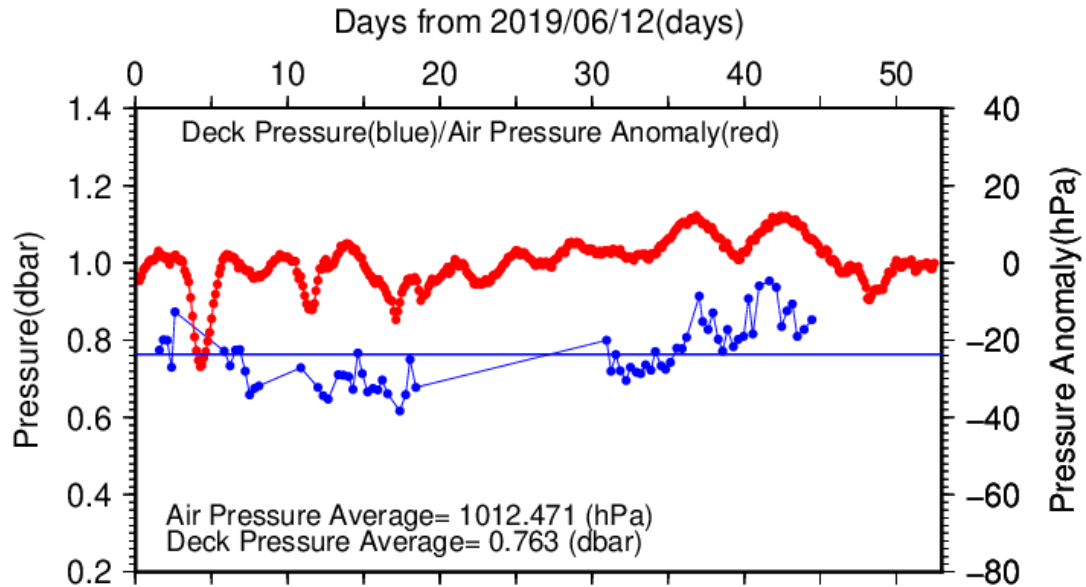


Figure C.1.1. Time series of the CTD deck pressure. Red line indicates atmospheric pressure anomaly. Blue line and dots indicate pre-cast deck pressure and average.

### (4.2) Temperature sensor (SBE 3plus)

The practical corrections for the CTD temperature data can be made by using a SBE 35 and correcting the SBE 3plus so that it agrees with the SBE 35 (*McTaggart et al., 2010; Uchida et al., 2007*).

CTD temperature is corrected as follows:

$$\text{Corrected temperature} = T - (c_0 + c_1 \times P + c_2 \times P^2)$$

*T*: CTD temperature (degrees Celsius), *P*: pressure (dbar), and *c*<sub>0</sub>, *c*<sub>1</sub>, *c*<sub>2</sub>: coefficients

Table C.1.1. Temperature correction summary (pressure ≥ 2000dbar). (Bold: accepted sensor)

<i>S/N</i>	<i>Num</i>	<i>c</i> <sub>0</sub> (K)	<i>c</i> <sub>1</sub> (K/dbar)	<i>C</i> <sub>2</sub> (K/dbar <sup>2</sup> )	<i>Stations</i>
<b>03P4436</b>	<b>438</b>	<b>1.087056 × 10<sup>-4</sup></b>	<b>-2.456657 × 10<sup>-7</sup></b>	<b>2.462016 × 10<sup>-11</sup></b>	<b>RF6502 – 6533</b>
<b>03P4436</b>	<b>581</b>	<b>6.972219 × 10<sup>-4</sup></b>	<b>-4.596775 × 10<sup>-8</sup></b>	<b>1.879355 × 10<sup>-12</sup></b>	<b>RF6534 – 6571</b>
03P5184	438	1.480337 × 10 <sup>-4</sup>	-5.275556 × 10 <sup>-7</sup>	4.485962 × 10 <sup>-11</sup>	RF6502 – 6533
03P5184	581	8.288990 × 10 <sup>-4</sup>	-1.693084 × 10 <sup>-7</sup>	0.000000	RF6534 – 6571

Table C.1.2. Temperature correction summary for S/N 03P4436.

Stations	Pressure < 2000dbar			Pressure $\geq$ 2000 dbar		
	Num	Average (K)	Std (K)	Num	Average (K)	Std (K)
RF6501 – 6533	642	–0.0009	0.0190	438	0.0000	0.0001
RF6534 – 6571	772	–0.0003	0.0074	581	0.0000	0.0001

Table C.1.3. Temperature correction summary for S/N 03P5184.

Stations	Pressure < 2000dbar			Pressure $\geq$ 2000 dbar		
	Num	Average (K)	Std (K)	Num	Average (K)	Std (K)
RF6501 – 6533	642	–0.0009	0.0175	438	0.0000	0.0002
RF6534 – 6571	772	–0.0012	0.0082	581	0.0000	0.0002

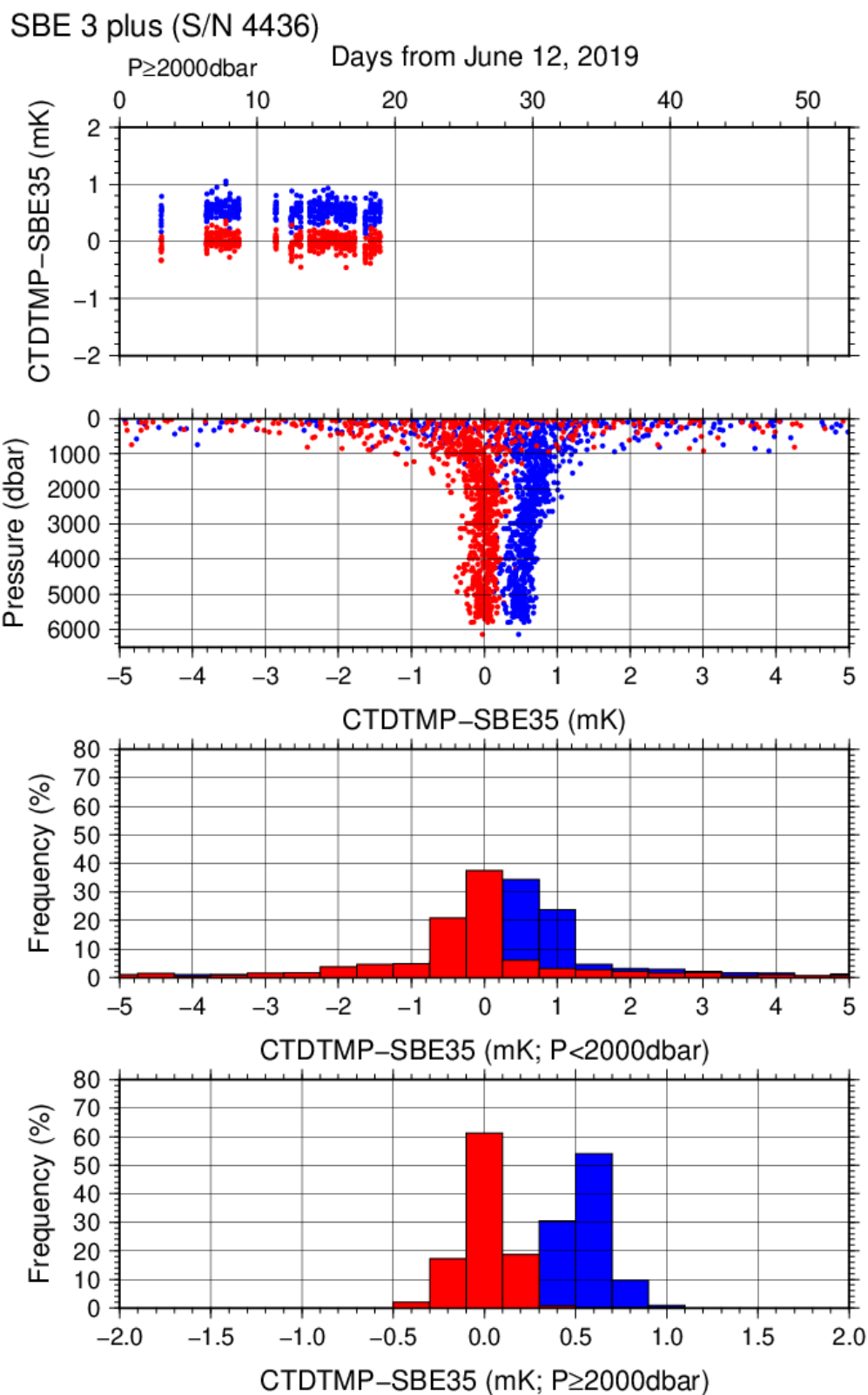


Figure C.1.2. Difference between the CTD temperature (*S/N 03P4436*) and the Deep Ocean Standards thermometer (SBE 35) on Leg 1. Blue and red dots indicate before and after the correction using SBE 35 data, respectively. Lower two panels show histograms of the differences after correction.

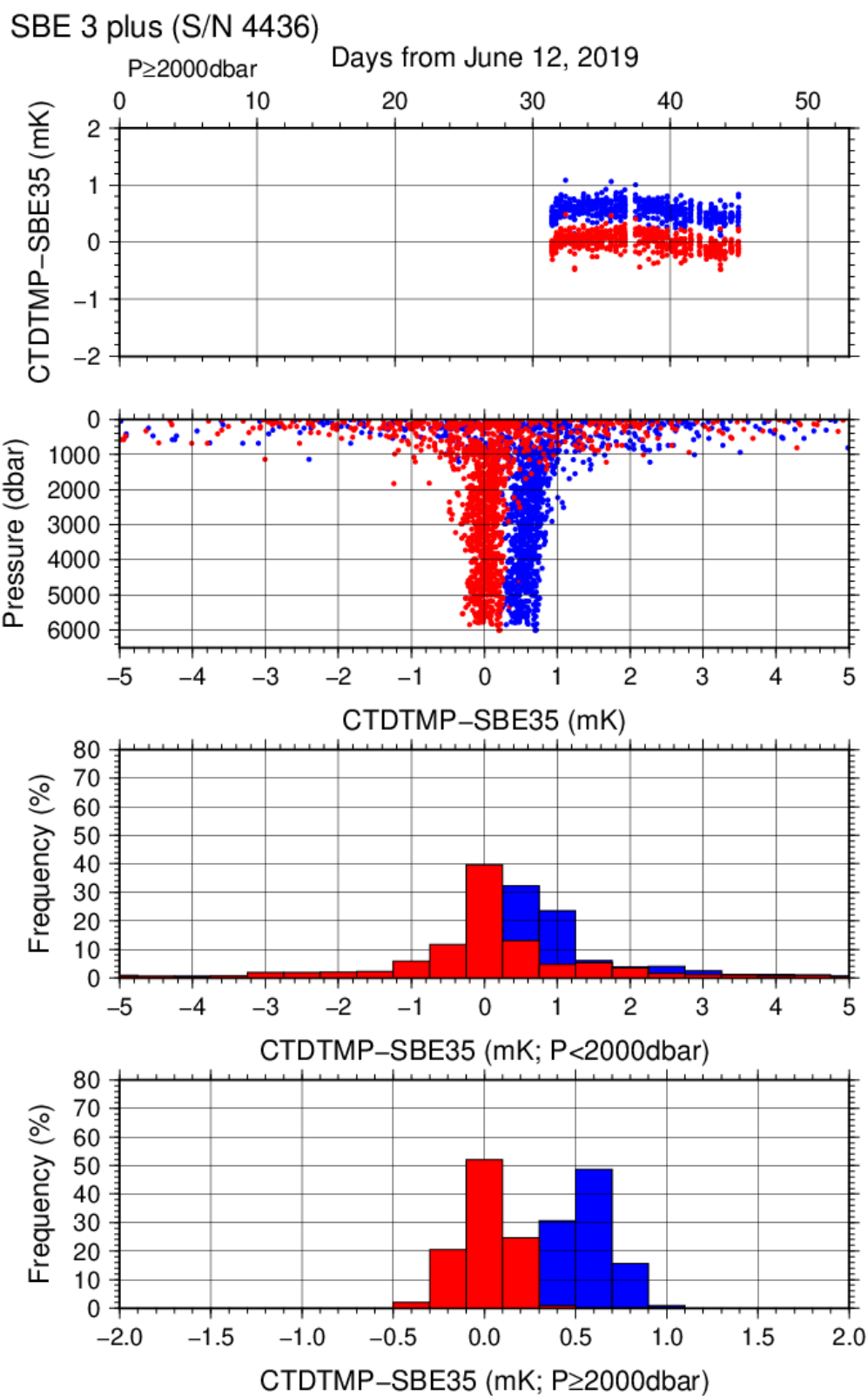


Figure C.1.3. Difference between the CTD temperature (*S/N 03P4436*) and the Deep Ocean Standards thermometer (SBE 35) on Leg 2. Blue and red dots indicate before and after the correction using SBE 35 data, respectively. Lower two panels show histograms of the differences after correction.

### (4.3) Conductivity sensor (SBE 4C)

The practical corrections for CTD conductivity data can be made by using bottle salinity data to correct the SBE 4C to agree with measured conductivity (*McTaggart et al., 2010*).

CTD conductivity was corrected as follows:

$$\text{Corrected Conductivity} = C - \left( \sum_{i=0}^I c_i \times C^i + \sum_{j=1}^J p_j \times P^j \right)$$

$C$ : CTD conductivity,  $c_i$  and  $p_j$ : calibration coefficients

$i, j$ : determined by use of the AIC (*Akaike, 1974*). In accord with *McTaggart et al. (2010)*, the maximum of  $I$  and  $J$  are 2.

Table C.1.4. Conductivity correction coefficient summary. (Bold: accepted sensor)

$S/N$	$Num$	$c_0(S/m)$	$c_1$	$c_2(m/S)$	$Stations$
			$p_1(S/m/dbar)$	$p_2(S/m/dbar^2)$	
<b>043697</b>	<b>1122</b>	<b><math>3.1142 \times 10^{-3}</math></b>	<b><math>-1.5209 \times 10^{-3}</math></b>	<b><math>1.7101 \times 10^{-4}</math></b>	<b>RF6502 – 6533</b>
			<b>0.0000</b>	<b>0.0000</b>	
<b>043697</b>	<b>1340</b>	<b><math>1.0175 \times 10^{-3}</math></b>	<b><math>-3.1676 \times 10^{-4}</math></b>	<b>0.0000</b>	<b>RF6534 – 6571</b>
			<b><math>2.6605 \times 10^{-8}</math></b>	<b><math>-4.1528 \times 10^{-12}</math></b>	
042987	1082	$2.6413 \times 10^{-3}$	$-1.3502 \times 10^{-3}$	$1.7745 \times 10^{-4}$	RF6502 – 6533
			$1.3335 \times 10^{-8}$	0.0000	
042987	1340	$5.3837 \times 10^{-4}$	$-1.2321 \times 10^{-4}$	0.0000	RF6534 – 6571
			$2.6432 \times 10^{-8}$	$-2.2120 \times 10^{-12}$	

Table C.1.5. Conductivity correction and salinity correction summary for S/N 043697.

Stations	Pressure < 1900dbar					
	Conductivity			Salinity		
	Num	Average (S/m)	Std (S/m)	Num	Average	Std
RF6502 – 6533	656	0.0000	0.0002	656	–0.0001	0.0024
RF6534 – 6571	820	0.0000	0.0004	820	0.0000	0.0036
Stations	Pressure ≥ 1900 dbar					
	Conductivity			Salinity		
	Num	Average (S/m)	Std (S/m)	Num	Average	Std
RF6502 – 6533	466	0.0000	0.0000	466	0.0001	0.0005
RF6534 – 6571	520	0.0000	0.0000	520	0.0000	0.0003

Table C.1.6. Conductivity correction and salinity correction summary for S/N 042987.

Stations	Pressure < 1900dbar					
	Conductivity			Salinity		
	Num	Average (S/m)	Std (S/m)	Num	Average	Std
RF6502 – 6533	635	0.0000	0.0002	635	0.0000	0.0024
RF6534 – 6571	820	0.0000	0.0004	820	0.0000	0.0033
Stations	Pressure ≥ 1900 dbar					
	Conductivity			Salinity		
	Num	Average (S/m)	Std (S/m)	Num	Average	Std
RF6502 – 6533	447	0.0000	0.0000	447	–0.0001	0.0005
RF6534 – 6571	520	0.0000	0.0000	520	0.0000	0.0004

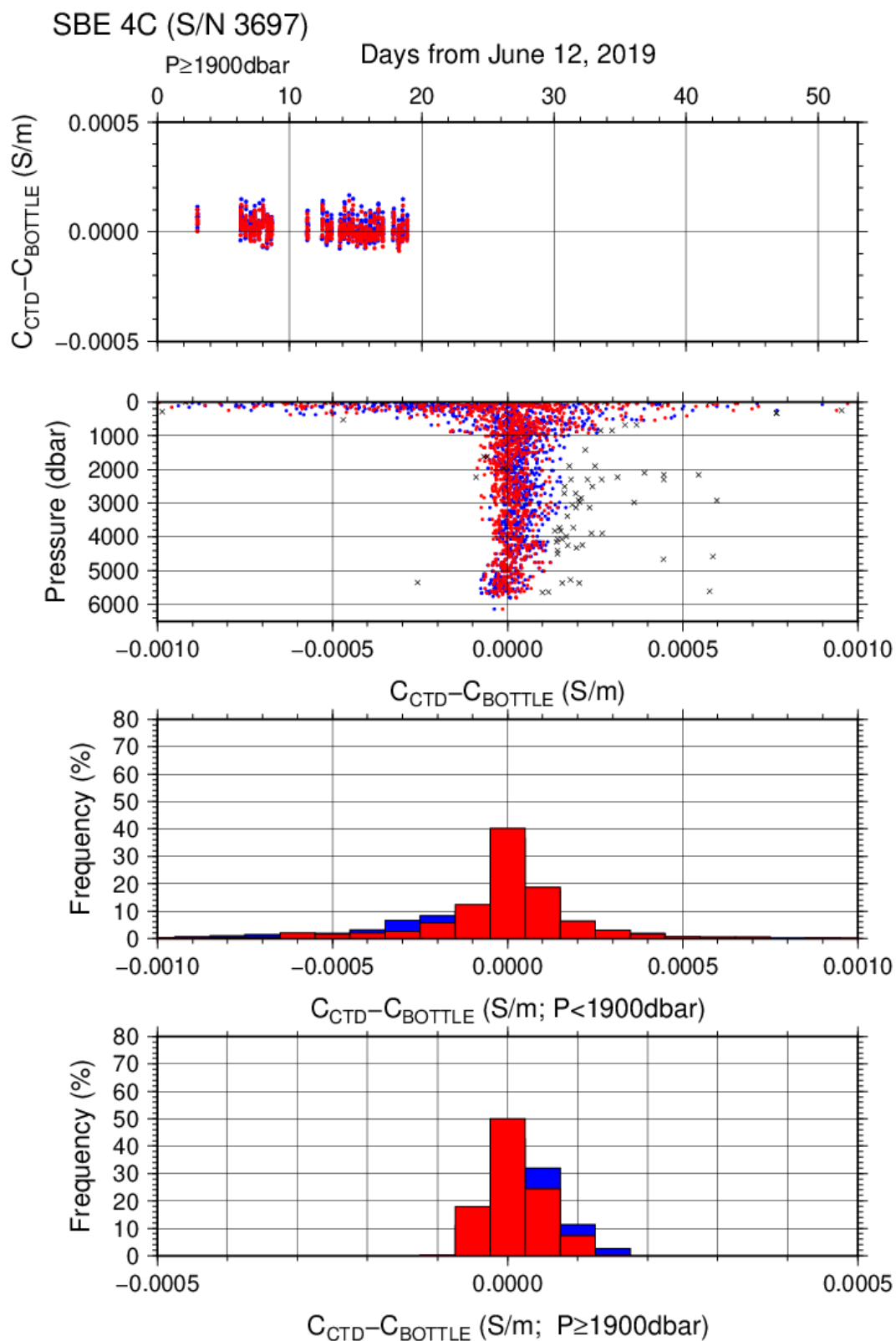


Figure C.1.4. Difference between the CTD conductivity (S/N 043697) and the bottle conductivity on Leg 1. Blue and red dots indicate before and after the calibration using bottle data, respectively. Lower two panels show histograms of the differences before and after calibration.

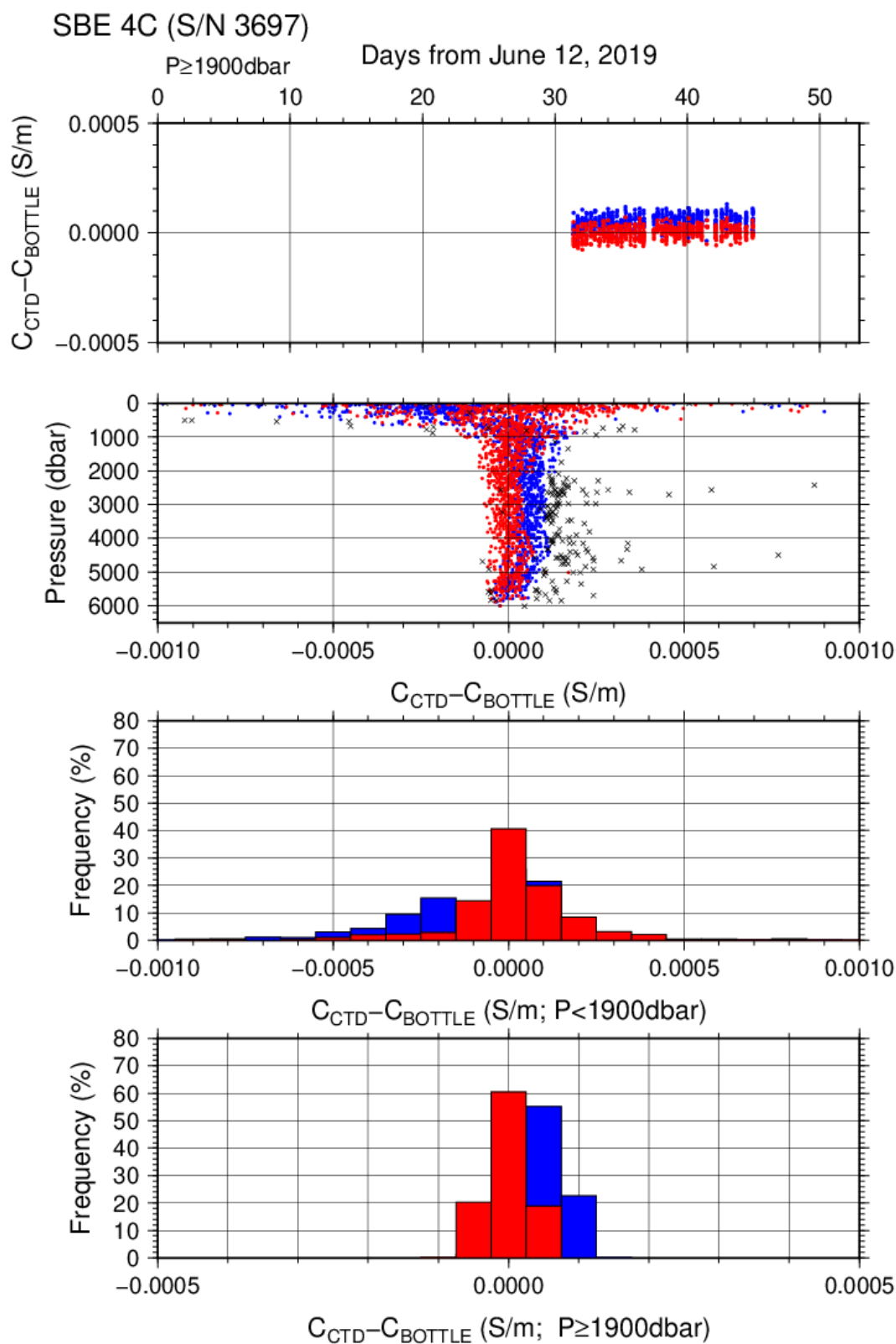


Figure C.1.5. Difference between the CTD conductivity (S/N 043697) and the bottle conductivity on Leg 2. Blue and red dots indicate before and after the calibration using bottle data, respectively. Lower two panels show histograms of the differences before and after calibration.



#### **(4.4) Oxygen sensor (RINKO III)**

The CTD oxygen concentration was calculated using the RINKO III output (voltage) with the Stern-Volmer equation in accord with the method of Uchida et al. (2008) and Uchida et al. (2010). The pressure hysteresis for the RINKO III output (voltage) was corrected in accord with Sea-bird Electronics (2009) and Uchida et al. (2010). The equations were as follows:

$P$ : pressure (dbar),  $t$ : potential temperature,  $v$ : RINKO output voltage (volt)

$T$ : elapsed time of the sensor from the beginning of first station in calculation group in day

$O_2^{\text{sat}}$ : dissolved oxygen saturation by Garcia and Gordon (1992) ( $\mu\text{mol/kg}$ )

$[O_2]$ : dissolved oxygen concentration ( $\mu\text{mol/kg}$ )

$c_1-c_9$ : determined by minimizing differences between CTD oxygen concentration and bottle dissolved oxygen concentration by quasi-newton method (*Shanno, 1970*).

Table C.1.7. Dissolved oxygen correction coefficient summary. (Bold: accepted sensor)

S/N	Stations	$c_1$	$c_2$	$c_3$	$c_4$	$c_5$
		$c_6$	$c_7$	$c_8$	$c_9$	
0007	RF6502 – 6533	<b>1.69328</b>	<b><math>3.08942 \times 10^{-2}</math></b>	<b><math>2.58009 \times 10^{-4}</math></b>	<b><math>1.42215 \times 10^{-3}</math></b>	<b><math>-1.50185 \times 10^{-1}</math></b>
		$3.23422 \times 10^{-1}$	$-6.71890 \times 10^{-4}$	$7.53719 \times 10^{-4}$	$6.78341 \times 10^{-2}$	
0007	RF6534 – 6571	<b>1.67409</b>	<b><math>2.39069 \times 10^{-2}</math></b>	<b><math>2.75124 \times 10^{-4}</math></b>	<b><math>2.00501 \times 10^{-4}</math></b>	<b><math>-1.46253 \times 10^{-1}</math></b>
		$3.23371 \times 10^{-1}$	$7.59088 \times 10^{-4}$	$5.29803 \times 10^{-5}$	$7.08813 \times 10^{-2}$	
0284	RF6502 – 6533	1.65277	$2.98490 \times 10^{-2}$	$3.49575 \times 10^{-4}$	$1.78525 \times 10^{-3}$	$-2.16280 \times 10^{-1}$
		$3.12320 \times 10^{-1}$	$-9.62855 \times 10^{-4}$	$7.06602 \times 10^{-4}$	$7.69413 \times 10^{-2}$	
0284	RF6534 – 6571	1.62357	$2.14475 \times 10^{-2}$	$3.28339 \times 10^{-4}$	$3.18233 \times 10^{-4}$	$-2.06872 \times 10^{-1}$
		$3.10692 \times 10^{-1}$	$6.78548 \times 10^{-4}$	$4.51383 \times 10^{-5}$	$8.14780 \times 10^{-2}$	

Table C.1.8. Dissolved oxygen correction summary for S/N 0007.

Stations	Pressure < 950dbar			Pressure $\geq$ 950 dbar		
	Num	Average ( $\mu\text{mol/kg}$ )	Std ( $\mu\text{mol/kg}$ )	Num	Average ( $\mu\text{mol/kg}$ )	Std ( $\mu\text{mol/kg}$ )
RF6502 – 6533	481	-0.02	1.23	583	0.02	0.38
RF6534 – 6571	569	-0.03	1.13	760	0.01	0.36

Table C.1.9. Dissolved oxygen correction summary for S/N 0284.

Stations	Pressure < 950dbar			Pressure $\geq$ 950 dbar		
	Num	Average ( $\mu\text{mol/kg}$ )	Std ( $\mu\text{mol/kg}$ )	Num	Average ( $\mu\text{mol/kg}$ )	Std ( $\mu\text{mol/kg}$ )
RF6502 – 6533	481	-0.12	1.22	583	0.02	0.42
RF6534 – 6571	569	-0.20	1.20	760	0.02	0.38

RINKO (S/N 007)

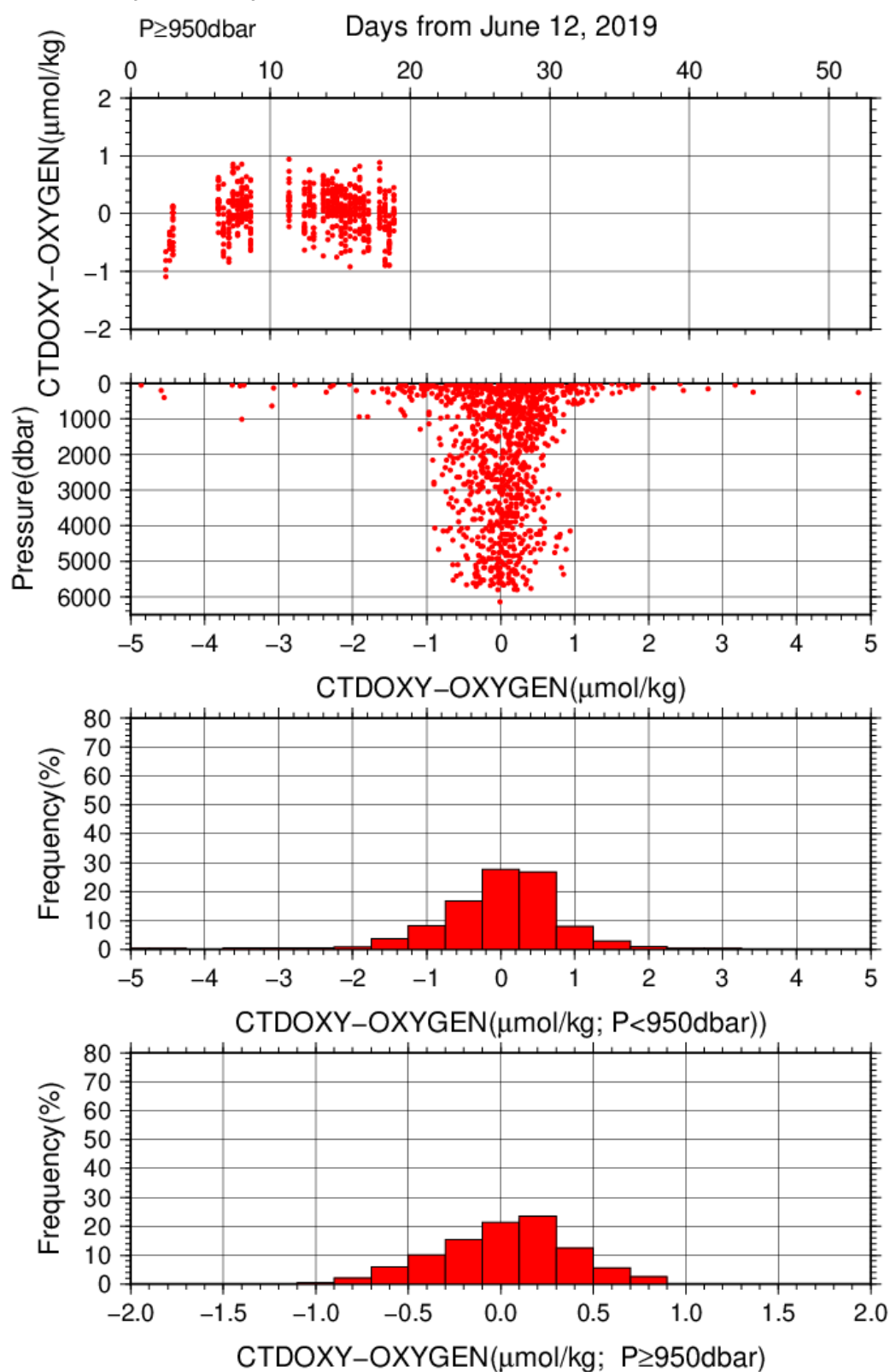


Figure C.1.6. Difference between the CTD oxygen (*S/N 0007*) and bottle dissolved oxygen on Leg 1. Red dots in upper two panels indicate the result of calibration. Lower two panels show histograms of the differences between calibrated oxygen concentration and bottle oxygen concentration.

RINKO (S/N 007)

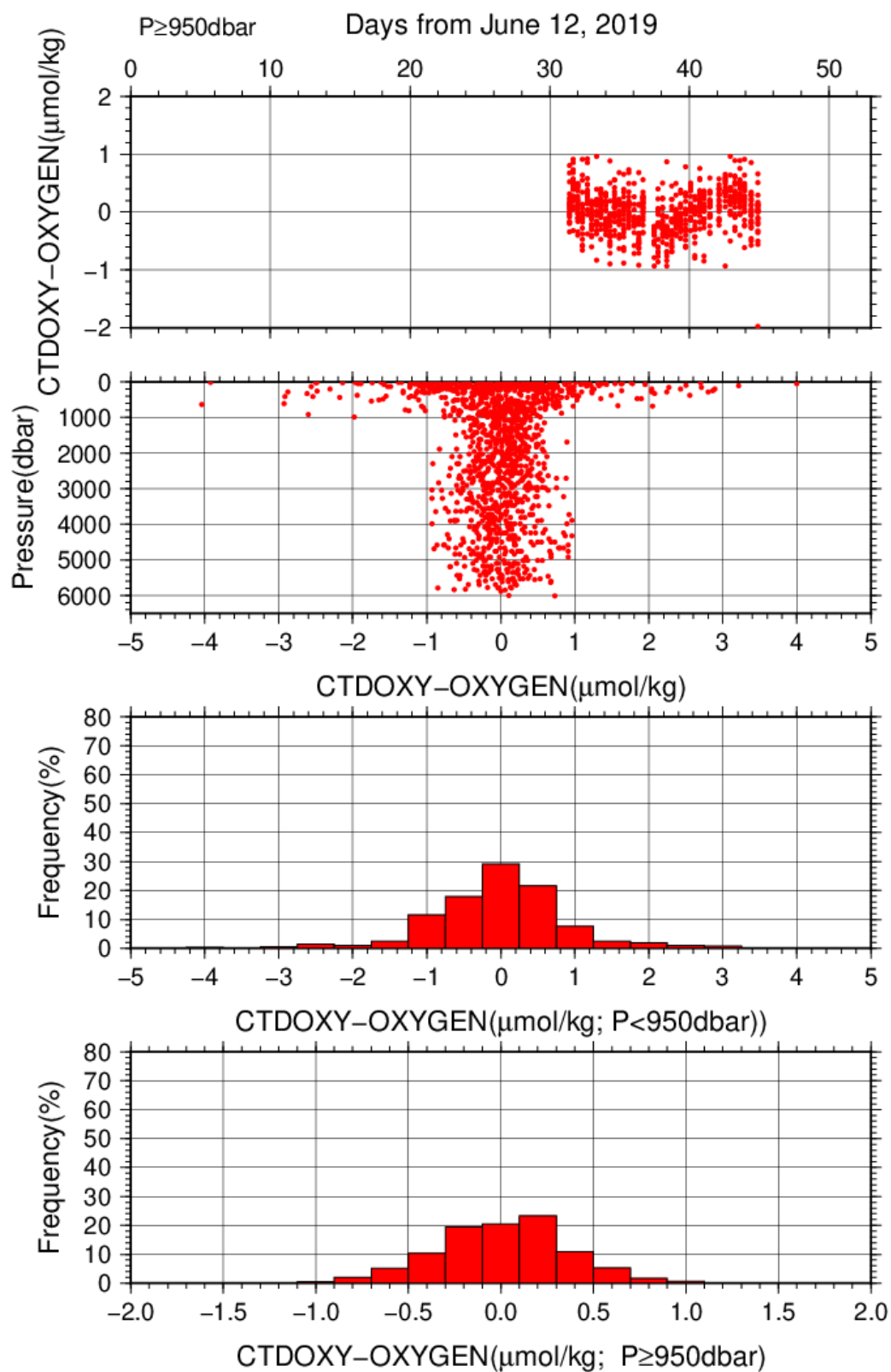


Figure C.1.7. Difference between the CTD oxygen (S/N 0007) and bottle dissolved oxygen on Leg 1. Red dots in upper two panels indicate the result of calibration. Lower two panels show histograms of

the differences between calibrated oxygen concentration and bottle oxygen concentration.

#### (4.5) Results of detection of sea floor by the altimeter (PSA-916D)

The altimeter detected the sea floor at 65 of 70 stations, the average distance of beginning detecting the sea floor was 45.5 m, and that of final detection of sea floor was 12.7 m. The summary of detection of PSA-916D was shown in Figure C.1.8.

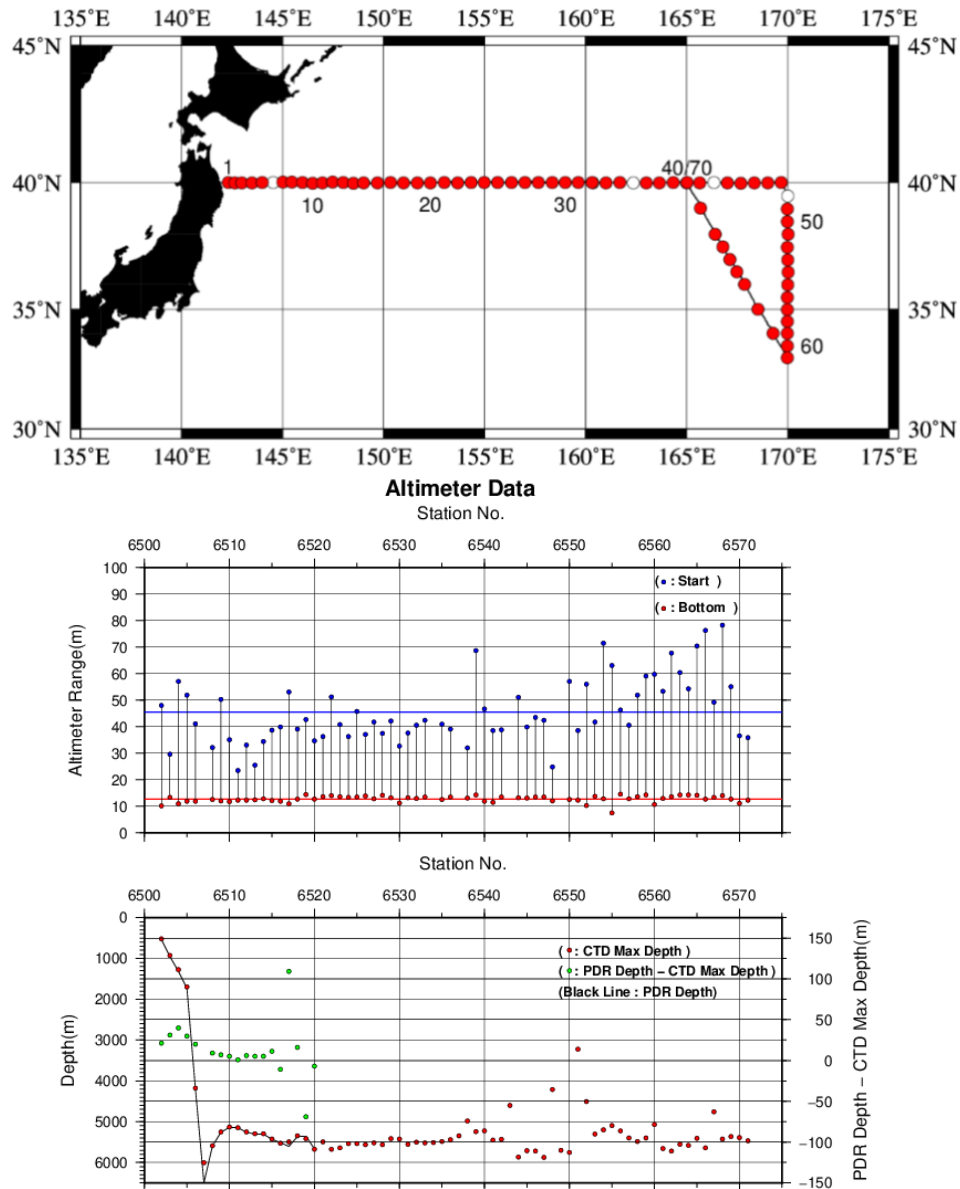


Figure C.1.8. The summary of detection of PSA-916D. The upper panel shows the stations of detection, the lower panel shows the relationship among PSA-916D, bathymetry and CTD depth. In the upper panel, closed and open circles indicate react and no-react stations, respectively.

## (9) Post-cruise calibration

After the cruise, post-cruise calibration of sensors was performed by the manufacturer, as shown below. We confirmed that the calibration of these sensors did not change significantly during the cruise.

### (5.1) Temperature (ITS-90): SBE 3plus

*S/N 03P4436 (primary), 16 Oct. 2019*

$$\begin{aligned} g &= 4.33674073 \times 10^{-3} & j &= 1.85113437 \times 10^{-6} \\ h &= 6.38225910 \times 10^{-4} & f_0 &= 1000.0 \\ i &= 2.13099806 \times 10^{-5} \end{aligned}$$

*S/N 03P5184 (secondary), 14 Feb. 2020*

$$\begin{aligned} g &= 4.34795864 \times 10^{-3} & j &= 1.96366585 \times 10^{-6} \\ h &= 6.36861968 \times 10^{-4} & f_0 &= 1000.0 \\ i &= 2.17766331 \times 10^{-5} \end{aligned}$$

### (5.2) Deep Ocean Standards Thermometer Temperature (ITS-90): SBE 35

*S/N 0093, 16 Oct. 2019*

$$\begin{aligned} a_0 &= 4.49398478 \times 10^{-3} & a_3 &= -1.00727358 \times 10^{-5} \\ a_1 &= -1.19680954 \times 10^{-3} & a_4 &= 2.14915542 \times 10^{-7} \\ a_2 &= 1.81023620 \times 10^{-4} \end{aligned}$$

Formula:

$$\text{Linearized temperature(ITS-90)} = 1/\{a_0 + a_1 \times \ln(n) + a_2 \times \ln^2(n) + a_3 \times \ln^3(n) + a_4 \times \ln^4(n)\} - 273.15$$

$n$ : instrument output

The slow time drift of the SBE 35

*S/N 0093, 10 Oct. 2019 (2nd step: fixed point calibration)*

$$\text{Slope} = 1.000002, \text{Offset} = -0.000037$$

Formula:

$$\text{Temperature(ITS-90)} = \text{slope} \times (\text{Linearized temperature}) + \text{offset}$$

### (5.3) Conductivity: SBE 4C

*S/N 043697 (primary), 10 Oct. 2019*

$$\begin{array}{llll} g & = & -9.73131524 & j & = & 6.60463693 \times 10^{-5} \\ h & = & 1.24469215 & CP_{cor} & = & -9.5700 \times 10^{-8} \\ i & = & -6.70333348 \times 10^{-5} & CT_{cor} & = & 3.2500 \times 10^{-6} \end{array}$$

*S/N 042987 (secondary), 22 Nov. 2019*

$$\begin{array}{llll} g & = & -9.92975809 & j & = & 1.35274502 \times 10^{-4} \\ h & = & 1.36552800 & CP_{cor} & = & -9.5700 \times 10^{-8} \\ i & = & -4.96841577 \times 10^{-4} & CT_{cor} & = & 3.2500 \times 10^{-6} \end{array}$$

### References

- Akaike, H. (1974): A new look at the statistical model identification. *IEEE Transactions on Automatic Control*, **19**:716–722.
- García, H. E., and L. I. Gordon (1992): Oxygen solubility in seawater: Better fitting equations. *Limnol. Oceanogr.*, **37**, 1307–1312.
- McTaggart, K. E., G. C. Johnson, M. C. Johnson, F. M. Delahoyde, and J. H. Swift (2010): The GO-SHIP Repeat Hydrography Manual: A Collection of Expert Reports and guidelines. IOCCP Report No **14**, ICPO Publication Series No. 134, version 1, 2010.
- Sea-Bird Electronics (2009): SBE 43 dissolved oxygen (DO) sensor – hysteresis corrections, *Application note no. 64-3*, 7 pp.
- Shanno, David F. (1970): Conditioning of quasi-Newton methods for function minimization. *Math. Comput.* **24**, 647–656. MR 42 #8905.
- Uchida, H., G. C. Johnson, McTaggart, K. E. (2010): CTD oxygen sensor calibration procedures. In: The GO-SHIP repeat hydrography manual: A Collection of Expert Reports and guidelines. IOCCP Report No **14**, ICPO Publication Series No. 134, version 1, 2010.
- Uchida, H., K. Ohyama, S. Ozawa, and M. Fukasawa (2007): In-situ calibration of the Sea-Bird 9plus CTD thermometer. *J. Atmos. Oceanic Technol.*, **24**, 1961–1967.
- Uchida, H., T. Kawano, I. Kaneko, and M. Fukasawa (2008): In-situ calibration of optode-based oxygen sensors. *J. Atmos. Oceanic Technol.*, **25**, 2271–2281.



## 2. Bottle Salinity

8 June 2020

### (1) Personnel

Noriyuki OKUNO (GEMD/JMA)

Kiyoshi TANAKA (GEMD/JMA)

Keita KAKUYA (GEMD/JMA)

Togo IDA (GEMD/JMA)

(Leg 1) Yoshikazu HIGASHI (GEMD/JMA)

(Leg 2) Yuma KAWAKAMI (GEMD/JMA)

### (2) Salinity measurement

Salinometer: AUTOSAL 8400B (Guildline Instruments Ltd., Canada ; S/N 69677 for stations before RF6506, S/N 72103 for stations after RF6507)

Thermometer: Guildline platinum thermometers model 9450 (to monitor ambient temperature and bath temperature) (Guildline Instruments Ltd., Canada)

IAPSO Standard Seawater: P162 ( $K_{15}=0.99983$ )

### (3) Sampling and measurement

The measurement system was almost the same as the system described by Kawano (2010).

Algorithm for practical salinity scale, 1978 (PSS-78; UNESCO, 1981) was employed to convert the conductivity ratios to salinities.

### (4) Station occupied

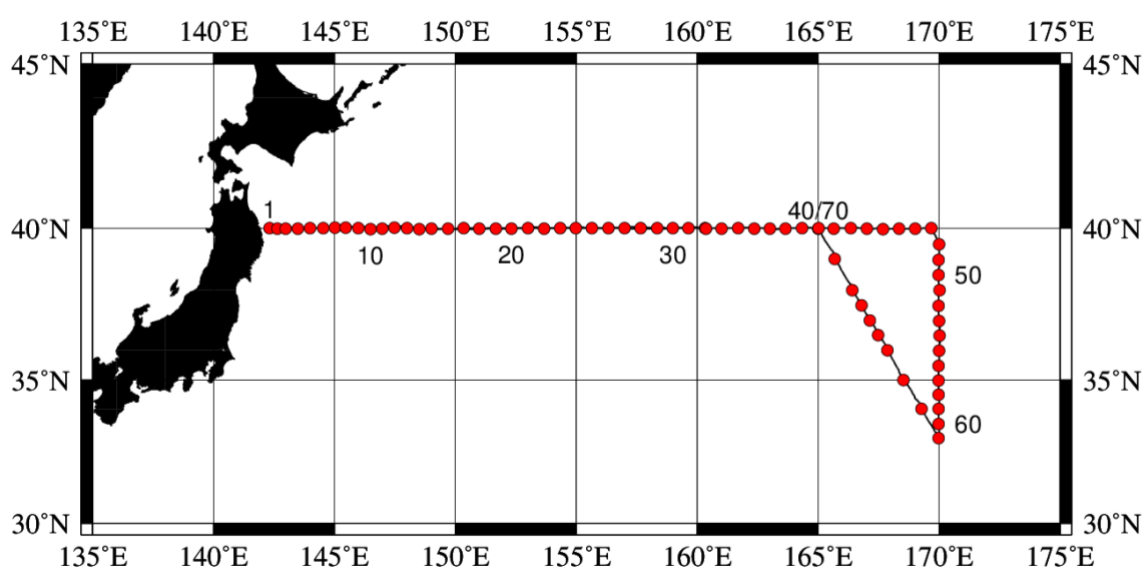


Figure C.2.1. Location of observation stations of bottle salinity.

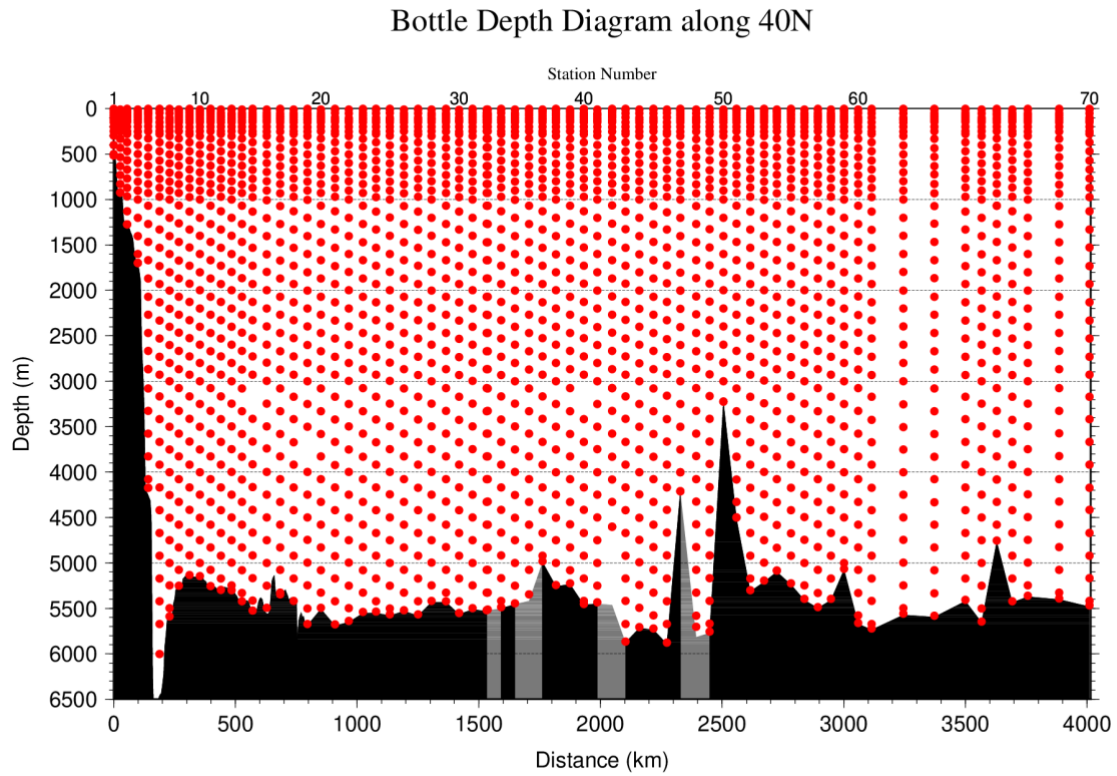


Figure C.2.2. Distance-depth distribution of sampling layers of bottle salinity. Seafloor filled with black before RF6520 station indicates data measured continuously by a single beam echo sounder, and after RF6521 station indicates data estimated by CTD observation with altimeter measurement. Seafloor filled with gray indicates data missing station during this cruise and is referred from our previous cruise in 2012.

## (5) Result

### (5.1) Ambient temperature, bath temperature and Standard Seawater measurements

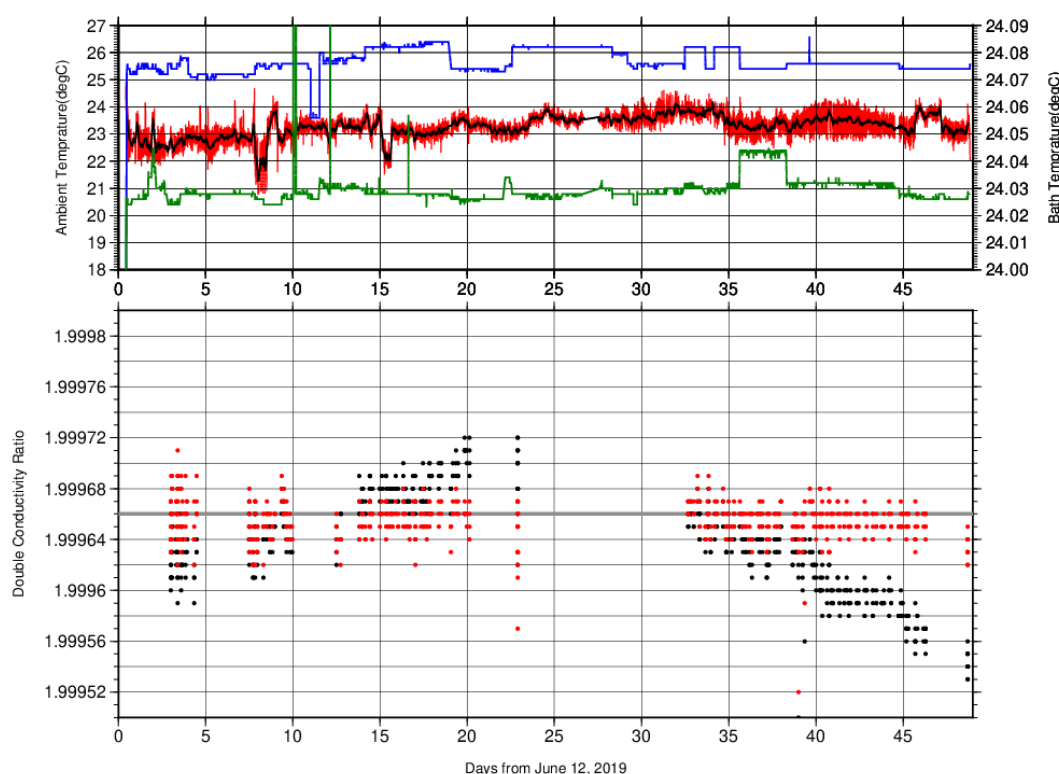


Figure C.2.3. The upper panel, red line, black line, green line, and blue line indicate time-series of ambient temperature, average ambient temperature, bath temperature (Autosal S/N 69677), and bath temperature (Autosal S/N 72103) during cruise. The lower panel, black dots, and red dots indicate raw and corrected time-series of the double conductivity ratio of the standard seawater (P162).

### (5.2) Replicate and duplicate samples

We took replicate (pair of water samples taken from a single Niskin bottle) and duplicate (pair of water samples taken from different Niskin bottles closed at the same depth) samples for bottle salinity throughout the cruise. Table C.2.1 summarizes the results of the analyses. Figure C.2.4 shows details of the results. The calculation of the standard deviation from the difference of sets was based on a procedure (SOP 23) in DOE (1994).

Table C.2.1. Summary of replicate and duplicate salinity analyses.

Measurement	Average difference $\pm$ S.D.
Replicate sample	$0.0002 \pm 0.0002$ (N = 207)
Duplicate sample	$0.0007 \pm 0.0008$ (N = 14)

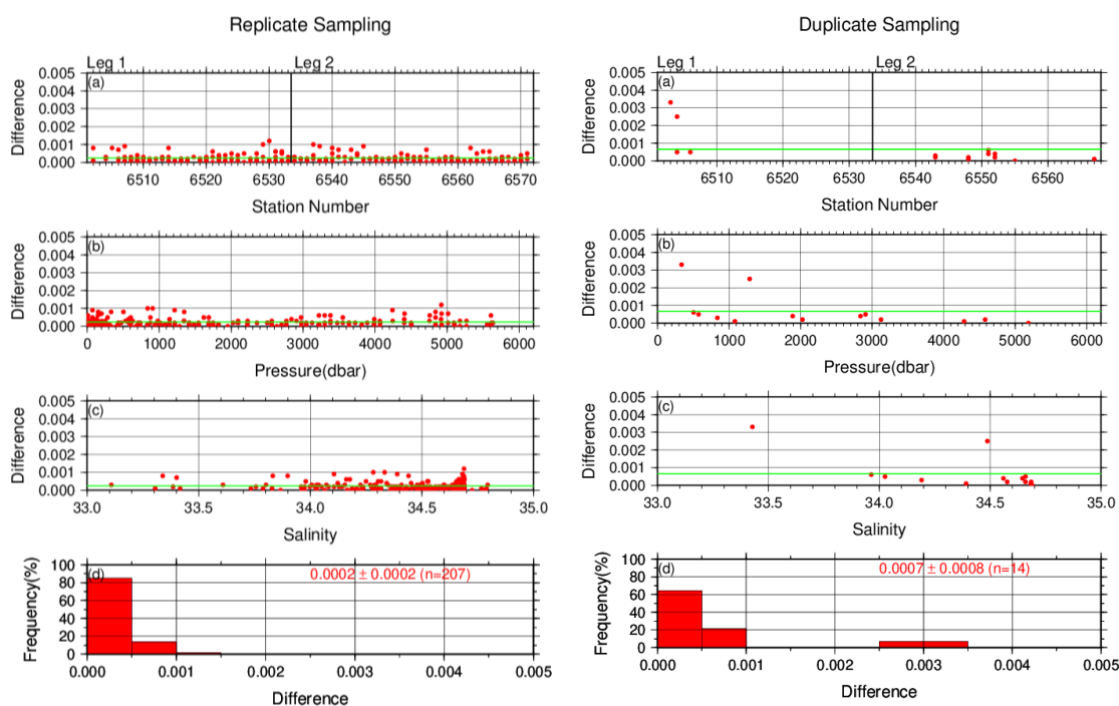


Figure C.2.4. Results of (left) replicate and (right) duplicate analyses during the cruise against (a) station number, (b) pressure, (c) salinity, and (d) histogram of the measurements. Green line indicates the mean of the differences of salinity of replicate/duplicate analyses.

### (5.3) Summary of assigned quality control flags

Table C.2.2. Summary of assigned quality control flags

Flag	Definition	Number
2	Good	2036
3	Questionable	0
4	Bad (Faulty)	216
5	Not reported	0
6	Replicate measurements	233
Total number of samples		2485

### References

- DOE (1994), Handbook of methods for the analysis of the various parameters of the carbon dioxide system in sea water; version 2. *A. G. Dickson and C. Goyet (eds), ORNL/CDIAC-74.*
- Kawano (2010), The GO-SHIP Repeat Hydrography Manual: A Collection of Expert Reports and Guidelines. *IOCCP Report No. 14, ICPO Publication Series No. 134, Version 1.*
- UNESCO (1981), Tenth report of the Joint Panel on Oceanographic Tables and Standards. *UNESCO Tech. Papers in Mar. Sci.*, **36**, 25 pp.

### 3. Bottle Oxygen

8 June 2020

#### (1) Personnel

##### Leg 1

Hiroyuki HATAKEYAMA (GEMD/JMA)

Koichi WADA (GEMD/JMA)

Kei KONDO (GEMD/JMA)

Rie SANAI (GEMD/JMA)

Masakazu TAKAMI (GEMD/JMA)

##### Leg 2

Hiroyuki HATAKEYAMA (GEMD/JMA)

Tomohiro UEHARA (GEMD/JMA)

Kei KONDO (GEMD/JMA)

Rie SANAI (GEMD/JMA)

Masakazu TAKAMI (GEMD/JMA)

#### (2) Station occupied

A total of 70 stations (Leg 1: 32, Leg 2: 38) were occupied for dissolved oxygen measurements. Station location and sampling layers of bottle oxygen are shown in Figures C.3.1 and C.3.2, respectively.

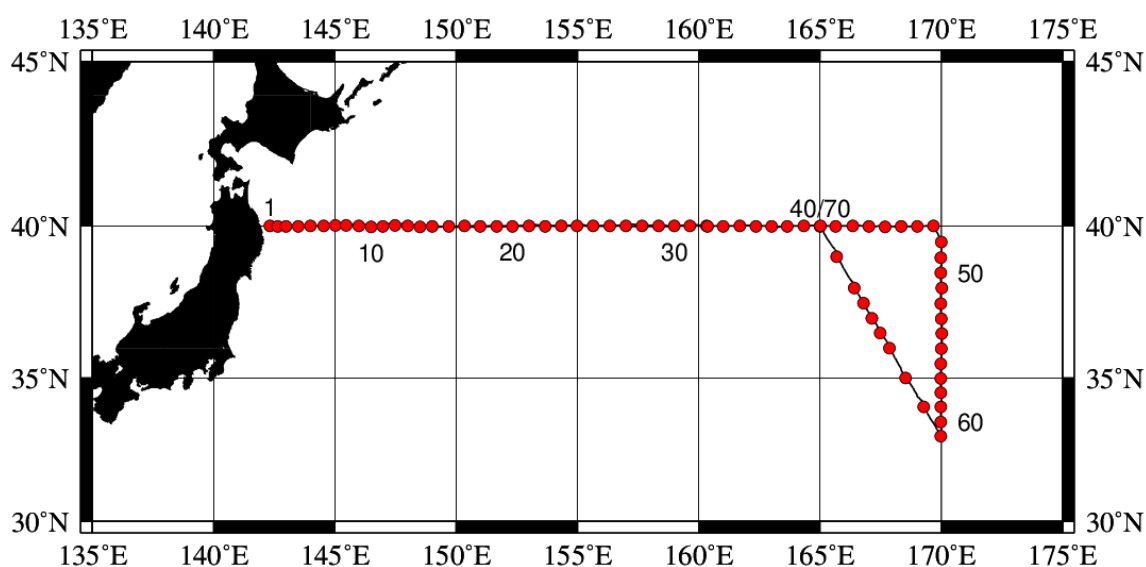


Figure C.3.1. Location of observation stations of bottle oxygen.

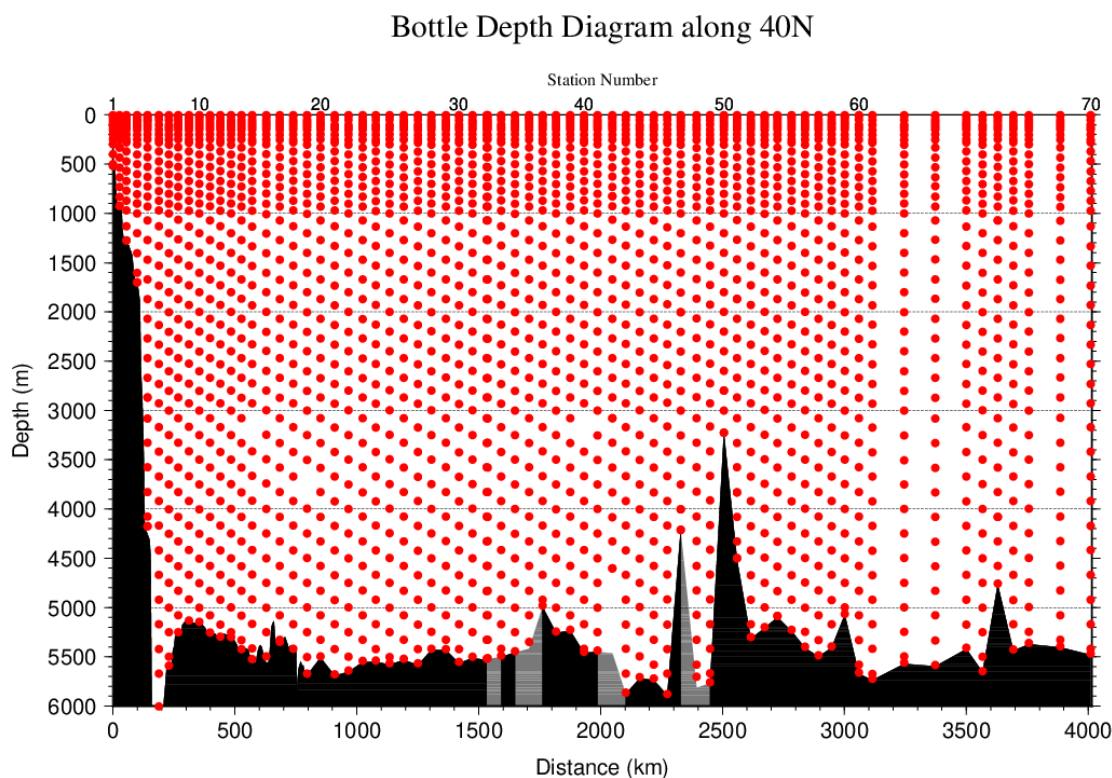


Figure C.3.2. Distance-depth distribution of sampling layers of bottle oxygen.

### (3) Instrument

Detector: DOT-15X (Kimoto Electronic, Japan)

Burette: APB-610 (Kyoto Electronic, Japan)

### (4) Sampling and measurement

Methods of seawater sampling, measurement, and calculation of dissolved oxygen concentration were based on an IOCCP Report (Langdon, 2010). Details of the methods are shown in Appendix A1.

The reagents for the measurement were prepared according to recipes described in Appendix A2. Standard  $\text{KIO}_3$  solutions were prepared gravimetrically using the highest purity standard substance  $\text{KIO}_3$  (Lot. No. ECG4358, Wako Pure Chemical, Japan). Table C.3.1 shows the batch list of prepared standard  $\text{KIO}_3$  solutions.

Table C.3.1. Batch list of the standard  $\text{KIO}_3$  solutions.

$\text{KIO}_3$ batch	Concentration and uncertainty ( $k=2$ ) at 20 °C. Unit is $\text{mol L}^{-1}$ .	Purpose of use
20181128-2	$0.0016646 \pm 0.0000068$	Standardization (main use)
20181205-2	$0.0016667 \pm 0.0000068$	Mutual comparison

### (5) Standardization

The concentration of the  $\text{Na}_2\text{S}_2\text{O}_3$  titrant was determined with the standard  $\text{KIO}_3$  solution “20181128-2”, based on the methods of an IOCCP Report (Langdon, 2010). Figure C.3.3 shows the results of standardization during the cruise. The standard deviation of the concentration at 20 °C was determined through standardization and was used in the calculation of uncertainty.

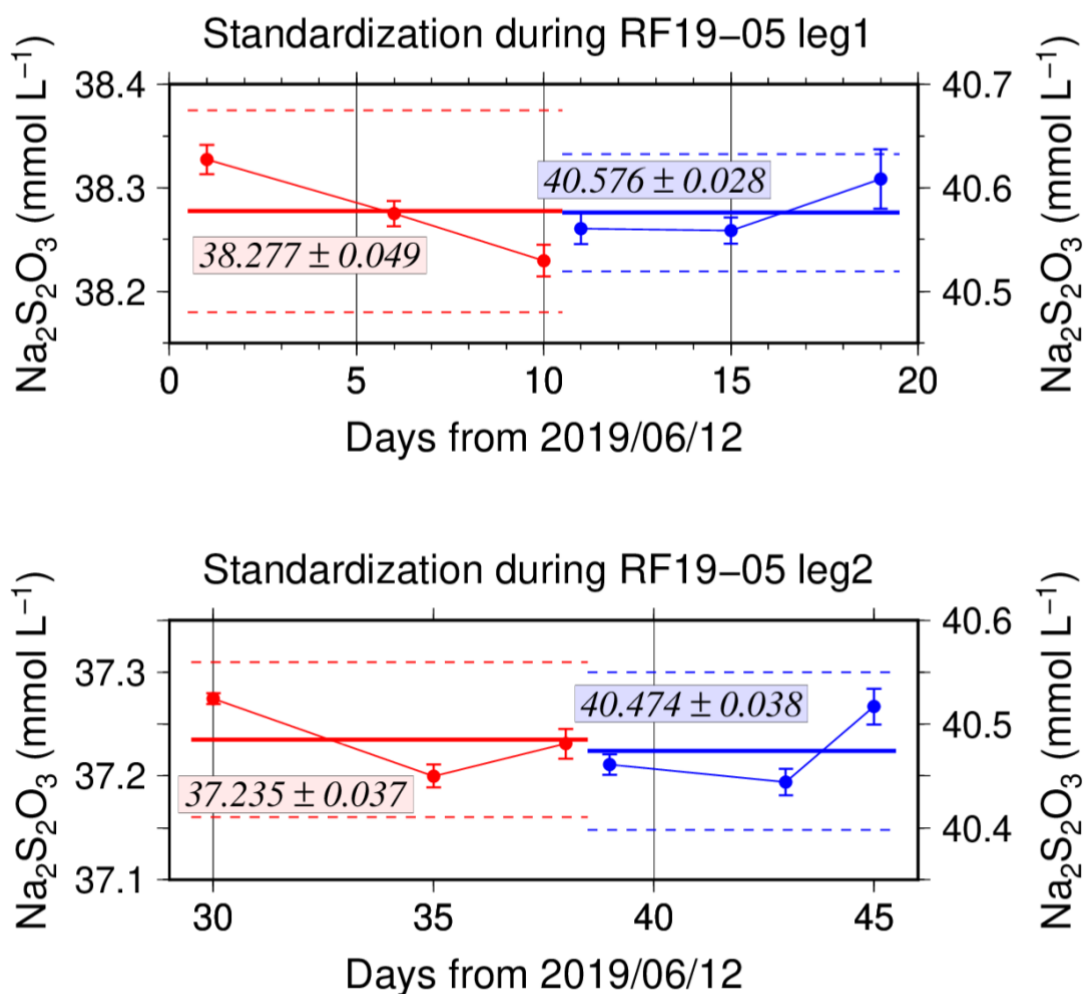


Figure C.3.3. Calculated concentration of  $\text{Na}_2\text{S}_2\text{O}_3$  solution at 20 °C in standardization during RF19-05 Leg 1 (top) and RF19-05 Leg 2 (bottom). Different colors of plots indicate different batches of  $\text{Na}_2\text{S}_2\text{O}_3$  solution; red (blue) plots correspond to the left (right) y-axis. Error bars of plots show standard deviations of concentration of  $\text{Na}_2\text{S}_2\text{O}_3$  in the measurements. Thick and dashed lines denote the mean and twice the standard deviations for the batch measurements, respectively.

## (6) Blank

### (6.1) Reagent blank

The blank in an oxygen measurement (reagent blank in distilled water;  $V_{\text{reg-blk}}$ ) was determined by the methods described in the IOCCP Report (Langdon, 2010) using pure water. The blank reflects not only the interfering substances (oxidants or reductants) in the reagents but also the differences between the measured end-point and the equivalence point due to unknown causes in the titrator. Because we used two sets (set A and B) of pickling reagent-I and -II, the blanks in each set were determined separately (Figure C.3.4).

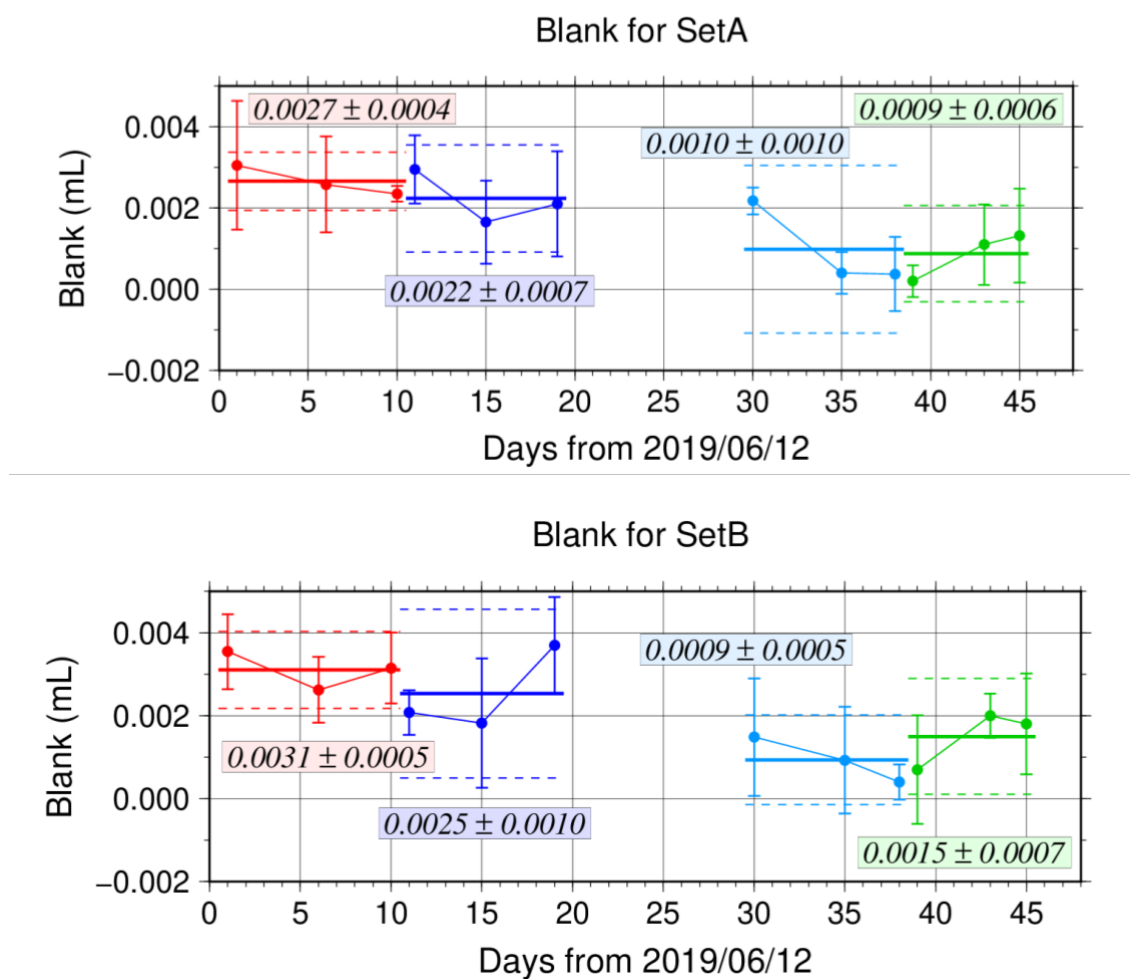


Figure C.3.4. Reagent blank ( $V_{\text{reg-blk}}$ ) determination for set A (top) and set B (bottom). Error bars of plots show standard deviations of the measurements. Thick and dashed lines denote the mean and the mean  $\pm$  twice the standard deviation for the batch measurement, respectively.

### (6.2) Seawater blank

We also determined seawater blank ( $V_{\text{sw-blk}}$ ) which reflects interfering substances in seawater. Although this blank is not included in determination of oxygen concentration, measurement of the blank would be necessary to improve traceability and comparability in dissolved



oxygen concentration. Details are described in Appendix A3.

## (7) Quality Control

### (7.1) Replicate and duplicate analyses

We took replicate (pair of water samples taken from a single Niskin bottle) and duplicate (pair of water samples taken from different Niskin bottles closed at the same depth) samples of dissolved oxygen throughout the cruise. Table C.3.2 summarizes the results of the analyses. Figure C.3.5 shows details of the results. The calculation of the standard deviation from the difference of sets was based on a procedure (SOP 23) in DOE (1994).

Table C.3.2. Summary of replicate and duplicate measurements.

Measurement	Ave. $\pm$ S.D. ( $\mu\text{mol kg}^{-1}$ )
Replicate	$0.20 \pm 0.26$ (N=273)
Duplicate	$0.57 \pm 0.84$ (N=23)

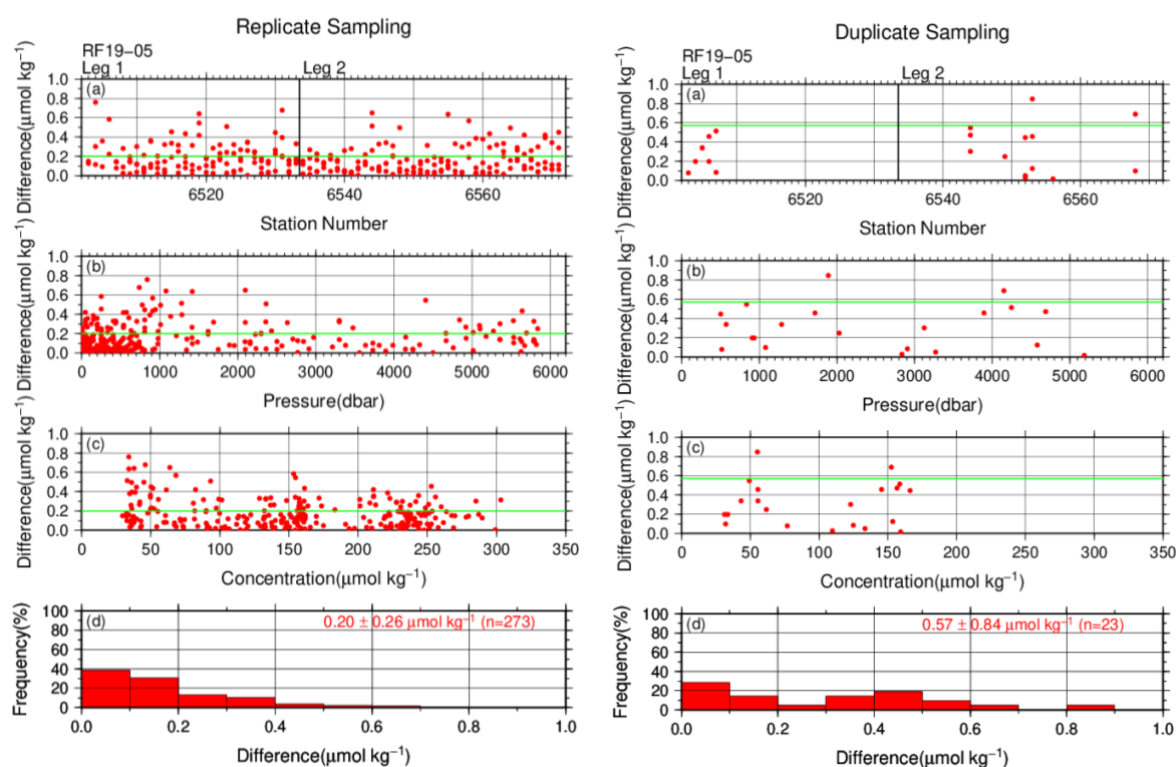


Figure C.3.5. Results of (left) replicate and (right) duplicate measurements during the cruise against (a) station number, (b) pressure, and (c) concentration of dissolved oxygen. Green lines denote the average of the measurements. Bottom panels (d) show histograms of the measurements.

### (7.2) Comparisons between standard KIO<sub>3</sub> solutions

During the cruise, comparisons were made between different lots of standard KIO<sub>3</sub> solutions to confirm the accuracy of our oxygen measurements and the bias of a standard KIO<sub>3</sub> solution. A concentration of the standard KIO<sub>3</sub> solution “20181205-2” was determined using Na<sub>2</sub>S<sub>2</sub>O<sub>3</sub> solution standardized with the KIO<sub>3</sub> solution “20181128-2”, and the difference between the measured value and the theoretical one. Good agreement between two standards confirmed that there was no systematic shift in oxygen measurements during the cruise (Figure C.3.6).

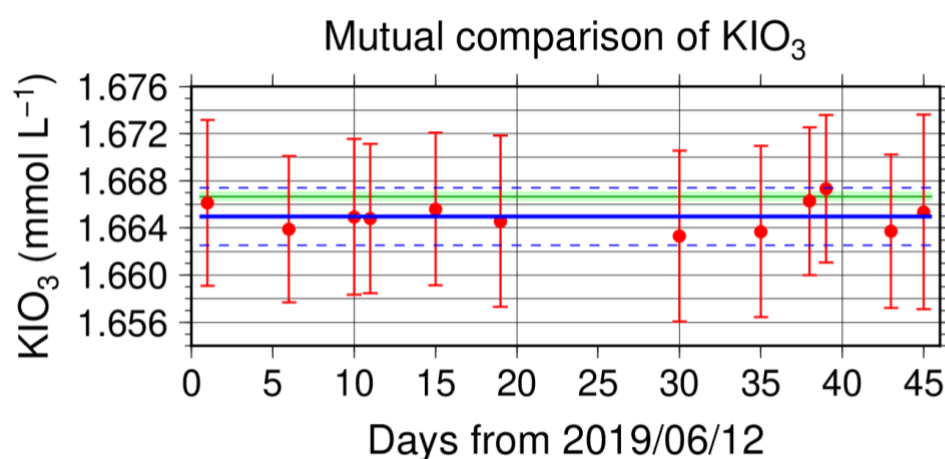


Figure C.3.6. Result of comparison of standard KIO<sub>3</sub> solutions during RF19-05. Circles and error bars show mean of the measured value and its uncertainty ( $k=2$ ), respectively. Thick and dashed lines in blue denote the mean and the mean  $\pm$  twice the standard deviations, respectively, for the measurements. Green thin line and light green thick line denote the nominal concentration and its uncertainty ( $k=2$ ) of standard KIO<sub>3</sub> solution “20181205-2”.

### (7.3) Quality control flag assignment

A quality flag value was assigned to oxygen measurements, as shown in Table C.3.3, using the code defined in IOCCP Report No.14 (Swift, 2010).

Table C.3.3. Summary of assigned quality control flags.

Flag	Definition	Number of samples
2	Good	2189
3	Questionable	28
4	Bad (Faulty)	25
5	Not reported	0
6	Replicate measurements	273
Total number of samples		2515

### (8) Uncertainty

Oxygen measurement involves various uncertainties; determination of glass bottles volume, repeatability and systematic error of burette discharge, repeatability of pickling reagent discharges, determination of reagent blank, standardization of  $\text{Na}_2\text{S}_2\text{O}_3$  solution, and uncertainty of  $\text{KIO}_3$  concentration. After taking into consideration the above uncertainties that could be evaluated, the expanded uncertainty of bottle oxygen concentrations ( $T=20$ ,  $S=34.5$ ) was estimated, as shown in Table C.3.4. However, it is difficult to determine a strict uncertainty for oxygen concentration because there is no reference material for oxygen measurement.

Table C.3.4. Expanded uncertainty ( $k=2$ ) of bottle oxygen during the cruise.

O <sub>2</sub> conc. ( $\mu\text{mol kg}^{-1}$ )	Uncertainty ( $\mu\text{mol kg}^{-1}$ )
20	0.31
30	0.32
50	0.34
70	0.36
100	0.40
150	0.49
200	0.59
250	0.70
300	0.81
400	1.05

## **Appendix**

### **A1. Methods**

#### **(A1.1) Seawater sampling**

Following procedure is based on a determination method in IOCCP Report (Langdon, 2010). Seawater samples were collected from 10-liters Niskin bottles attached the CTD-system and a stainless steel bucket for the surface. Seawater for bottle oxygen measurement was transferred from the Niskin bottle and a stainless steel bucket to a volumetrically calibrated dry glass bottles. At least three times the glass volume water was overflowed. Then, pickling reagent-I 1 mL and reagent-II 1mL were added immediately, and sample temperature was measured using a thermometer. After a stopper was inserted carefully into the glass, it was shaken vigorously to mix the content and to disperse the precipitate finely. After the precipitate has settled at least halfway down the glass, the glass was shaken again. The sample glasses containing pickled samples were stored in a laboratory until they were titrated. To prevent air from entering the glass, deionized water (DW) was added to its neck after sampling.

#### **(A1.2) Sample measurement**

At least 15 minutes after the re-shaking, the samples were measured on board. Added 1 mL  $\text{H}_2\text{SO}_4$  solution and a magnetic stirrer bar into the sample glass, samples were titrated with  $\text{Na}_2\text{S}_2\text{O}_3$  solution whose molarity was determined with  $\text{KIO}_3$  solution. During the titration, the absorbance of iodine in the solution was monitored using a detector. Also, temperature of  $\text{Na}_2\text{S}_2\text{O}_3$  solution during the titration was recorded using a thermometer. Dissolved oxygen concentration ( $\mu\text{mol kg}^{-1}$ ) was calculated from sample temperature at the fixation, CTD salinity, glass volume, and titrated volume of the  $\text{Na}_2\text{S}_2\text{O}_3$  solution, and oxygen in the pickling reagents-I (1 mL) and II (1 mL) ( $7.6 \times 10^{-8}$  mol; Murray *et al.*, 1968).

### **A2. Reagents recipes**

Pickling reagent-I; Manganous chloride solution ( $3 \text{ mol L}^{-1}$ )

Dissolve 600 g of  $\text{MnCl}_2 \cdot 4\text{H}_2\text{O}$  in DW, then dilute the solution with DW to a final volume of 1 L.

Pickling reagent-II; Sodium hydroxide ( $8 \text{ mol L}^{-1}$ ) / sodium iodide solution ( $4 \text{ mol L}^{-1}$ )

Dissolve 320 g of NaOH in about 500 mL of DW, allow to cool, then add 600 g NaI and dilute with DW to a final volume of 1 L.

$\text{H}_2\text{SO}_4$  solution; Sulfuric acid solution ( $5 \text{ mol L}^{-1}$ )

Slowly add 280 mL concentrated  $\text{H}_2\text{SO}_4$  to roughly 500 mL of DW. After cooling the final volume should be 1 L.

$\text{Na}_2\text{S}_2\text{O}_3$  solution; Sodium thiosulfate solution ( $0.04 \text{ mol L}^{-1}$ )

Dissolve 50 g of  $\text{Na}_2\text{S}_2\text{O}_3 \cdot 5\text{H}_2\text{O}$  and 0.4 g of  $\text{Na}_2\text{CO}_3$  in DW, then dilute the solution with DW to a final volume of 5 L.

$\text{KIO}_3$  solution; Potassium iodate solution ( $0.001667 \text{ mol L}^{-1}$ )

Dry high purity  $\text{KIO}_3$  for two hours in an oven at  $130^\circ\text{C}$ . After weight out accurately  $\text{KIO}_3$ , dissolve it in DW in a 5 L flask. Concentration of potassium iodate is determined by a gravimetric method.

### A3. Seawater blank

Blank due to redox species other than oxygen in seawater ( $V_{\text{sw-blk}}$ ) can be a potential source of measurement error. Total blank ( $V_{\text{tot-blk}}$ ) in seawater measurement can be represented as follows;

$$V_{\text{tot-blk}} = V_{\text{reg-blk}} + V_{\text{sw-blk}}. \quad (\text{C3.A1})$$

Because the reagent blank ( $V_{\text{reg-blk}}$ ) determined for pure water is expected to be equal to that in seawater, the difference between blanks for seawater ( $V_{\text{tot-blk}}$ ) and for pure water gives the  $V_{\text{sw-blk}}$ .

Here,  $V_{\text{sw-blk}}$  was determined by following procedure. Seawater was collected in the calibrated volumetric glass without the pickling solution. Then 1 mL of the standard  $\text{KIO}_3$  solution,  $\text{H}_2\text{SO}_4$  solution, and reagent solution-II and I each were added in sequence into the glass. After that, the sample was titrated to the end-point by  $\text{Na}_2\text{S}_2\text{O}_3$  solution. Similarly, a glass contained 100 mL of DW added with 1 mL of the standard  $\text{KIO}_3$  solution,  $\text{H}_2\text{SO}_4$  solution, pickling reagent solution-II and I were titrated with  $\text{Na}_2\text{S}_2\text{O}_3$  solution. The difference of the titrant volume of the seawater and DW glasses gave  $V_{\text{sw-blk}}$ .

The seawater blank has been reported from 0.4 to  $0.8 \mu\text{mol kg}^{-1}$  in the previous study (Culberson *et al.*, 1991). Additionally, these errors are expected to be the same to all investigators and not to affect the comparison of results from different investigators (Culberson, 1994). However, the magnitude and variability of the seawater blank have not yet been documented. Understanding of the magnitude and variability is important to improve traceability and comparability in oxygen concentration. The determined seawater blanks are shown in Table C.3.A1.

Table C.3.A1. Results of seawater blank determinations.

Station: RF6533 40°-01'N/160°-20'E		Station: RF6571 40°-01'N/165°-01'E	
Depth	Blank	Depth	Blank
(m)	( $\mu\text{mol kg}^{-1}$ )	(m)	( $\mu\text{mol kg}^{-1}$ )
11	1.83	101	0.70
248	0.92	280	0.64
428	0.91	672	0.74
631	0.85	672	0.77
930	1.03	973	0.72
1669	1.21	1529	0.71
2270	0.84	2332	0.76
3077	1.10	3170	0.70
3828	1.12	4172	0.69
5327	1.69	4922	0.89
		5419	0.71
		5419	0.75

### Reference

- Culberson, A.H. (1994), Dissolved oxygen, in WHPO Pub. 91-1 Rev. 1, November 1994, Woods Hole, Mass., USA.
- Culberson, A.H., G. Knapp, M.C. Stalcup, R.T. Williams, and F. Zemlyak (1991), A comparison of methods for the determination of dissolved oxygen in seawater, WHPO Pub. 91-2, August 1991, Woods Hole, Mass., USA.
- Langdon, C. (2010), Determination of dissolved oxygen in seawater by Winkler titration using the amperometric technique, *IOCCP Report No.14, ICPO Pub. 134, 2010 ver.1*
- Murray, C. N., J. P. Riley and T. R. S. Wilson (1968), The solubility of oxygen in Winkler reagents used for the determination of dissolved oxygen. *Deep-Sea Res.* 15, 237–238.
- Swift, J. H. (2010), Reference-quality water sample data: Notes on acquisition, record keeping, and evaluation. *IOCCP Report No.14, ICPO Pub. 134, 2010 ver.1*.

#### 4. Nutrients

10 June 2020

##### (1) Personnel

###### Leg 1

Hiroyuki HATAKEYAMA (GEMD/JMA)

Koichi WADA (GEMD/JMA)

Kei KONDO (GEMD/JMA)

Rie SANAI (GEMD/JMA)

Masakazu TAKAMI (GEMD/JMA)

###### Leg 2

Hiroyuki HATAKEYAMA (GEMD/JMA)

Tomohiro UEHARA (GEMD/JMA)

Kei KONDO (GEMD/JMA)

Rie SANAI (GEMD/JMA)

Masakazu TAKAMI (GEMD/JMA)

##### (2) Station occupied

A total of 70 stations (Leg 1: 32, Leg 2: 38) were occupied for nutrients measurements. Station location and sampling layers of nutrients are shown in Figures C.4.1 and C.4.2.

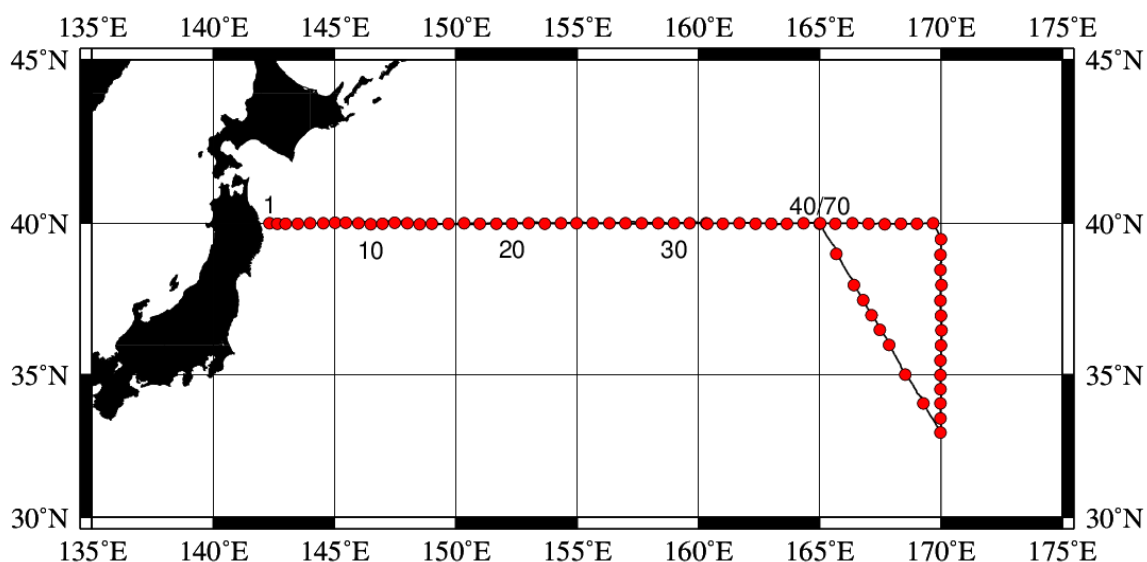


Figure C.4.1. Location of observation stations of nutrients.



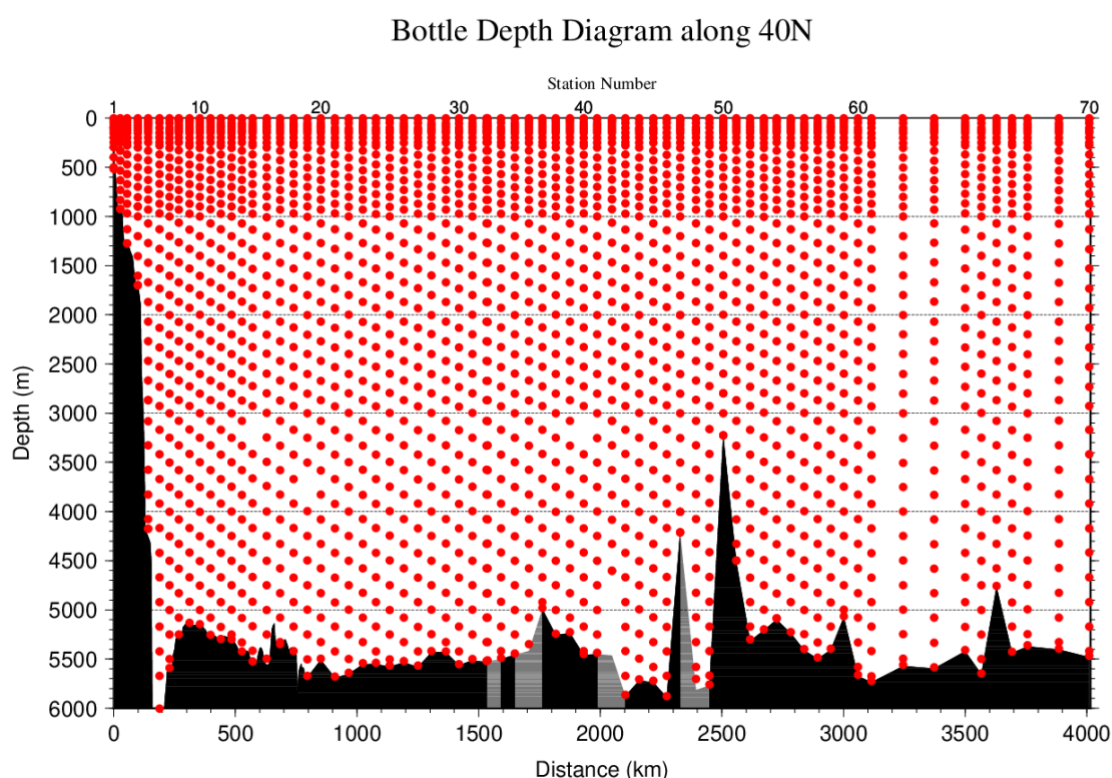


Figure C.4.2. Distance-depth distributions of sampling layers of nutrients.

### (3) Instrument

The nutrients analyses were carried out on a four-channel Auto Analyzer III (BL TEC K.K., Japan) for four nutrients nitrate+nitrite, nitrite, phosphate, and silicate.

### (4) Sampling and measurement

Methods of seawater sampling, measurement, and data processing of nutrient concentration were described in Appendixes A1, A2, and A3, respectively. The reagents for the measurement were prepared according to recipes shown in Appendix A4.

### (5) Nutrients standards

#### (5.1) Volumetric laboratory ware of in-house standards

All volumetric wares were gravimetrically calibrated. The weights obtained in the calibration weighing were corrected for the density of water and for air buoyancy. Polymethylpenten volumetric flasks were gravimetrically calibrated at the temperature of use within 4–6 °C. All pipettes have nominal calibration tolerances of 0.1 % or better. These were gravimetrically calibrated in order to verify and improve upon this nominal tolerance.

### (5.2) Reagents of standard

The batches of the reagents used for standards are listed in Table C.4.1.

Table C.4.1. List of reagents for the standards used in the cruise.

	Name	CAS No	Lot. No	Industries
<b>Nitrate</b>	Potassium nitrate 99.995 suprapur®	7757-79-1	B1452165	Merck KGaA
<b>Nitrite</b>	Sodium nitrite GR for analysis ACS, Reag. Ph Eur	7632-00-0	A1276649	Merck KGaA
<b>Phosphate</b>	Potassium dihydrogen phosphate anhydrous 99.995 suprapur®	7778-77-0	B1642608	Merck KGaA
<b>Silicate</b>	Silicon standard solution 1000 mg/l Si*	-	HC86788836	Merck KGaA

\* Traceable to NIST-SRM3150

### (5.3) Low nutrient seawater (LNSW)

Surface water with sufficiently low nutrient concentration was taken and filtered using 10 µm pore size membrane filter in our previous cruise. This water was stored in 15 liter flexible container with paper box.

### (5.4) In-house standard solutions

Nutrient concentrations for A, B and C standards were set as shown in Table C.4.2. A and B standards were prepared with deionized water (DW). C standard (full scale of working standard) was mixture of B-1 and B-2 standards, and was prepared with LNSW. C-1 standard, whose concentrations of nutrient were nearly zero, was prepared as LNSW slightly added with DW to be equal with mixing ratio of LNSW and DW in C standard. The C-2 to -5 standards were prepared with mixture of C-1 and C standards in stages as 1/4, 2/4, 3/4, and 4/4 (i.e., pure “C standard”) concentration for full scale, respectively. The actual concentration of nutrients in each standard was calculated based on the solution temperature and factors of volumetric laboratory wares calibrated prior to use. Nominal zero concentration of nutrient was determined in measurement of DW after refraction error correction. The calibration curves for each run were obtained using 5 levels of C-1 to -5 standards. These standard solutions were periodically renewed as shown in Table C.4.3.

Table C.4.2. Nominal concentrations of nutrients for A, B, and C standards at 20 °C. Unit is  $\mu\text{mol L}^{-1}$ .

	A	B	C
Nitrate	28761	575	46.0
Nitrite	12505	250	2.0
Phosphate	2202	44.0	3.52
Silicate	35819	2328	186

Table C.4.3. Schedule of renewal of in-house standards.

Standard	Renewal
A-1 std. ( $\text{NO}_3$ )	No renewal
A-2 std. ( $\text{NO}_2$ )	No renewal
A-3 std. ( $\text{PO}_4$ )	No renewal
A-4 std. (Si)	Commercial prepared solution
B-1 std. (mixture of A-1, A-3, and A-4 stds.)	Maximum 8 days
B-2 std. (diluted A-2 std.)	Maximum 15 days
C-std. (mixture of B-1 and B-2 stds.)	Every measurement
C-1 to -5 stds.	Every measurement

## (6) Certified reference material

Certified reference material for nutrients in seawater (hereafter CRM), which was prepared by the General Environmental Technos company (KANSO Technos, Japan), was used for every analysis at each hydrographic station. Use of CRMs for the analysis of seawater ensures stable comparability and uncertainty of data. CRMs used in the cruise are shown in Table C.4.4.

Table C.4.4. Certified concentration and uncertainty ( $k=2$ ) of CRMs. Unit is  $\mu\text{mol kg}^{-1}$ .

	Nitrate	Nitrite	Phosphate	Silicate
CRM-CK	0.020±0.031*	0.011±0.008*	0.048±0.012*	0.730±0.080
CRM-CJ	16.2±0.2	0.031±0.007	1.19±0.02	38.5±0.4
CRM-CB	35.79±0.27	0.116±0.0057	2.520±0.022	109.2±0.62
CRM-BZ	43.35±0.33	0.215±0.011	3.056±0.033	161.0±0.93

\* Reference value because concentration is under limit of quantitation

The CRMs were analyzed every run but were newly opened every two runs. Although this usage of CRM might be less common, we have confirmed a stability of the opened CRM bottles to be tolerance in our observation. The CRM bottles were stored at a laboratory in the ship, where the temperature was maintained at around 25 °C.

It is noted that nutrient data in our report are calibrated not on CRM but on in-house standard solutions. Therefore, to calculate data based on CRM, it is necessary that values of nutrient concentration in our report are correlated with CRM values measured in the same analysis run. The result of CRM measurements is attached as 49UP20190612\_40N\_nut\_CRM\_measurement.csv.

## (7) Quality Control

### (7.1) Replicate and duplicate analyses

We took replicate (pair of water samples taken from a single Niskin bottle) and duplicate (pair of water samples taken from different Niskin bottles closed at the same depth) samples of nutrients throughout the cruise. Table C.4.5 summarizes the results of the analyses. Figures C.4.3–C.4.5 show details of the results. The calculation of the standard deviation from the difference of sets of samples was based on a procedure (SOP 23) in DOE (1994).

Table C.4.5. Average and standard deviation of difference of replicate and duplicate measurements throughout the cruise. Unit is  $\mu\text{mol kg}^{-1}$ .

Samples	Nitrate+nitrite	Phosphate	Silicate
Replicate	0.032±0.033 (N=273)	0.002±0.002 (N=273)	0.055±0.055 (N=273)

Duplicate  $0.071 \pm 0.069$  (N=25)  $0.004 \pm 0.004$  (N=25)  $0.150 \pm 0.137$  (N=25)

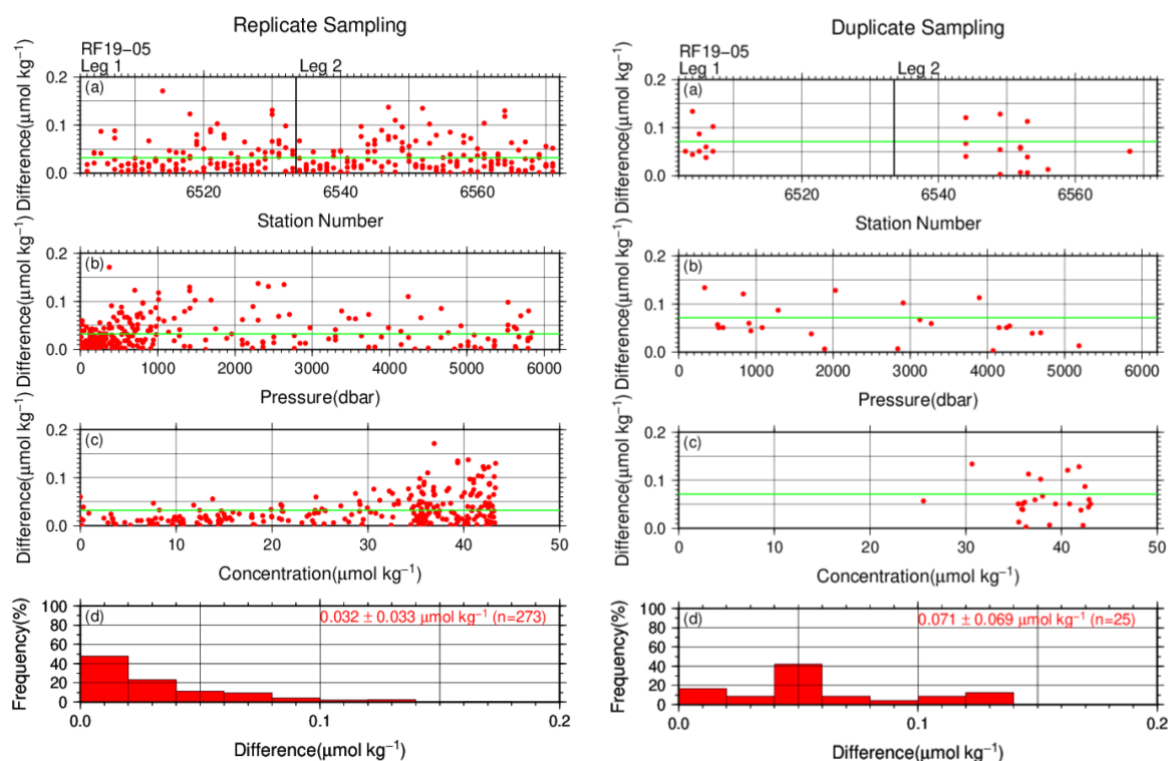


Figure C.4.3. Results of (left) replicate and (right) duplicate measurements of nitrate+nitrite throughout the cruise versus (a) station number, (b) sampling pressure, (c) concentration, and (d) histogram of the measurements. Green lines indicates the mean of the differences of concentrations based on replicate/duplicate analyses.

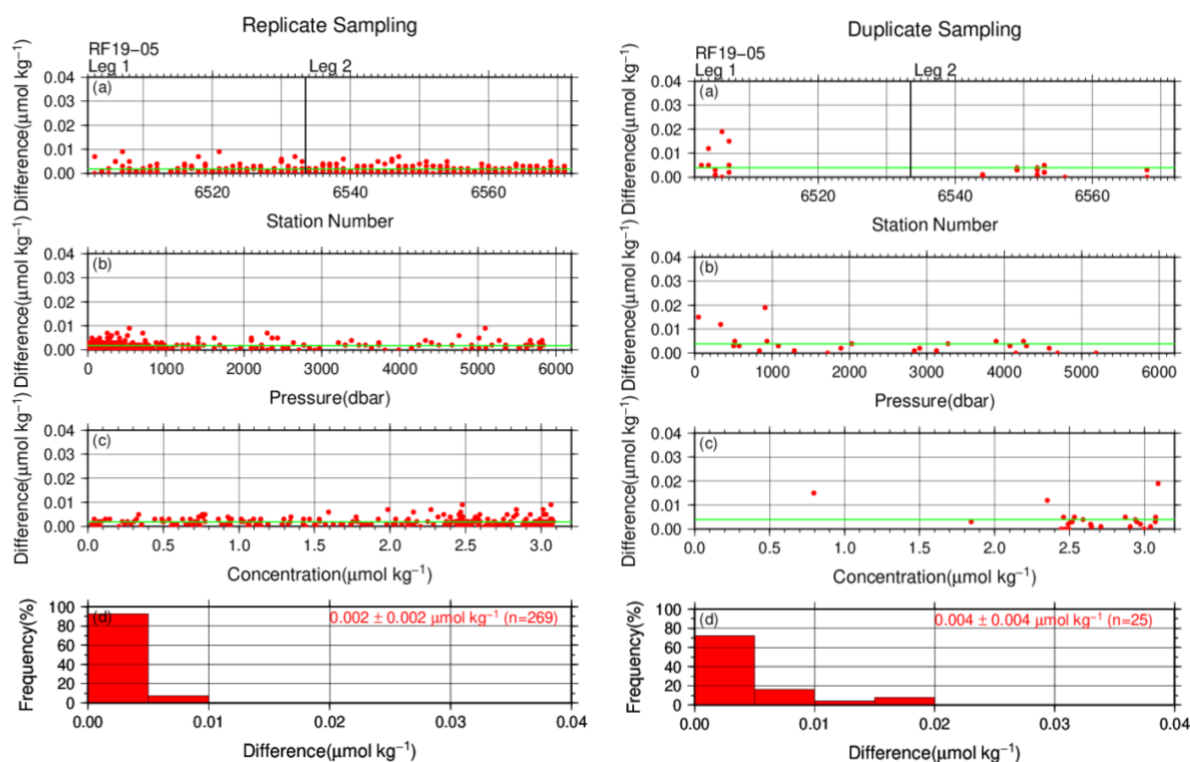


Figure C.4.4. Same as Figure C.4.3, but for phosphate.

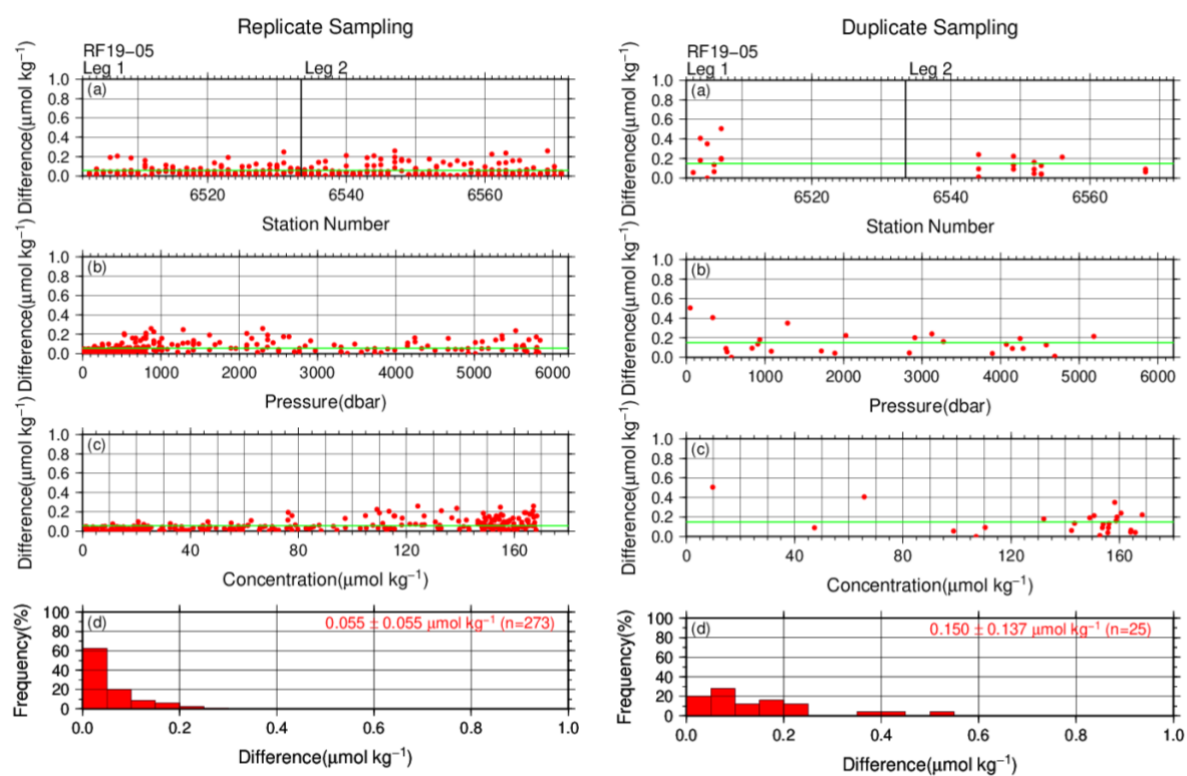


Figure C.4.5. Same as Figure C.4.3, but for silicate.

## (7.2) Measurement of CRMs

Table C.4.6 summarizes the CRM measurements during the cruise. The CRM concentrations were assigned with in-house standard solutions. Figures C.4.6–C.4.9 show the measured concentrations of CRM-BZ throughout the cruise.

Table C.4.6. Summary of (upper) mean concentration and its standard deviation (unit:  $\mu\text{mol kg}^{-1}$ ), (middle) coefficient of variation (%), and (lower) total number of CRMs measurements throughout the cruise.

	Nitrate+nitrite	Nitrite	Phosphate	Silicate
	$0.061 \pm 0.022$	$0.035 \pm 0.002$	$0.056 \pm 0.003$	$0.84 \pm 0.05$
CRM-CK	36.14 %	4.70 %	5.16 %	6.37 %
	(N=105)	(N=105)	(N=103)	(N=105)
	$16.20 \pm 0.04$	$0.045 \pm 0.001$	$1.19 \pm 0.005$	$38.88 \pm 0.09$
CRM-CJ	0.24 %	2.94 %	0.41 %	0.22 %
	(N=105)	(N=104)	(N=103)	(N=105)
	$35.93 \pm 0.07$	$0.133 \pm 0.002$	$2.53 \pm 0.004$	$110.72 \pm 0.17$
CRM-CB	0.20 %	1.20 %	0.17 %	0.15 %
	(N=105)	(N=105)	(N=103)	(N=105)
	$43.63 \pm 0.09$	$0.231 \pm 0.007$	$3.06 \pm 0.006$	$162.92 \pm 0.23$
CRM-BZ	0.21 %	2.85 %	0.21 %	0.14 %
	(N=105)	(N=105)	(N=103)	(N=105)

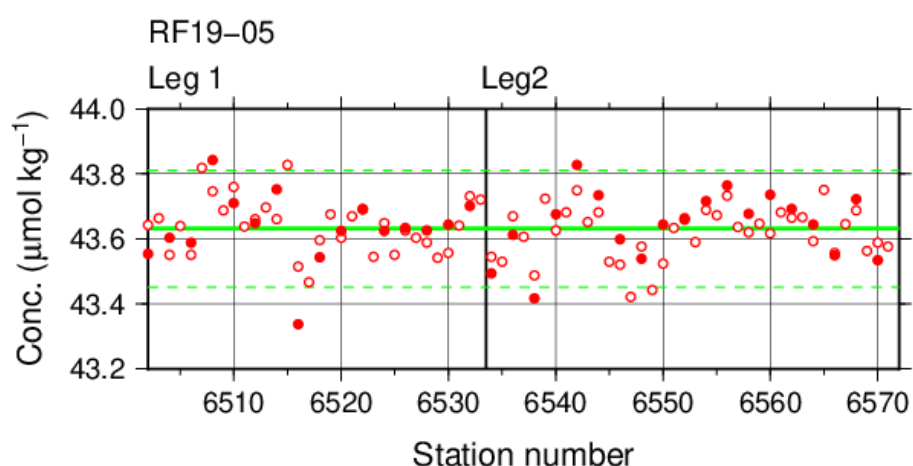


Figure C.4.6. Time-series of measured concentration of nitrate+nitrite of CRM-BZ throughout the cruise. Closed and open circles indicate the newly and previously opened bottle, respectively. Thick and dashed lines denote the mean and the mean  $\pm$  twice the standard deviations of the measurements throughout the cruise, respectively.

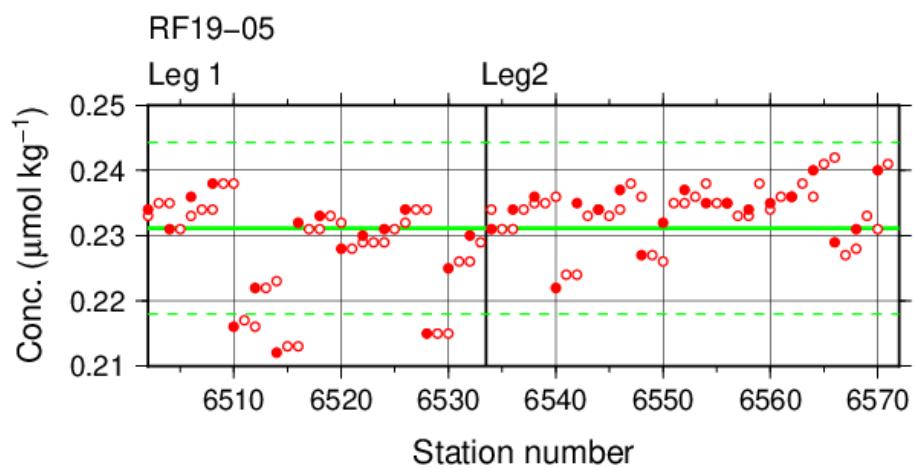


Figure C.4.7. Same as Figure C.4.6, but for nitrite.

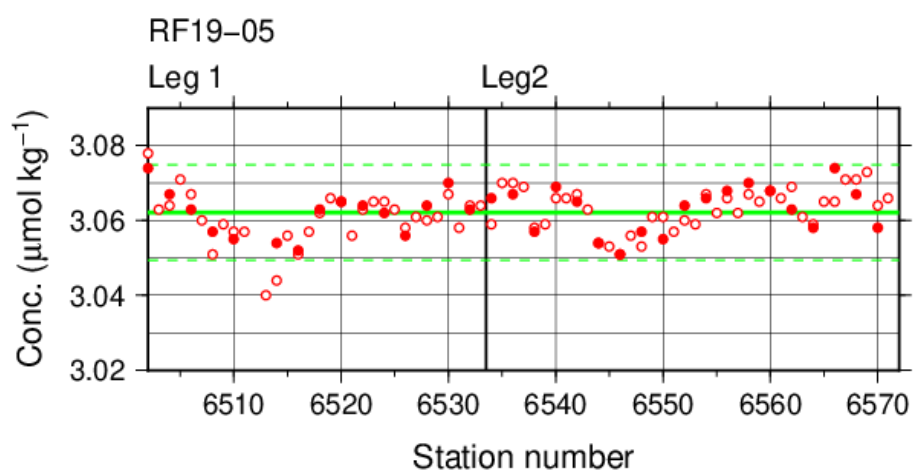


Figure C.4.8. Same as Figure C.4.6, but for phosphate.

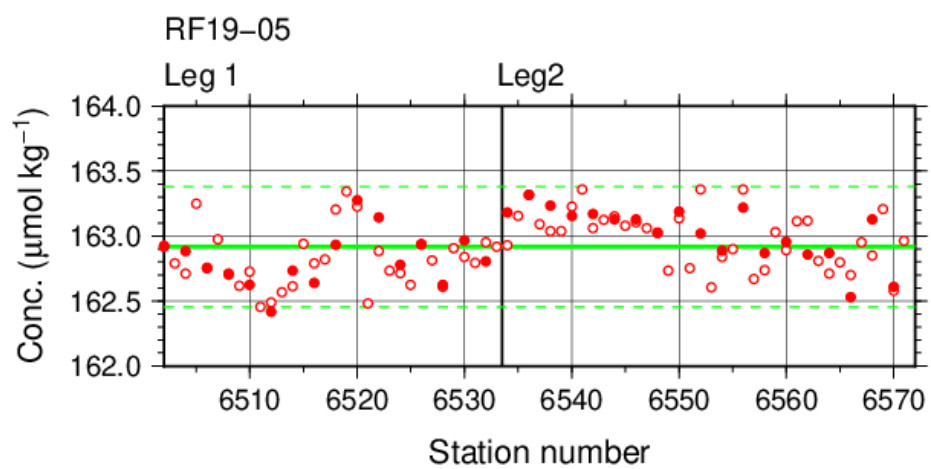


Figure C.4.9. Same as Figure C.4.6, but for silicate.



### (7.3) Precision of analysis in a run

To monitor the precision of the analyses, the same samples were repeatedly measured in a sample array during a run. For this purpose, a C-5 standard solution was randomly inserted in every 2–10 samples as a “check standard” (the number of standards was about 8–9) in the run. The precision was estimated in terms of the coefficient of variation of the measurements. Table C.4.7 summarizes the results. The time series are shown in Figures C.4.10–C.4.13.

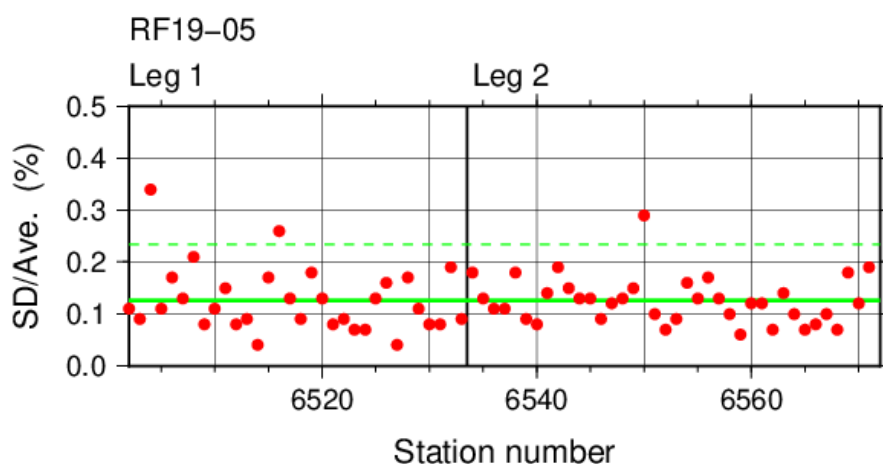


Figure C.4.10. Time-series of the coefficients of variation of “check standard” measurements of nitrate+nitrite throughout the cruise. Thick and dashed lines denote the mean and the mean  $\pm$  twice the standard deviations of the measurements throughout the cruise, respectively.

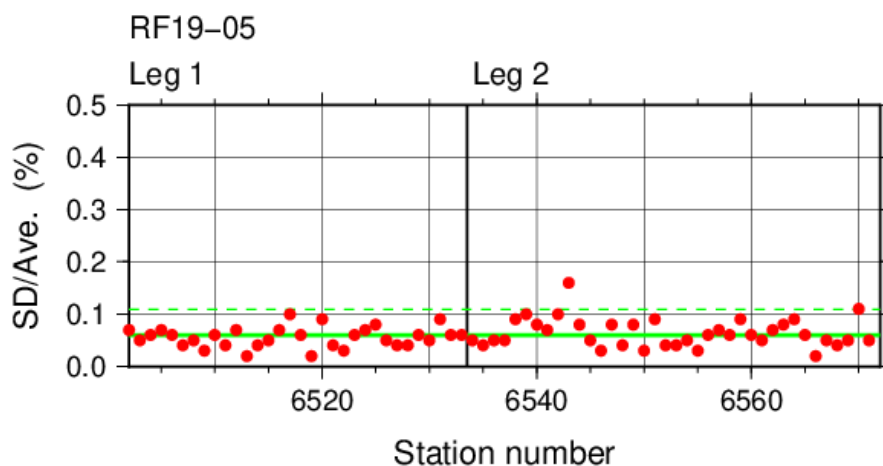


Figure C.4.11. Same as Figure C.4.10, but for nitrite.

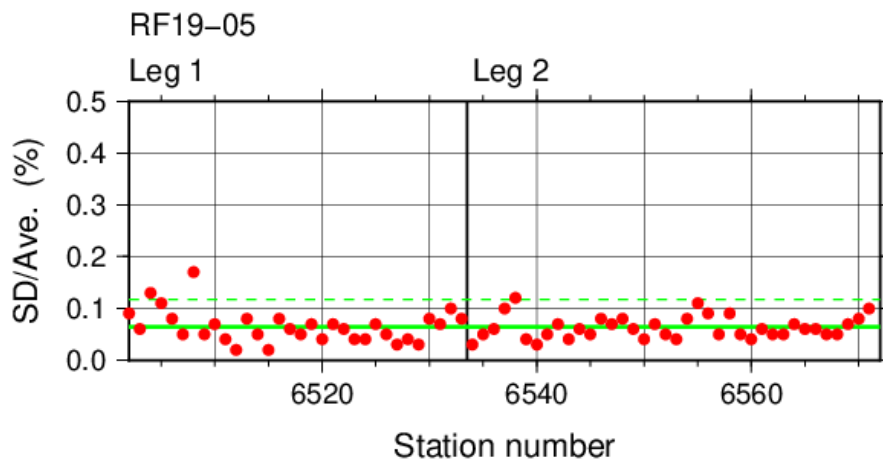


Figure C.4.12. Same as Figure C.4.10, but for phosphate.

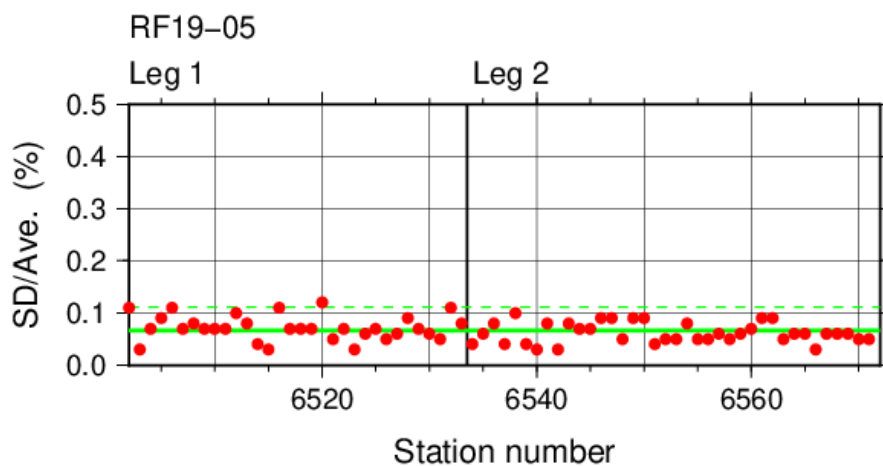


Figure C.4.13. Same as Figure C.4.10, but for silicate.

Table C.4.7. Summary of precisions of nutrient assays during the cruise.

	Nitrate+nitrite	Nitrite	Phosphate	Silicate
Median	0.12 %	0.06 %	0.06 %	0.07 %
Mean	0.13 %	0.06 %	0.06 %	0.07 %
Minimum	0.04 %	0.02 %	0.02 %	0.03 %
Maximum	0.34 %	0.16 %	0.17 %	0.12 %
Number	70	70	70	70

#### (7.4) Carryover

Carryover coefficients were determined during each analytical run. The C-5 standard (high standard) was followed by two C-1 standards (low standards). Figures C.4.14–17 show the time series of the carryover coefficients.

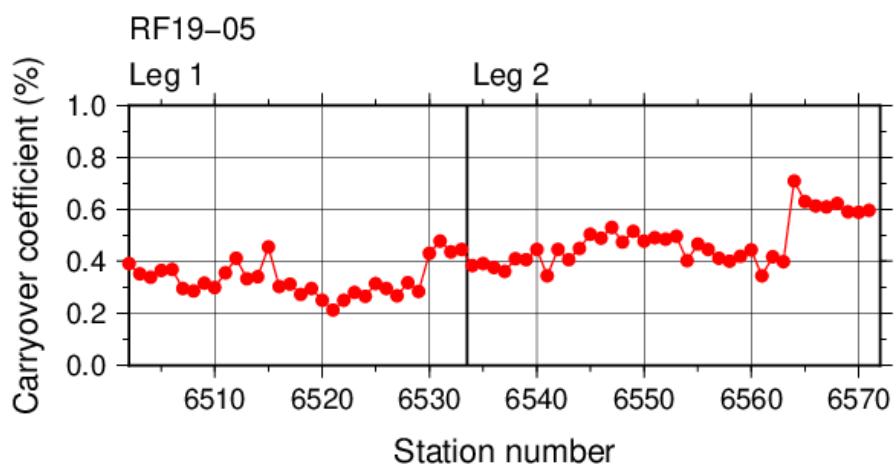


Figure C.4.14. Time-series of carryover coefficients in measurement of nitrate+nitrite throughout the cruise.

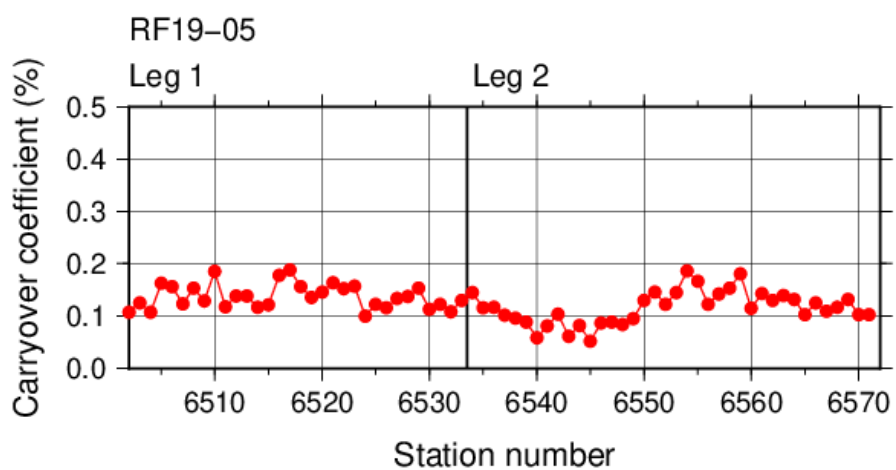


Figure C.4.15. Same as Figure C.4.14, but for nitrite.

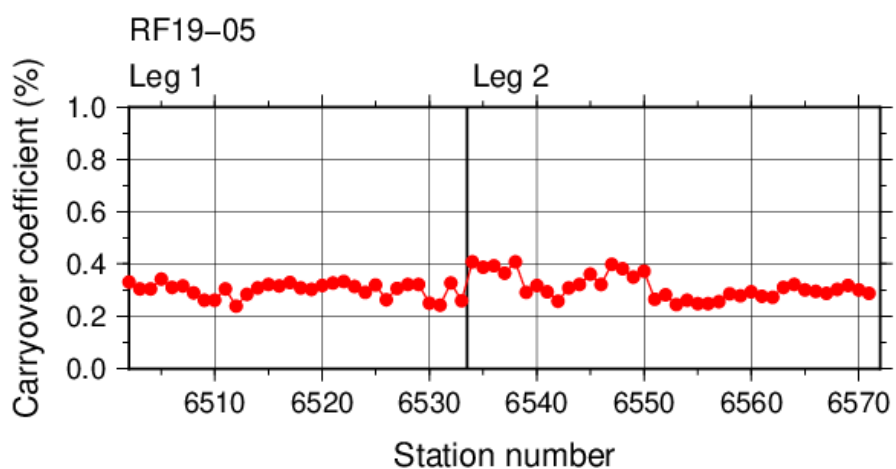


Figure C.4.16. Same as Figure C.4.14, but for phosphate.

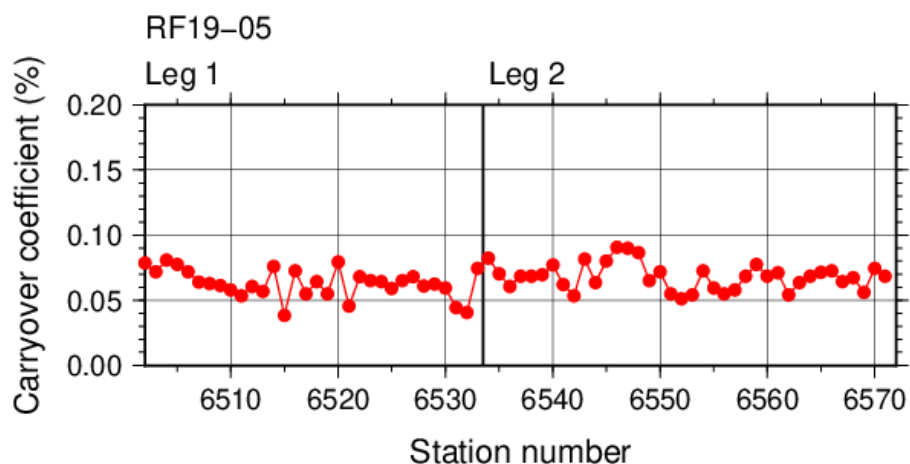


Figure C.4.17. Same as Figure C.4.14, but for silicate.

### (7.5) Limit of detection/quantitation of measurement

Limit of detection (LOD) and quantitation (LOQ) of nutrient measurement were estimated from standard deviation ( $\sigma$ ) of repeated measurements of nutrients concentration in C-1 standard as  $3\sigma$  and  $10\sigma$ , respectively. Summary of LOD and LOQ are shown in Table C.4.8.

Table C.4.8. Limit of detection (LOD) and quantitation (LOQ) of nutrient measurement in the cruise. Unit is  $\mu\text{mol kg}^{-1}$ .

	LOD	LOQ
Nitrate+nitrite	0.042	0.139
Nitrite	0.004	0.015
Phosphate	0.007	0.023
Silicate	0.073	0.243

### (7.6) Quality control flag assignment

A quality flag value was assigned to nutriment measurements as shown in Table C.4.9, using the code defined in IOCCP Report No.14 (Swift, 2010).

Table C.4.9. Summary of assigned quality control flags.

Flag	Definition	Nitrate+nitrite	Nitrite	Phosphate	Silicate
2	Good	2236	2238	2201	2237
3	Questionable	2	2	41	0
4	Bad (Faulty)	4	3	4	5
5	Not reported	0	0	0	0
6	Replicate measurements	273	272	269	273
Total number of samples		2515	2515	2515	2515

## (8) Uncertainty

### (8.1) Uncertainty associated with concentration level: $U_c$

Generally, an uncertainty of nutrient measurement is expressed as a function of its concentration level which reflects that some components of uncertainty are relatively large in low concentration. Empirically, the uncertainty associated with concentrations level ( $U_c$ ) can be expressed as follows;

$$U_c = \frac{C_x}{C_x} \quad (C4.1)$$

where  $C_x$  is the concentration of sample for parameter X.

Using the coefficients of variation of the CRM measurements throughout the cruise, uncertainty associated with concentrations of nitrate+nitrite, phosphate, and silicate were determined as follows:

$$U_c = \frac{C_{no3}}{C_{no3}} \quad (C4.2)$$

$$U_c = \frac{C_{po4}}{C_{po4}} \quad (C4.3)$$

$$U_c = \frac{C_{sil}}{C_{sil}} \quad (C4.4)$$

where  $C_{no3}$ ,  $C_{po4}$ , and  $C_{sil}$  represent concentrations of nitrate+nitrite, phosphate, and silicate, respectively, in  $\mu\text{mol kg}^{-1}$ . Figures C.4.18–C.4.20 show the calculated uncertainty graphically.

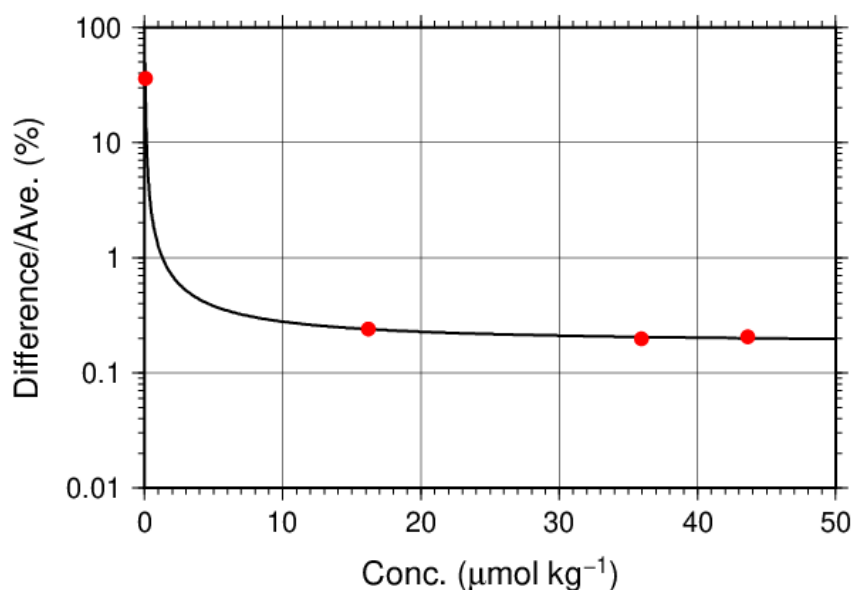


Figure C.4.18. Uncertainty of nitrate+nitrite associated with concentrations.

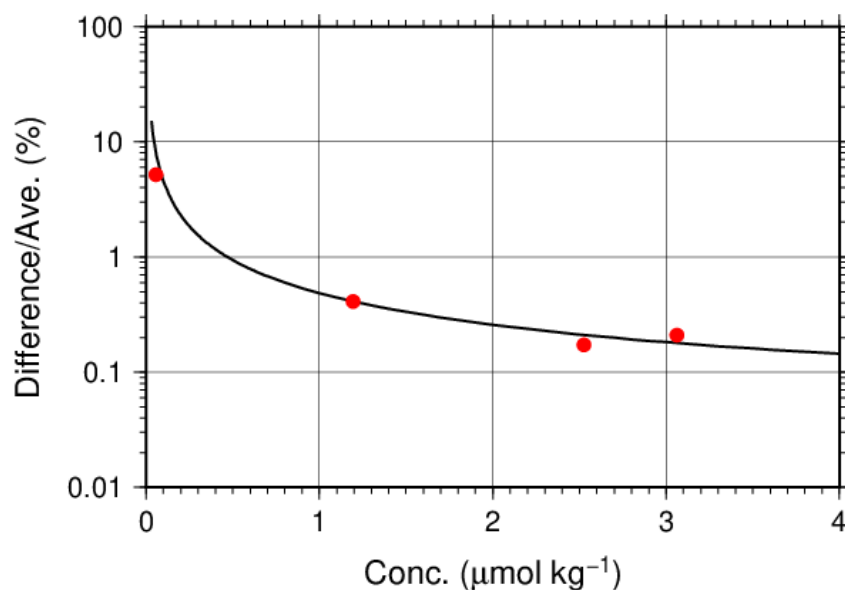


Figure C.4.19. Same as Figure C.4.18, but for phosphate.

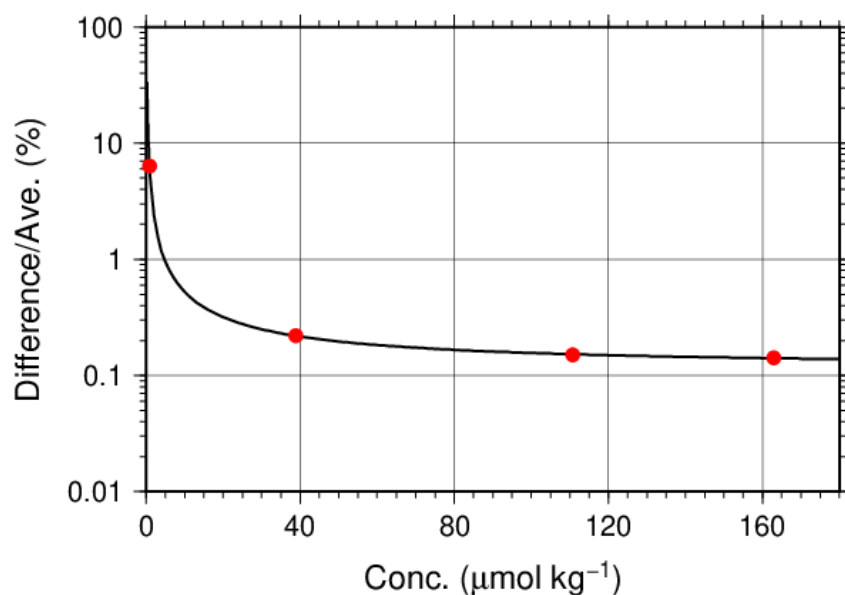


Figure C.4.20. Same as Figure C.4.18, but for silicate.

### (8.2) Uncertainty of analysis between runs: $U_s$

Uncertainty of analysis among runs ( $U_s$ ) was evaluated based on the coefficient of variation of measured concentrations of CRM-BZ with the highest concentration among the CRM lots throughout the cruise, as shown in subsection (7.2). The reason for using the CRM lot to state  $U_s$  is to exclude the effect of uncertainty associated with lower concentration described previously. As is clear from the definition of  $U_c$ ,  $U_s$  is equal to  $U_c$  at nutrients concentrations of the lot. It is important to note that  $U_s$  includes all of uncertainties during the measurements

throughout stations, namely uncertainties of concentrations of in-house standard solutions prepared for each run, uncertainties of slopes and intercepts of the calibration curve in each run, precision of measurement in a run ( $U_a$ ), and between-bottle homogeneity of the CRM.

### **(8.3) Uncertainty of analysis in a run: $U_a$**

Uncertainty of analysis in a run ( $U_a$ ) was evaluated based on the coefficient of variation of repeated measurements of the “check standard” solution, as shown in subsection (7.3). The  $U_a$  reflects the conditions associated with chemistry of colorimetric measurement of nutrients, and stability of electronic and optical parts of the instrument throughout a run. Under a well-controlled condition of the measurements,  $U_a$  might show Poisson distribution with a mean as shown in Figures C.4.10–C.4.13 and Table C.4.7 and treated as a precision of measurement.  $U_a$  is a part of  $U_c$  at the concentration as stated in a previous section for  $U_c$ .

However,  $U_a$  may show larger value which was not expected from Poisson distribution of  $U_a$  due to the malfunction of the instruments, larger ambient temperature change, human errors in handling samples and chemistries, and contaminations of samples in a run. In the cruise, we observed that  $U_a$  of our measurement was usually small and well-controlled in most runs as shown in Figures C.4.10–C.4.13 and Table C.4.7. However, in a few runs,  $U_a$  showed high values which were over the mean  $\pm$  twice the standard deviations of  $U_a$ , suggesting that the measurement system might have some problems.

### **(8.4) Uncertainty of CRM concentration: $U_r$**

In the certification of CRM, the uncertainty of CRM concentrations ( $U_r$ ) was stated by the manufacturer (Table C.4.4) as expanded uncertainty at  $k=2$ . This expanded uncertainty reflects the uncertainty of the Japan Calibration Service System (JCSS) solutions, characterization in assignment, between-bottle homogeneity, and long term stability. We have ensured comparability between cruises by ensuring that at least two lots of CRMs overlap between cruises. In comparison of nutrient concentrations between cruises using KANSO CRMs in an organization, it was not necessary to include  $U_r$  in the conclusive uncertainty of concentration of measured samples because comparability of measurements was ensured in an organization as stated previously.

### **(8.5) Conclusive uncertainty of nutrient measurements of samples: $U$**

To determine the conclusive uncertainty of nutrient measurements of samples ( $U$ ), we use two functions depending on  $U_a$  value acquired at each run as follows:

When  $U_a$  was small and measurement was well-controlled condition, the conclusive uncertainty of nutrient measurements of samples,  $U$ , might be as below:

$$\cdot \quad (C4.5)$$

When  $U_a$  was relative large and the measurement might have some problems, the conclusive uncertainty of nutrient measurements of samples,  $U$ , can be expanded as below:

$$\cdot \quad (C4.6)$$

When  $U_a$  was relative large and the measurement might have some problems, the equation of  $U$  is defined as to include  $U_a$  to evaluate  $U$ , although  $U_a$  partly overlaps with  $U_c$ . It means that the equation overestimates the conclusive uncertainty of samples. On the other hand, for low concentration there is a possibility that the equation not only overestimates but also underestimates the conclusive uncertainty because the functional shape of  $U_c$  in lower concentration might not be the same and cannot be verified. However, we believe that the applying the above function might be better way to evaluate the conclusive uncertainty of nutrient measurements of samples because we can do realistic evaluation of uncertainties of nutrient concentrations of samples which were obtained under relatively unstable conditions, larger  $U_a$  as well as the evaluation of them under normal and good conditions of measurements of nutrients.



## **Appendix**

### **A1. Seawater sampling**

Seawater samples were collected from 10-liters Niskin bottle attached CTD-system and a stainless steel bucket for the surface. Samples were drawn into 10 mL polymethylpenten vials using sample drawing tubes. The vials were rinsed three times before water filling and were capped immediately after the drawing.

No transfer was made and the vials were set on an auto sampler tray directly. Samples were analyzed immediately after collection.

### **A2. Measurement**

#### **(A2.1) General**

Auto Analyzer III is based on Continuous Flow Analysis method and consists of sampler, pump, manifolds, and colorimeters. As a baseline, we used artificial seawater (ASW).

#### **(A2.2) Nitrate+nitrite and nitrite**

Nitrate+nitrite and nitrite were analyzed according to the modification method of Armstrong (1967). The sample nitrate was reduced to nitrite in a glass tube which was filled with granular cadmium coated with copper. The sample stream with its equivalent nitrite was treated with an acidic, sulfanilamide reagent and the nitrite forms nitrous acid which reacts with the sulfanilamide to produce a diazonium ion. N-1-naphthylethylene-diamine was added to the sample stream then coupled with the diazonium ion to produce a red, azo dye. With reduction of the nitrate to nitrite, sum of nitrate and nitrite were measured; without reduction, only nitrite was measured. Thus, for the nitrite analysis, no reduction was performed and the alkaline buffer was not necessary. The flow diagrams for each parameter are shown in Figures C.4.A1 and C.4.A2. If the reduction efficiency of the cadmium column became lower than 95 %, the column was replaced.

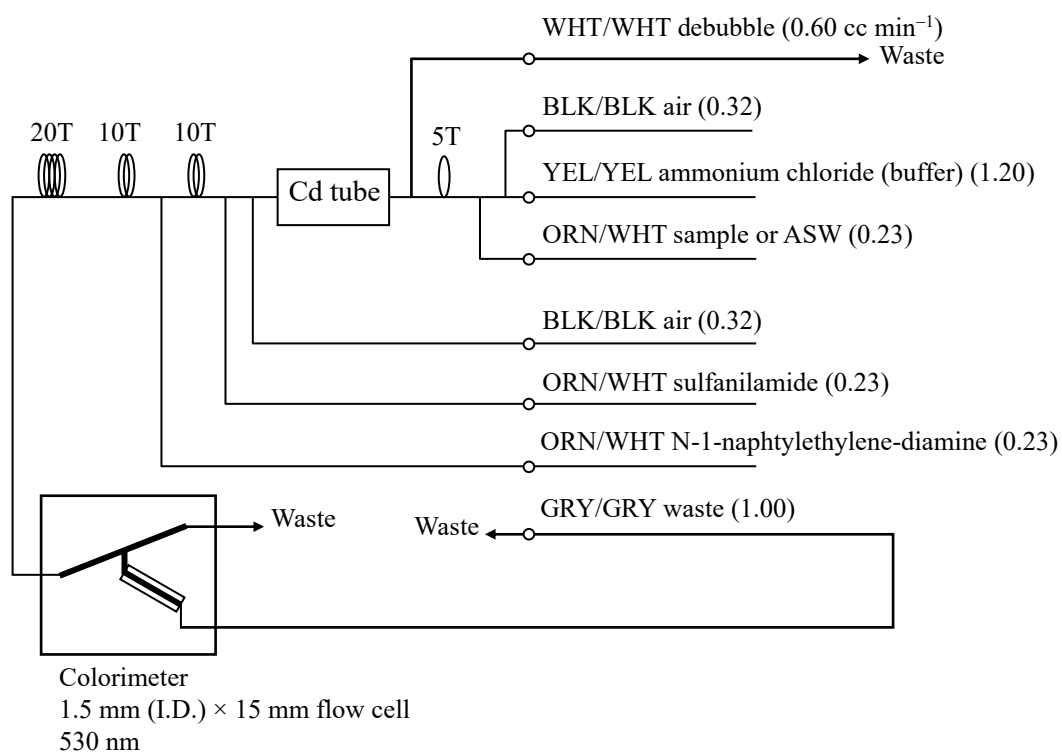


Figure C.4.A1. Nitrate+nitrite (ch. 1) flow diagram.

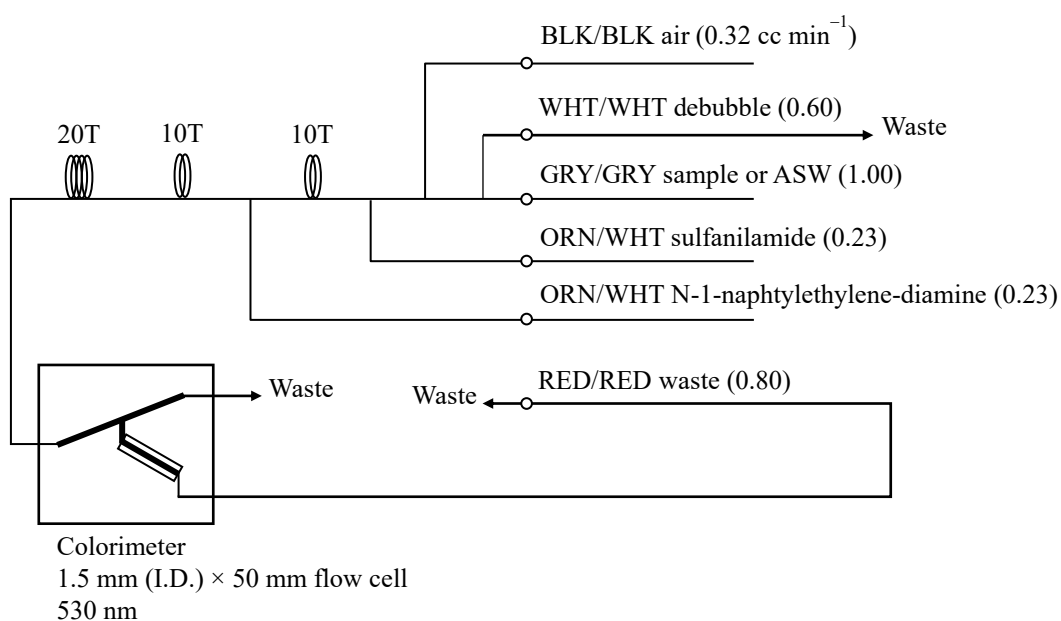


Figure C.4.A2. Nitrite (ch. 2) flow diagram.

### (A2.3) Phosphate

The phosphate analysis was a modification of the procedure of Murphy and Riley (1962). Molybdic acid was added to the seawater sample to form phosphomolybdic acid which was in turn reduced to phosphomolybdous acid using L-ascorbic acid as the reductant. The flow diagram for phosphate is shown in Figure C.4.A3.

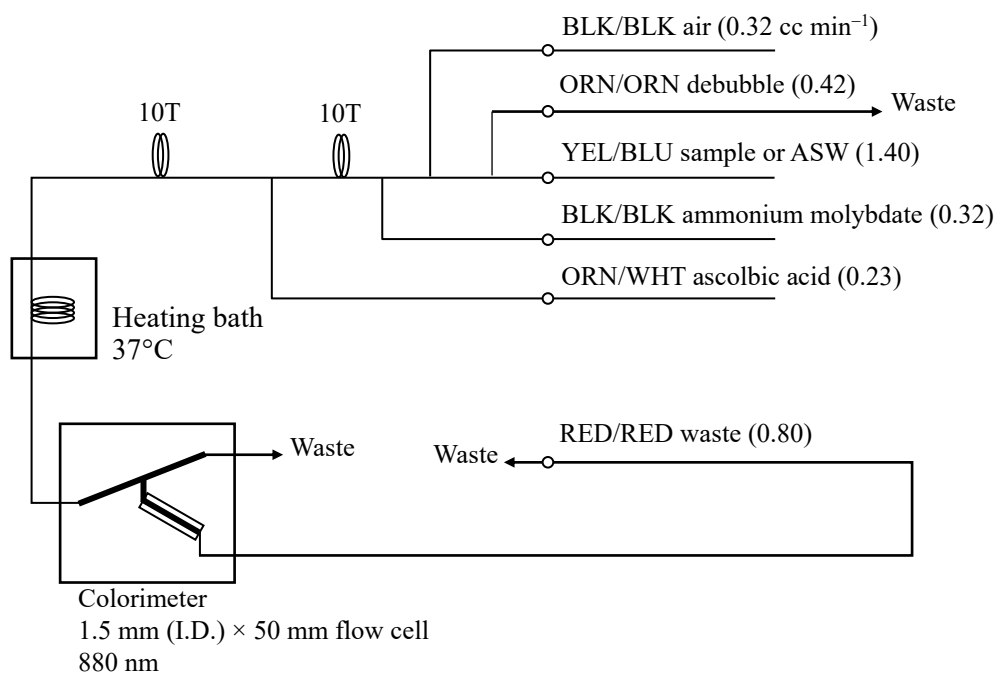


Figure C.4.A3. Phosphate (ch. 3) flow diagram.

#### (A2.4) Silicate

The silicate was analyzed according to the modification method of Grasshoff *et al.* (1983), wherein silicomolybdic acid was first formed from the silicate in the sample and added molybdic acid, then the silicomolybdic acid was reduced to silicomolybdous acid, or "molybdenum blue," using L-ascorbic acid as the reductant. The flow diagram for silicate is shown in Figure C.4.A4.

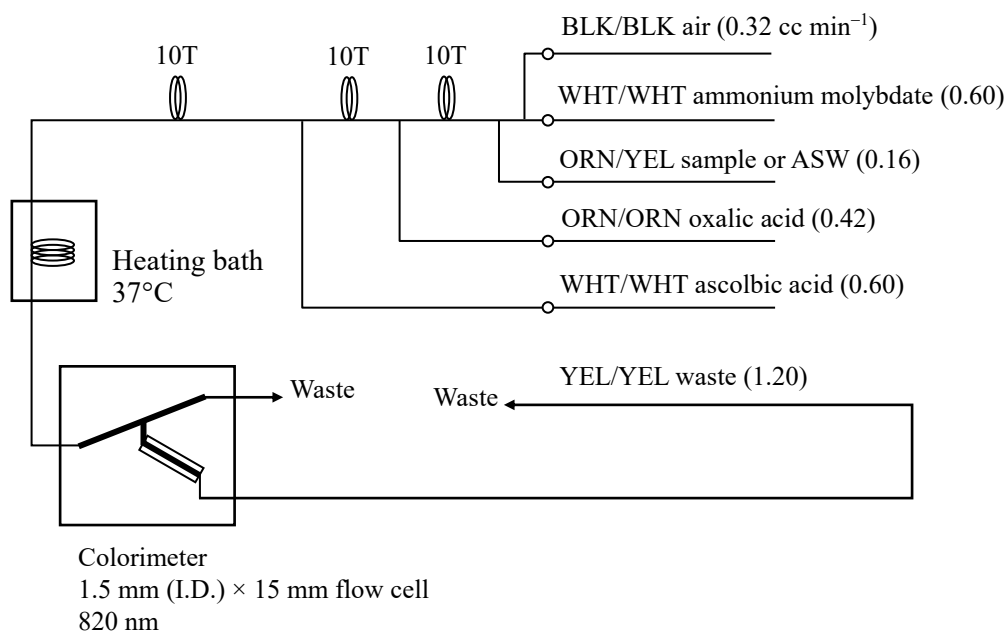


Figure C.4.A4. Silicate (ch. 4) flow diagram.

#### A3. Data processing

Raw data from Auto Analyzer III were recorded at 1-second interval and were treated as follows;

- Check the shape of each peak and position of peak values taken, and then change the positions of peak values taken if necessary.
- Baseline correction was done basically using liner regression.
- Reagent blank correction was done basically using liner regression.
- Carryover correction was applied to peak heights of each sample.
- Sensitivity correction was applied to peak heights of each sample.
- Refraction error correction was applied to peak heights of each seawater sample.
- Calibration curves to get nutrients concentration were assumed quadratic expression.
- Concentrations were converted from  $\mu\text{mol L}^{-1}$  to  $\mu\text{mol kg}^{-1}$  using seawater density.

#### A4. Reagents recipes

##### (A4.1) Nitrate+nitrite

Ammonium chloride (buffer),  $0.7 \mu\text{mol L}^{-1}$  (0.04 % w/v);

Dissolve 190 g ammonium chloride,  $\text{NH}_4\text{Cl}$ , in ca. 5 L of DW, add about 5 mL ammonia(aq) to adjust pH of 8.2–8.5.

Sulfanilamide,  $0.06 \mu\text{mol L}^{-1}$  (1 % w/v);

Dissolve 5 g sulfanilamide,  $4\text{-NH}_2\text{C}_6\text{H}_4\text{SO}_3\text{H}$ , in 430 mL DW, add 70 mL concentrated HCl. After mixing, add 1 mL Brij-35 (22 % w/w).

N-1-naphtylethylene-diamine dihydrochloride (NEDA),  $0.004 \mu\text{mol L}^{-1}$  (0.1 % w/v);

Dissolve 0.5 g NEDA,  $\text{C}_{10}\text{H}_7\text{NH}_2\text{CH}_2\text{CH}_2\text{NH}_2 \cdot 2\text{HCl}$ , in 500 mL DW.

#### (A4.2) Nitrite

Sulfanilamide,  $0.06 \mu\text{mol L}^{-1}$  (1 % w/v); Shared from nitrate reagent.

N-1-naphtylethylene-diamine dihydrochloride (NEDA),  $0.004 \mu\text{mol L}^{-1}$  (0.1 % w/v); Shared from nitrate reagent.

#### (A4.3) Phosphate

Ammonium molybdate,  $0.005 \mu\text{mol L}^{-1}$  (0.6 % w/v);

Dissolve 3 g ammonium molybdate(VI) tetrahydrate,  $(\text{NH}_4)_6\text{Mo}_7\text{O}_{24} \cdot 4\text{H}_2\text{O}$ , and 0.05 g potassium antimonyl tartrate,  $\text{C}_8\text{H}_4\text{K}_2\text{O}_{12}\text{Sb}_2 \cdot 3\text{H}_2\text{O}$ , in 400 mL DW and add 40 mL concentrated  $\text{H}_2\text{SO}_4$ . After mixing, dilute the solution with DW to final volume of 500 mL and add 2 mL sodium dodecyl sulfate (15 % solution in water).

L(+)-ascorbic acid,  $0.08 \mu\text{mol L}^{-1}$  (1.5 % w/v);

Dissolve 4.5 g L(+)-ascorbic acid,  $\text{C}_6\text{H}_8\text{O}_6$ , in 300 mL DW. After mixing, add 10 mL acetone. This reagent was freshly prepared before every measurement.

#### (A4.4) Silicate

Ammonium molybdate,  $0.005 \mu\text{mol L}^{-1}$  (0.6 % w/v);

Dissolve 3 g ammonium molybdate(VI) tetrahydrate,  $(\text{NH}_4)_6\text{Mo}_7\text{O}_{24} \cdot 4\text{H}_2\text{O}$ , in 500 mL DW and added concentrated 2 mL  $\text{H}_2\text{SO}_4$ . After mixing, add 2 mL sodium dodecyl sulfate (15 % solution in water).

Oxalic acid,  $0.4 \mu\text{mol L}^{-1}$  (5 % w/v);

Dissolve 25 g oxalic acid dihydrate,  $(\text{COOH})_2 \cdot 2\text{H}_2\text{O}$ , in 500 mL DW.

L(+)-ascorbic acid,  $0.08 \mu\text{mol L}^{-1}$  (1.5 % w/v); Shared from phosphate reagent.

#### (A4.5) Baseline

Artificial seawater (salinity is ~34.7);

Dissolve 160.6 g sodium chloride,  $\text{NaCl}$ , 35.6 g magnesium sulfate heptahydrate,  $\text{MgSO}_4 \cdot 7\text{H}_2\text{O}$ , and 0.84 g sodium hydrogen carbonate,  $\text{NaHCO}_3$ , in 5 L DW.

## ***References***

- Armstrong, F. A. J., C. R. Stearns and J. D. H. Strickland (1967), The measurement of upwelling and subsequent biological processes by means of the Technicon TM Autoanalyzer TM and associated equipment, *Deep-Sea Res.*, 14(3), 381–389.
- Grasshoff, K., Ehrhardt, M., Kremling K. et al. (1983), Methods of seawater analysis. 2nd rev, *Weinheim: Verlag Chemie, Germany, West.*
- Murphy, J. and Riley, J.P. (1962), *Analytica chimica Acta*, 27, 31-36.
- Swift, J. H. (2010), Reference-quality water sample data: Notes on acquisition, record keeping, and evaluation. *IOCCP Report No.14, ICPO Pub. 134, 2010 ver.1.*

## 5. *Phytopigments (chlorophyll-*a* and phaeopigment)*

8 June 2020

### (1) Personnel

#### Leg 1

Hiroyuki HATAKEYAMA (GEMD/JMA)

Koichi WADA (GEMD/JMA)

Kei KONDO (GEMD/JMA)

Rie SANAI (GEMD/JMA)

Masakazu TAKAMI (GEMD/JMA)

#### Leg 2

Hiroyuki HATAKEYAMA (GEMD/JMA)

Tomohiro UEHARA (GEMD/JMA)

Kei KONDO (GEMD/JMA)

Rie SANAI (GEMD/JMA)

Masakazu TAKAMI (GEMD/JMA)

### (2) Station occupied

A total of 40 stations (Leg 1: 18, Leg 2: 22) were occupied for phytopigment measurements. Station location and sampling layers of phytopigment are shown in Figures C.5.1 and C.5.2.

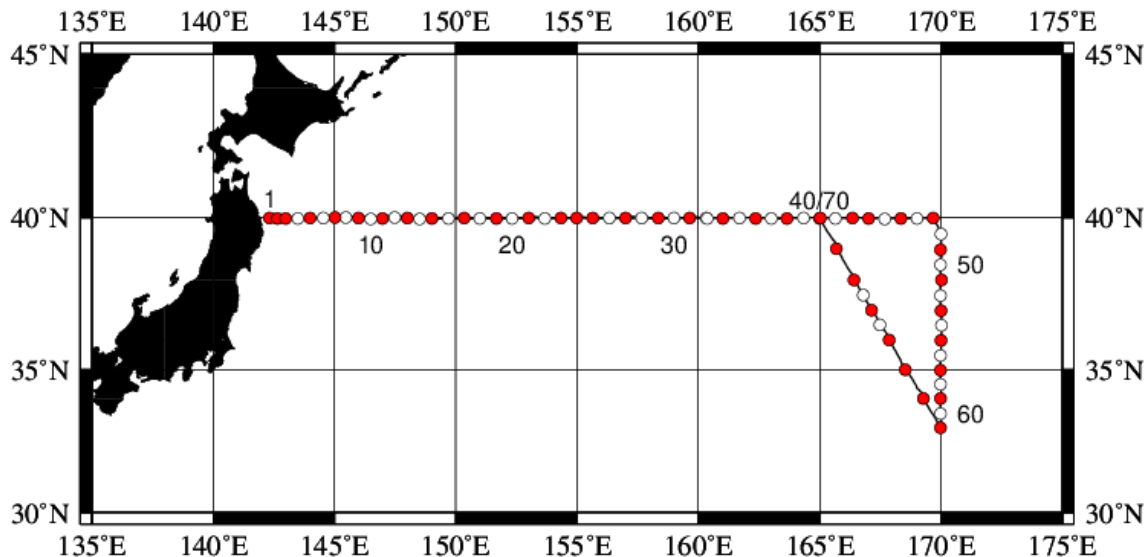


Figure C.5.1. Location of observation stations of chlorophyll-*a*. Closed and open circles indicate sampling and no-sampling stations, respectively.

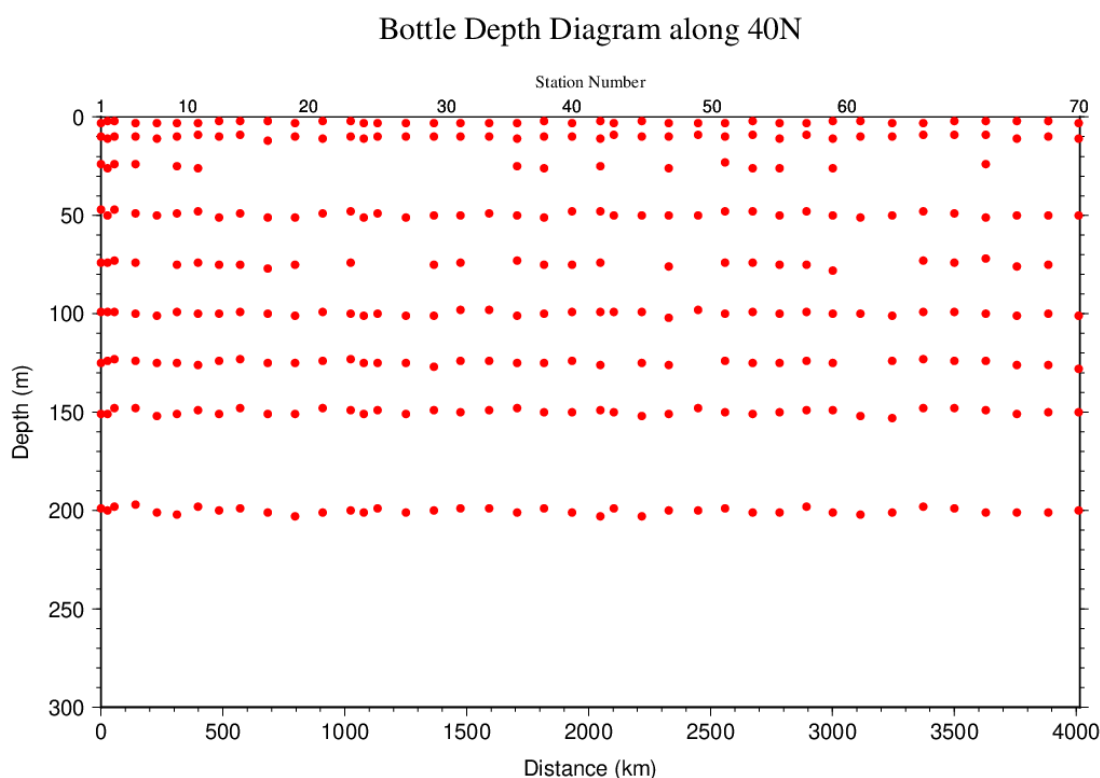


Figure C.5.2. Distance-depth distribution of sampling layers of chlorophyll-*a*.

### (3) Reagents

N,N-dimethylformamide (DMF)

Hydrochloric acid (HCl), 0.5 mol L<sup>-1</sup>

Chlorophyll-*a* standard from *Anacystis nidulans* algae (Sigma-Aldrich, United States)

Rhodamine WT (Turner Designs, United States)

### (4) Instruments

Fluorometer: 10-AU (Turner Designs, United States)

Spectrophotometer: UV-1800 (Shimadzu, Japan)

### (5) Standardization

#### (5.1) Determination of chlorophyll-*a* concentration of standard solution

To prepare the pure chlorophyll-*a* standard solution, reagent powder of chlorophyll-*a* standard was dissolved in DMF. A concentration of the chlorophyll-*a* solution was determined with the spectrophotometer as follows:

$$\text{chl. } a \text{ concentration } (\mu\text{g mL}^{-1}) = A_{\text{chl}} / a_{\text{phy}}^* \quad (\text{C5.1})$$

where  $A_{\text{chl}}$  is the difference between absorbance at 663.8 nm and 750 nm, and  $a_{\text{phy}}^*$  is specific absorption coefficient (UNESCO, 1994). The specific absorption coefficient is 88.74 L g<sup>-1</sup> cm<sup>-1</sup> (Porra *et al.*, 1989).

#### (5.2) Determination of R and $f_{\text{ph}}$



Before measurements, sensitivity of the fluorometer was calibrated with pure DMF and a rhodamine 1 ppm solution (diluted with deionized water).

The chlorophyll-*a* standard solution, whose concentration was precisely determined in subsection (5.1), was measured with the fluorometer, and after acidified with 1–2 drops 0.5 mol L<sup>-1</sup> HCl the solution was also measured. The acidification coefficient (R) of the fluorometer was also calculated as the ratio of the unacidified and acidified readings of chlorophyll-*a* standard solution. The linear calibration factor (f<sub>ph</sub>) of the fluorometer was calculated as the slope of the acidified reading against chlorophyll-*a* concentration. The R and f<sub>ph</sub> in the cruise are shown in Table C.9.1.

Table C.5.1. R and f<sub>ph</sub> in the cruise.

Acidification coefficient (R)	1.933
Linear calibration factor (f <sub>ph</sub> )	5.971

## (6) Seawater sampling and measurement

Water samples were collected from 10-liters Niskin bottle attached the CTD-system and a stainless steel bucket for the surface. A 200 mL seawater sample was immediately filtered through 25 mm GF/F filters by low vacuum pressure below 15 cmHg, the particulate matter collected on the filter. Phytopigments were extracted in vial with 9 mL of DMF. The extracts were stored for 24 hours in the refrigerator at –30 °C until analysis.

After the extracts were put on the room temperature for at least one hour in the dark, the extracts were decanted from the vial to the cuvette. Fluorometer readings for each cuvette were taken before and after acidification with 1–2 drops 0.5 mol L<sup>-1</sup> HCl. Chlorophyll-*a* and phaeopigment concentrations (µg mL<sup>-1</sup>) in the sample are calculated as follows:

$$\text{chl } a \text{ conc.} = \frac{F_0 - F_a}{f_{\text{ph}} \cdot (R - 1)} \cdot \frac{v}{V} \quad (\text{C5.2})$$

$$\text{phaeo. conc.} = \frac{R \cdot F_0 - F_a}{f_{\text{ph}} \cdot (R - 1)} \cdot \frac{v}{V} \quad (\text{C5.3})$$

F<sub>0</sub>: reading before acidification

F<sub>a</sub>: reading after acidification

R: acidification coefficient (F<sub>0</sub>/F<sub>a</sub>) for pure chlorophyll-*a*

f<sub>ph</sub>: linear calibration factor

v: extraction volume

V: sample volume.

### (7) Quality control flag assignment

Quality flag value was assigned to oxygen measurements as shown in Table C.5.2, using the code defined in IOCCP Report No.14 (Swift, 2010).

Table C.5.2 Summary of assigned quality control flags.

Flag	Definition	Chl. <i>a</i>	Phaeo.
2	Good	302	302
3	Questionable	0	0
4	Bad (Faulty)	18	18
5	Not reported	0	0
Total number		320	320

### References

- Porra, R. J., W. A. Thompson and P. E. Kriedemann (1989), Determination of accurate coefficients and simultaneous equations for assaying chlorophylls *a* and *b* extracted with four different solvents: verification of the concentration of chlorophyll standards by atomic absorption spectroscopy. *Biochem. Biophys. Acta*, 975, 384-394.
- Swift, J. H. (2010), Reference-quality water sample data: Notes on acquisition, record keeping, and evaluation. *IOCCP Report No.14, ICPO Pub. 134, 2010 ver.1*.
- UNESCO (1994), Protocols for the joint global ocean flux study (JGOFS) core measurements: Measurement of chlorophyll *a* and phaeopigments by fluorometric analysis, *IOC manuals and guides 29, Chapter 14*.

## 6. *Total Dissolved Inorganic Carbon (DIC)*

30 September 2023

### (8) Personnel

OKA Takahiro

INAMI Haruna (Leg 1)

USHIO Nobuyasu (Leg 1)

AKIEDA Chikako (Leg 2)

TANIZAKI Chiho (Leg 2)

### (9) Station occupied

A total of 40 stations (Leg 1: 18, Leg 2: 22) were occupied for total dissolved inorganic carbon (DIC). Station location and sampling layers of them are shown in Figures C.6.1 and C.6.2, respectively.

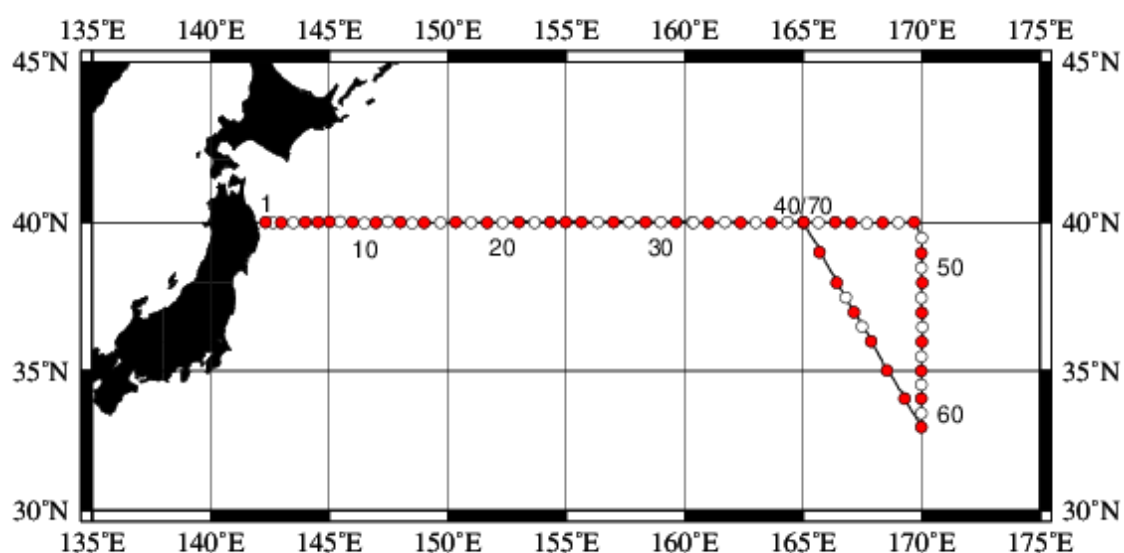


Figure C.6.1. Location of observation stations of DIC. Closed and open circles indicate sampling and no-sampling stations, respectively.

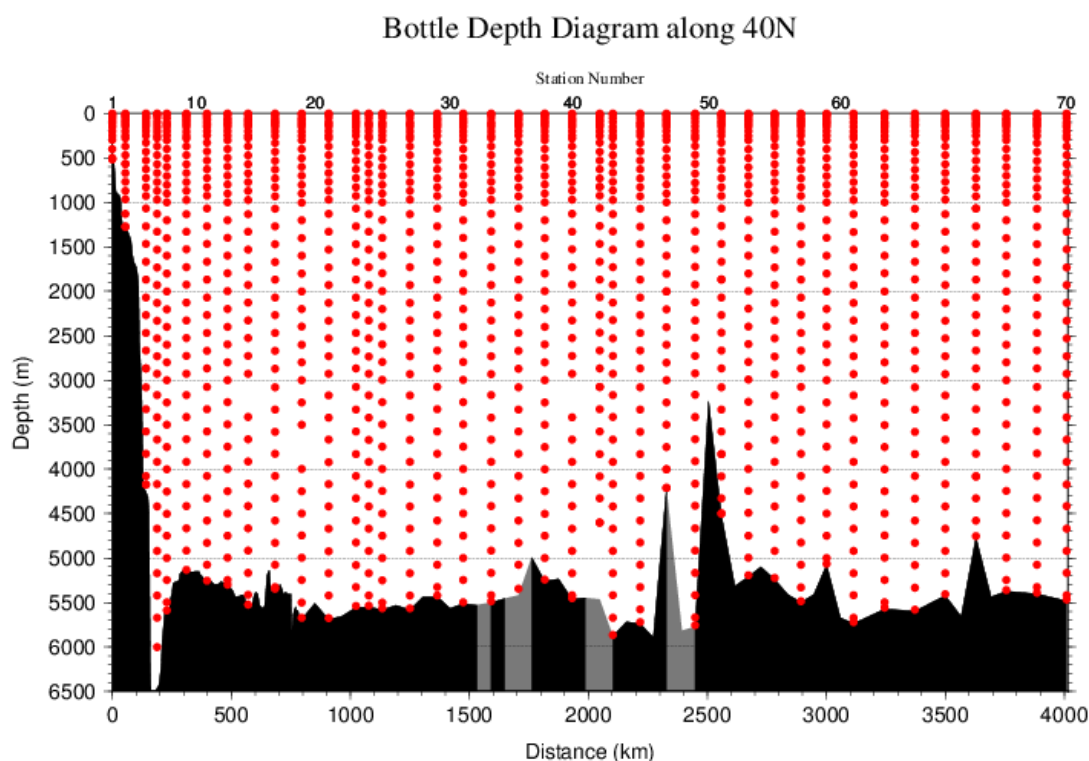


Figure C.6.2. Distance-depth distribution of sampling layers of DIC.

#### (10) Instrument

The measurement of DIC was carried out with DIC/TA analyzers (Nihon ANS Co. Ltd, Japan). We used two analyzers concurrently. These analyzers are designated as apparatus A and B.

#### (11) Sampling and measurement

Methods of seawater sampling, poisoning, measurement, and calculation of DIC concentrations were based on the Standard Operating Procedure (SOP) described in PICES Special Publication 3, SOP-2 (Dickson et al., 2007). DIC was determined by coulometric analysis (Johnson et al., 1985, 1987) using an automated CO<sub>2</sub> extraction unit and a coulometer. Details of sampling and measurement are shown in Appendix A1.

#### (12) Calibration

The concentration of DIC ( $C_T$ ) in moles per kilogram ( $\text{mol kg}^{-1}$ ) of seawater was calculated from the following equation:

$$(C6.1)$$

where  $N_s$  is the counts of the coulometer (gC),  $cV$  is the calibration factor ( $\text{gC (mol L}^{-1})^{-1}$ ), and  $\rho_s$  is density of seawater ( $\text{kg L}^{-1}$ ), which is calculated from the salinity of the sample and the water temperature of the water-jacket for the sample pipette.

The values of  $cV$  were determined by measurements of Certified Reference Materials (CRMs) that were provided by Dr. Andrew G. Dickson of the Scripps Institution of Oceanography. Table C.6.1 provides information about the CRM batches used in this cruise.

Table C.6.1. Certified  $C_T$  and standard deviation of CRM. Unit of  $C_T$  is  $\mu\text{mol kg}^{-1}$ . More information is available at the NOAA web site ([https://www.ncei.noaa.gov/access/ocean-carbon-acidification-data-system/oceans/Dickson\\_CRM/batches.html](https://www.ncei.noaa.gov/access/ocean-carbon-acidification-data-system/oceans/Dickson_CRM/batches.html)).

Batch number	179
$C_T$	$1941.92 \pm 0.68$
Salinity	33.841

The CRM measurement was carried out at every station. After the cruise, a value of  $cV$  was assigned to each apparatus (A, B). Table C.6.2 summarizes the  $cV$  values. Figure C.6.3 shows details.

Table C.6.2. Assigned  $cV$  and its standard deviation for each apparatus during the cruise. Unit is  $\text{gC (mol L}^{-1})^{-1}$ .

Apparatus	$cV$
A	$0.189057 \pm 0.000249$ (N=83)
B	$0.189722 \pm 0.000168$ (N=77)

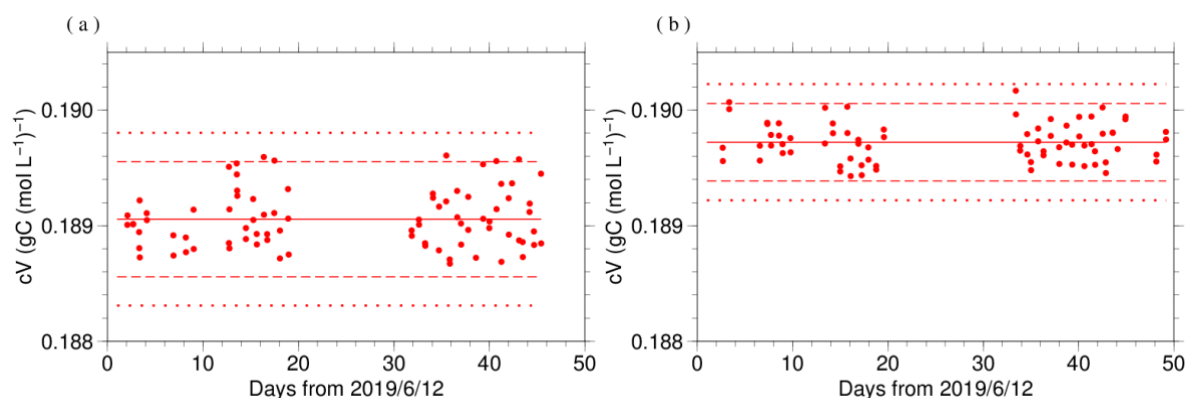


Figure C.6.3. Results of the  $cV$  at each station assigned for apparatus (a) A and (b) B. The solid, dashed, and dotted lines denote the mean, the mean  $\pm$  twice the S.D., and the mean  $\pm$  thrice the S.D. for all measurements, respectively.

The precisions of the  $cV$  is equated to its coefficient of variation ( $= \text{S.D.} / \text{mean}$ ). They were 0.132 % for apparatus A and 0.089 % for apparatus B. They correspond to  $2.56 \mu\text{mol kg}^{-1}$  and  $1.72 \mu\text{mol kg}^{-1}$  in  $C_T$  of CRM batch 179, respectively.

Finally, the value of  $C_T$  was multiplied by 1.00067 ( $= 300.2 / 300.0$ ) to correct dilution effect induced by addition of 0.2 mL of mercury (II) chloride ( $\text{HgCl}_2$ ) solution in a sampling bottle with a volume of  $\sim 300$  mL.

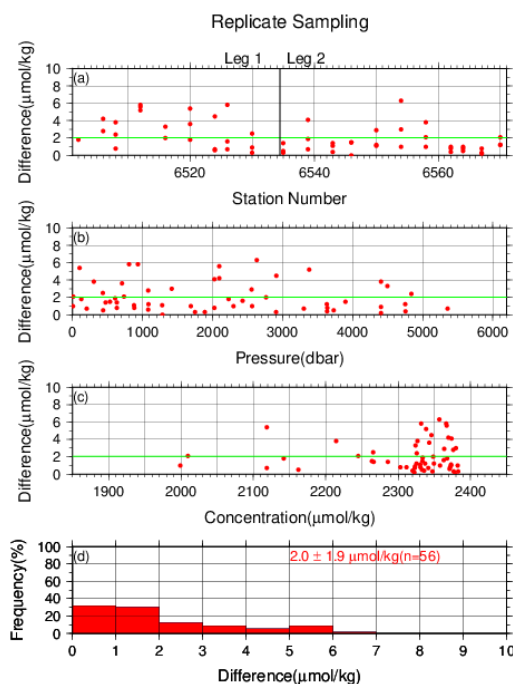
### (13) Quality Control

### (6.1) Replicate and duplicate analyses

We took replicate (pair of water samples taken from a single Niskin bottle) and duplicate (pair of water samples taken from different Niskin bottles closed at the same depth) samples of DIC throughout the cruise. Table C.6.3 summarizes the results of the measurements with each apparatus. Figures C.6.4–C.6.5 show details of the results. The calculation of the standard deviation from the difference of sets of measurements was based on a procedure (SOP 23) in DOE (1994).

Table C.6.3. Summary of replicate and duplicate measurements. Unit is  $\mu\text{mol kg}^{-1}$ .

	Apparatus A	Apparatus B
Measurement	Average magnitude of difference $\pm$ S.D.	
Replicate	$2.0 \pm 1.9$ (N=56)	$0.9 \pm 0.9$ (N=59)
Duplicate	$2.7 \pm 2.2$ (N=9)	$1.1 \pm 1.0$ (N=8)



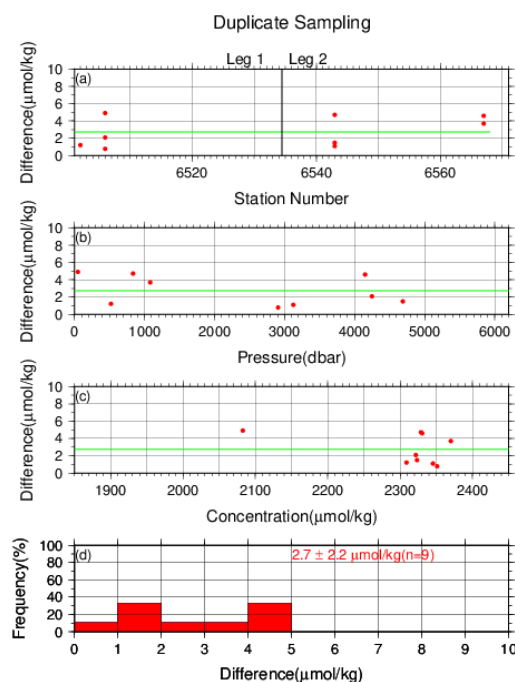


Figure C.6.4. Results of (left) replicate and (right) duplicate measurements during the cruise versus (a) station number, (b) pressure, and (c)  $C_T$  determined by apparatus A. The green lines denote the averages of the measurements. The bottom panels (d) show histograms of the measurements.

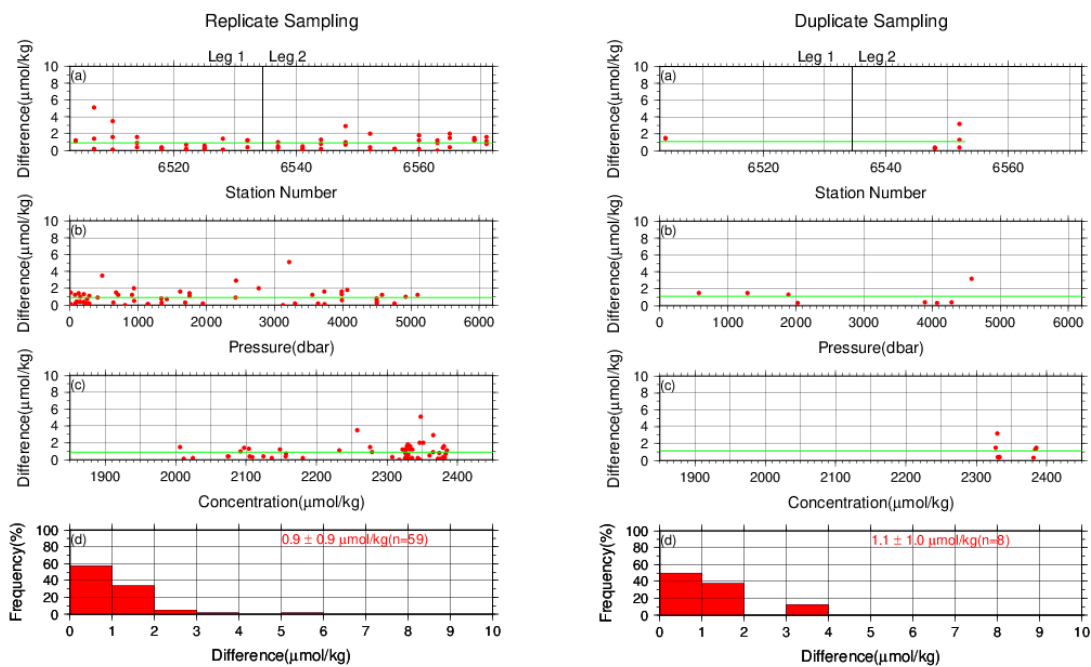


Figure C.6.5. Same as Figure C.6.4, but for apparatus B.

## (6.2) Measurements of CRM and working reference materials

The precision of the measurements was monitored by using the CRMs and working reference materials bottled in our laboratory (Appendix A2). The CRM (batch 179) and working reference material measurements were carried out at every station. At the beginning of the measurement of each station, we measured a working reference material and a CRM. If the results of these measurements were confirmed to be good, measurements on seawater samples were begun. At the end of a sequence of measurements at a station, another CRM bottle was measured. A CRM measurement was repeated twice from the same bottle. Table C.6.4 summarizes the differences in the repeated measurements of the CRMs, the mean  $C_T$  of the CRM measurements, and the mean  $C_T$  of the working reference material measurements. Figures C.6.6–C.6.8 show detailed results.

Table C.6.4. Summary of difference and mean of  $C_T$  in the repeated measurements of CRM and the mean  $C_T$  of the working reference material. These data are based on good measurements. Unit is  $\mu\text{mol kg}^{-1}$ .

Apparatus	CRM	Working reference material	
	Average magnitude of difference $\pm$ S.D.	Mean Ave. $\pm$ S.D.	Mean Ave. $\pm$ S.D.
A	$2.5 \pm 2.3$ (N=40)	$1942.0 \pm 2.0$ (N=40)	$2053.2 \pm 1.1$ (N=21)
B	$1.2 \pm 1.0$ (N=37)	$1942.0 \pm 1.6$ (N=37)	$2053.8 \pm 1.0$ (N=20)

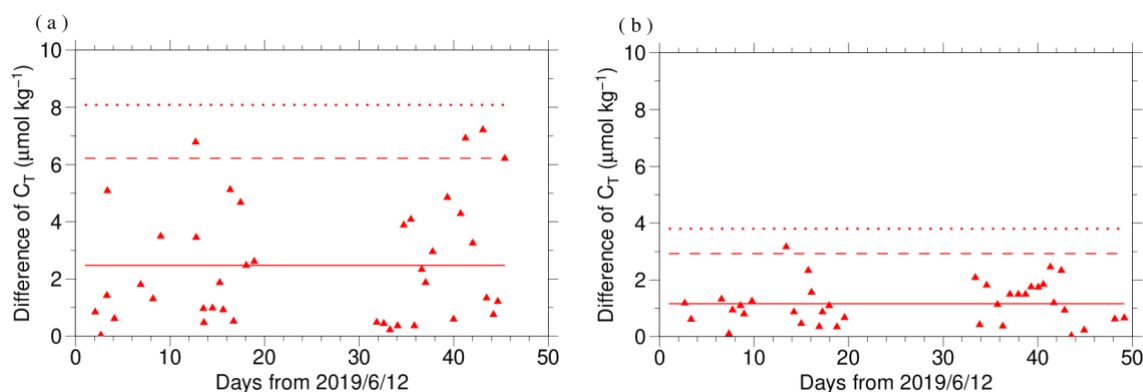


Figure C.6.6. The absolute difference ( $R$ ) of  $C_T$  in repeated measurements of CRM determined by apparatus (a) A and (b) B. The solid line indicates the average of  $R$  ( $\bar{R}$ ). The dashed and dotted lines denote the upper warning limit (2.512) and upper control limit (3.267), respectively (see Dickson et al., 2007).



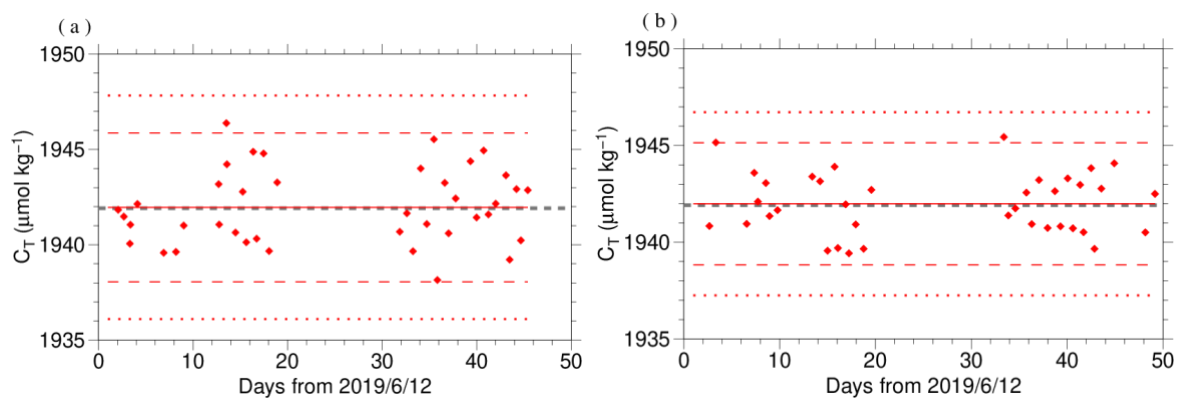


Figure C.6.7. The mean  $C_T$  of measurements of CRM. The panels show the results for apparatus (a) A and (b) B. The solid line indicates the mean of the measurements throughout the cruise. The dashed and dotted lines denote the upper/lower warning limit (mean  $\pm$  2S.D.) and the upper/lower control limit (mean  $\pm$  3S.D.), respectively. The gray dashed line denotes certified  $C_T$  of CRM.

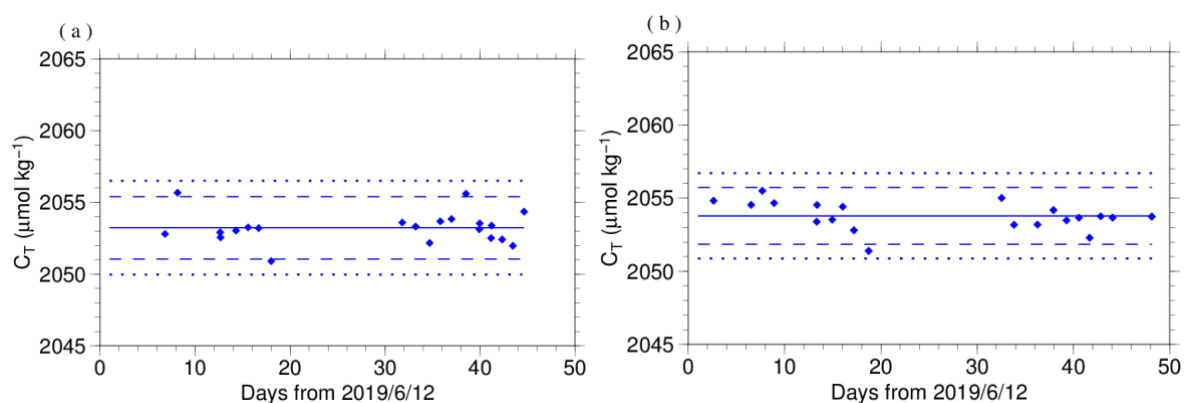


Figure C.6.8. Calculated  $C_T$  of working reference material measured by apparatus (a) A and (b) B. The solid, dashed and dotted lines are the same as in Figure C.6.7.

### (6.3) Comparisons with other CRM batches

At every few stations, other CRM batches (175 and 182) were measured to provide comparisons with batch 179 to confirm the determination of  $C_T$  in our measurements. For these CRM measurements,  $C_T$  was calculated from the  $cV$  determined from batch 179 measurement. Figures C.6.9 show the differences between the calculated and certified  $C_T$ .

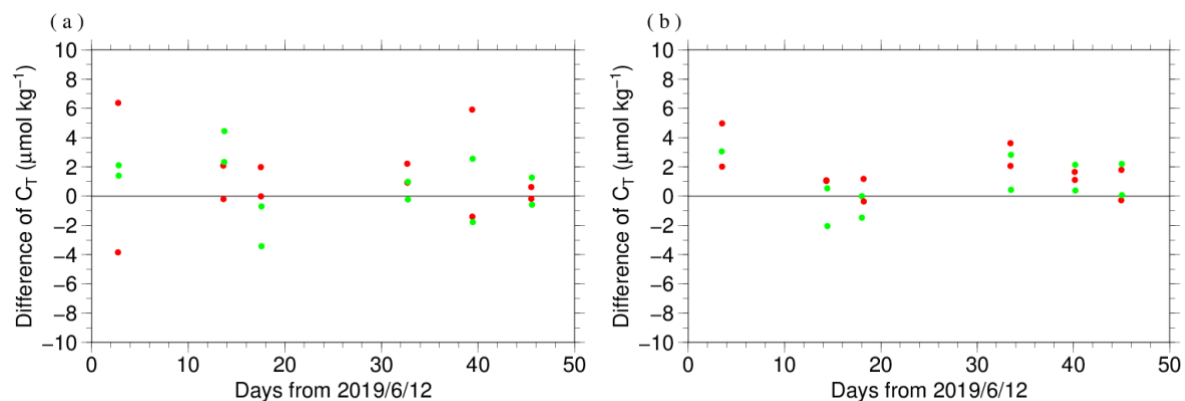


Figure C.6.9. The differences between the calculated  $C_T$  from batch 179 measurements and the certified  $C_T$ . The panels show the results for apparatus (a) A and (b) B. Colors indicate CRM batches; red: 175 and green: 182.

### (6.4) Quality control flag assignment

A quality control flag value was assigned to the DIC measurements (Table C.6.5) using the code defined in the IOCCP Report No.14 (Swift, 2010).

Table C.6.5. Summary of assigned quality control flags.

Flag	Definition	Number of samples
2	Good	1315
3	Questionable	8
4	Bad (Faulty)	3
5	Not reported	0
6	Replicate measurements	115
Total number of samples		1441

## **Appendix**

### **A1. Methods**

#### **(A1.1) Seawater sampling**

Seawater samples were collected from 10-liters Niskin bottles mounted on CTD-system and a stainless steel bucket for the surface. Samples for DIC/TA were transferred to Schott Duran® glass bottles (screw top) using sample drawing tubes. Bottles were filled smoothly from the bottom after overflowing double a volume while taking care of not entraining any bubbles, and lid temporarily with inner polyethylene cover and screw cap.

After all sampling finished, 2 mL of sample is removed from each bottle to make a headspace to allow thermal expansion, and then samples were poisoned with 0.2 mL of saturated HgCl<sub>2</sub> solution and covered tight again.

#### **(A1.2) Measurement**

The unit for DIC measurement in the coupled DIC/TA analyzer consists of a coulometer with a quartz coulometric titration cell, a CO<sub>2</sub> extraction unit and a reference gas injection unit. The CO<sub>2</sub> extraction unit, which is connected to a bottle of 20 % v/v phosphoric acid and a carrier N<sub>2</sub> gas supply, includes a sample pipette (approx. 12 mL) and a CO<sub>2</sub> extraction chamber, two thermoelectric cooling units and switching valves. The coulometric titration cell and the sample pipette are water-jacketed and are connected to a thermostated (25 °C) water bath. The automated procedures of DIC analysis in seawater were as follows (Ishii et al., 1998):

- (a) Approximately 2 mL of 20 % v/v phosphoric acid was injected to an “extraction chamber”, *i.e.*, a glass tube with a coarse glass frit placed near the bottom. Purified N<sub>2</sub> was then allowed to flow through the extraction chamber to purge CO<sub>2</sub> and other volatile acids dissolved in the phosphoric acid.
- (b) A portion of sample seawater was delivered from the sample bottle into the sample pipette of CO<sub>2</sub> extraction unit by pressurizing the headspace in the sample bottle. After temperature of the pipette was recorded, the sample seawater was transferred into the extraction chamber and mixed with phosphoric acid to convert all carbonate species to CO<sub>2</sub> (aq).
- (c) The acidified sample seawater was then stripped of CO<sub>2</sub> with a stream of purified N<sub>2</sub>. After being dehumidified in a series of two thermoelectric cooling units, the evolved CO<sub>2</sub> in the N<sub>2</sub> stream was introduced into the carbon cathode solution in the coulometric titration cell and then CO<sub>2</sub> was electrically titrated.

#### **A2. Working reference material recipe**

The surface seawater in the western North Pacific was taken until at least a half year ago. Seawater was firstly filtered by membrane filter (0.45 µm-mesh) using magnetic pump and transfer into large tank. After first filtration finished, corrected seawater in the tank was processed in cycle filtration again for 3 hours and agitated in clean condition air for 6 hours. On the next day, agitated 5 minutes to remove small bubbles on the tank and transfer to Schott Duran® glass bottles as same method as samples (Appendix A1.1) except for overflowing a

half of volume, not double. Created of headspace and poisoned with HgCl<sub>2</sub> was as same as samples, finally, sealed by ground glass stoppers lubricated with Apiezon<sup>®</sup> grease (L).

### **References**

- Dickson, A. G., C. L. Sabine, and J. R. Christian (Eds.) (2007), Guide to best practices for ocean CO<sub>2</sub> measurements. *PICES Special Publication 3*, 191 pp.
- DOE (1994), Handbook of methods for the analysis of the various parameters of the carbon dioxide system in sea water; version 2. *A. G. Dickson and C. Goyet (eds), ORNL/CDIAC-74*.
- Ishii, M., H. Y. Inoue, H. Matsueda, and E. Tanoue (1998), Close coupling between seasonal biological production and dynamics of dissolved inorganic carbon in the Indian Ocean sector and the western Pacific Ocean sector of the Antarctic Ocean, *Deep Sea Res. Part I*, **45**, 1187–1209, doi:10.1016/S0967-0637(98)00010-7.
- Johnson, K. M., A. E. King and J. McN. Sieburth (1985), Coulometric TCO<sub>2</sub> analyses for marine studies; an introduction. *Marine Chemistry*, **16**, 61–82.
- Johnson, K. M., J. M. Sieburth, P. J. L. Williams and L. Brändström (1987), Coulometric total carbon dioxide analysis for marine studies: Automation and calibration. *Marine Chemistry*, **21**, 117–133.
- Swift, J. H. (2010): Reference-quality water sample data, Notes on acquisition, record keeping, and evaluation. *IOCCP Report No.14, ICPO Pub. 134*, 2010 ver.1.

## 7. *Total Alkalinity (TA)*

30 September 2023

### (14) Personnel

OKA Takahiro

INAMI Haruna (Leg 1)

USHIO Nobuyasu (Leg 1)

AKIEDA Chikako (Leg 2)

TANIZAKI Chiho (Leg 2)

### (15) Station occupied

A total of 40 stations (Leg 1: 18, Leg 2: 22) were occupied for total alkalinity (TA). Station location and sampling layers of them are shown in Figures C.7.1 and C.7.2, respectively.

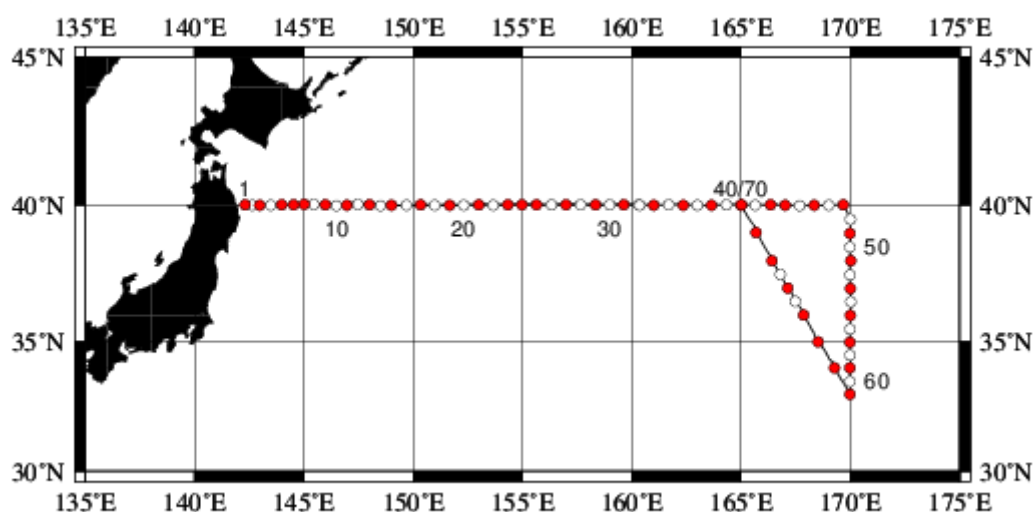


Figure C.7.1. Location of observation stations of TA. Closed and open circles indicate sampling and no-sampling stations, respectively.

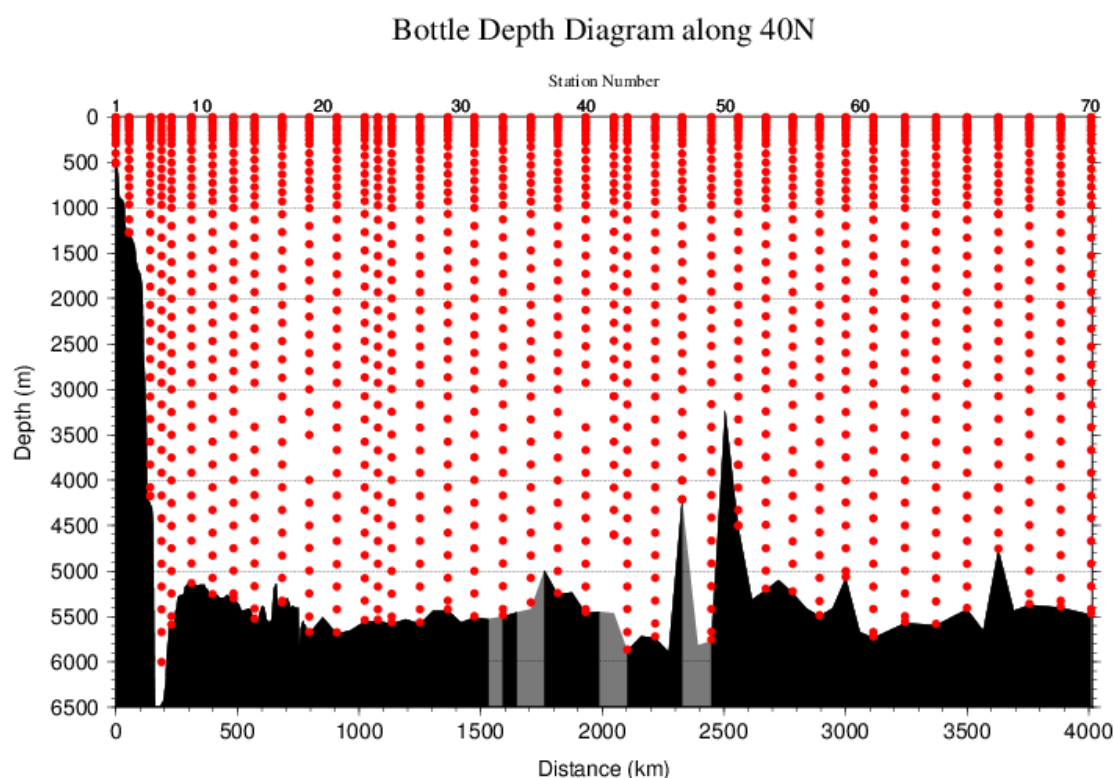


Figure C.7.2. Distance-depth distribution of sampling layers of TA.

## (16) Instrument

The measurement of TA was carried out with DIC/TA analyzers (Nihon ANS Co. Ltd., Japan). The methodology that these analyzers use is based on an open titration cell. We used two analyzers concurrently. These analyzers are designated as apparatus A and B.

## (17) Sampling and measurement

The procedure of seawater sampling of TA bottles and poisoning with mercury (II) chloride ( $\text{HgCl}_2$ ) were based on the Standard Operating Procedure (SOP) described in PICES Special Publication 3 (Dickson et al., 2007). Details are shown in Appendix A1 in C.6.

TA measurement is based on a one-step volumetric addition of hydrochloric acid (HCl) to a known amount of sample seawater with prompt spectrophotometric measurement of excess acid using the sulfonephthalein indicator bromo cresol green sodium salt (BCG) (Breland and Byrne, 1993). We used a mixed solution of HCl, BCG, and sodium chloride (NaCl) as reagent. Details of measurement are shown in Appendix A1.

## (18) Calculation

### (5.1) Volume of sample seawater

The volumes of pipette  $V_s$  using in apparatus A and B was calibrated gravimetrically in our laboratory. Table C.7.1 shows the summary.

Table C.7.1. Summary of sample volumes of seawater  $V_S$  for TA measurements.

Apparatus	$V_S$ / mL
A	42.8099
B	41.4764

### (5.2) $\text{pH}_T$ calculation in spectrophotometric measurement

The data of absorbance  $A$  and pipette temperature  $T$  (in  $^{\circ}\text{C}$ ) were processed to calculate  $\text{pH}_T$  (in total hydrogen ion scale; details shown in Appendix A1 in C.8) and the concentration of excess acid  $[\text{H}^+]_T$  ( $\text{mol kg}^{-1}$ ) in the following equations (C7.1)–(C7.3) (Yao and Byrne, 1998),

$$\begin{aligned} \text{pH}_T &= -\log_{10}([\text{H}^+]_T) \\ &= 4.2699 + 0.02578 \cdot (35 - S) + \log\{(R_{25} - 0.00131) / (2.3148 - 0.1299 \cdot R_{25})\} \\ &\quad - \log(1 - 0.001005 \cdot S) \end{aligned} \quad (\text{C7.1})$$

$$R_{25} = R_T \cdot \{1 + 0.00909 \cdot (25 - T)\} \quad (\text{C7.2})$$

$$. \quad (\text{C7.3})$$

In the equation (C7.1),  $R_T$  is absorbance ratio at temperature  $T$ ,  $R_{25}$  is absorbance ratio at temperature  $25^{\circ}\text{C}$  and  $S$  is salinity. and denote absorbance of seawater before and after acidification, respectively, at wavelength  $\lambda$  nm.

### (5.3) TA calculation

The calculated  $[\text{H}^+]_T$  was then combined with the volume of sample seawater  $V_S$ , the volume of titrant  $V_A$  added to the sample, and molarity of hydrochloric acid  $\text{HCl}_A$  (in  $\text{mmol L}^{-1}$ ) in the titrant to determine to TA concentration  $A_T$  (in  $\mu\text{mol kg}^{-1}$ ) as follows:

$$A_T = (-[\text{H}^+]_T \cdot (V_S + V_A) \cdot \rho_{SA} + \text{HCl}_A \cdot V_A) / (V_S \cdot \rho_S) \quad (\text{C7.4})$$

$\rho_S$  and  $\rho_{SA}$  denote the density of seawater sample before and after the addition of titrant, respectively. Here we assumed that  $\rho_{SA}$  is equal to  $\rho_S$ , since the density of titrant has been adjusted to that of seawater by adding NaCl and the volume of titrant (approx. 2.5 mL) is no more than approx. 6 % of seawater sample.

Finally, the value of  $A_T$  was multiplied by 1.00067 ( $= 300.2 / 300.0$ ) to correct dilution effect in  $A_T$  induced by addition of  $\text{HgCl}_2$  solution.

### (19) Standardization of HCl reagent

HCl reagents were prepared in our laboratory (Appendix A2) and divided into bottles (HCl batches).  $\text{HCl}_A$  in the bottles were determined from CRMs provided by Dr. Andrew G. Dickson in Scripps Institution of Oceanography. Table C.7.2 provides information about the CRM batch used during this cruise.

Table C.7.2. Certified  $A_T$  and standard deviation of CRM. Unit of  $A_T$  is  $\mu\text{mol kg}^{-1}$ . More information is available at the NOAA web site ([https://www.ncei.noaa.gov/access/ocean-carbon-acidification-data-system/oceans/Dickson\\_CRM/batches.html](https://www.ncei.noaa.gov/access/ocean-carbon-acidification-data-system/oceans/Dickson_CRM/batches.html)).

Batch number	179
$A_T$	$2219.26 \pm 0.86$
Salinity	33.841

The CRM measurement was carried out at every station. The apparent  $HCl_A$  of the titrant was determined from CRM using equation (C7.4).

$HCl_A$  was assigned for each HCl batches for each apparatus, as summarized in Table C.7.3 and detailed in Figure C.7.3.

Table C.7.3. Summary of assigned  $HCl_A$  for each HCl batches. The reported values are means and standard deviations. Unit is  $\text{mmol L}^{-1}$ .

Apparatus	HCl Batch	$HCl_A$
A	A_1	$50.0551 \pm 0.0354$ (N=36)
	A_2	$50.0324 \pm 0.0303$ (N=27)
	A_3	$50.1182 \pm 0.0363$ (N=30)
	A_4	$49.9933 \pm 0.0328$ (N=36)
B	B_1	$50.0756 \pm 0.0538$ (N=30)
	B_2	$50.0877 \pm 0.0359$ (N=29)
	B_3	$50.0127 \pm 0.0224$ (N=30)
	B_4	$50.0283 \pm 0.0236$ (N=36)

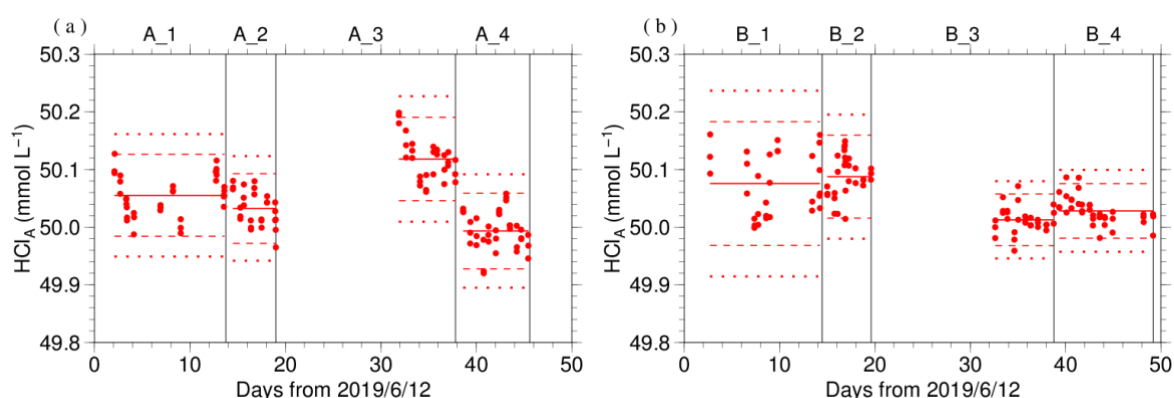


Figure C.7.3. Results of  $HCl_A$  measured by apparatus (a) A and (b) B. The HCl batch names are indicated at the top of each graph, and vertical lines denote the day when the HCl batch was switched. The red solid, dashed, and dotted lines denote the mean and the mean  $\pm$  twice the S.D. and thrice the S.D. for each HCl batches, respectively.



The precisions of  $HCl_A$ , defined as the coefficient of variation ( $= \text{S.D.} / \text{mean}$ ), were 0.0606–0.0724 % for apparatus A and 0.0448–0.1074 % for apparatus B. They correspond to 1.34–1.61  $\mu\text{mol kg}^{-1}$  and 0.99–2.38  $\mu\text{mol kg}^{-1}$  in  $A_T$  of CRM batch 179, respectively.

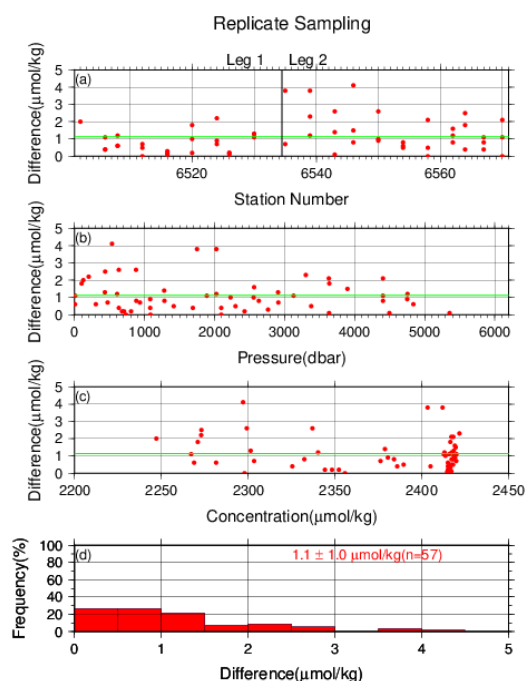
## (20) Quality Control

### (7.1) Replicate and duplicate analyses

We took replicate (pair of water samples taken from a single Niskin bottle) and duplicate (pair of water samples taken from different Niskin bottles closed at the same depth) samples of TA throughout the cruise. Table C.7.4 summarizes the results of the measurements with each apparatus. Figures C.7.4–C.7.5 show details of the results. The calculation of the standard deviation from the difference of sets of measurements was based on a procedure (SOP 23) in DOE (1994).

Table C.7.4. Summary of replicate and duplicate measurements. Unit is  $\mu\text{mol kg}^{-1}$ .

Measurement	Apparatus A	Apparatus B
	Average magnitude of difference $\pm$ S.D.	
Replicate	1.1 $\pm$ 1.0 (N=57)	1.1 $\pm$ 1.1 (N=58)
Duplicate	1.3 $\pm$ 1.0 (N=9)	1.6 $\pm$ 1.3 (N=8)



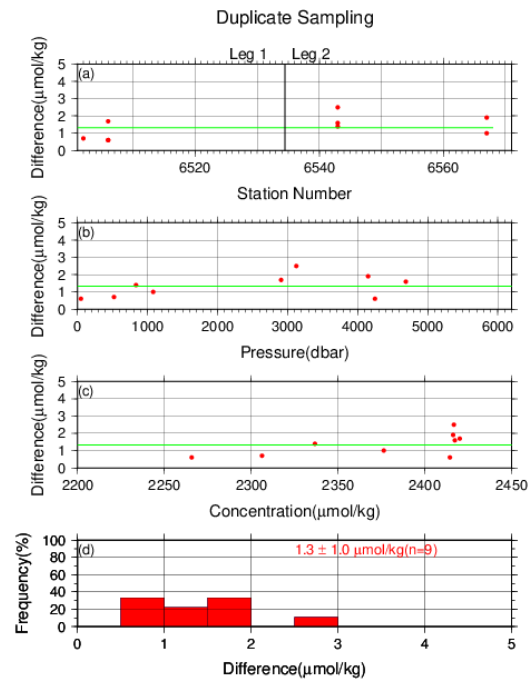
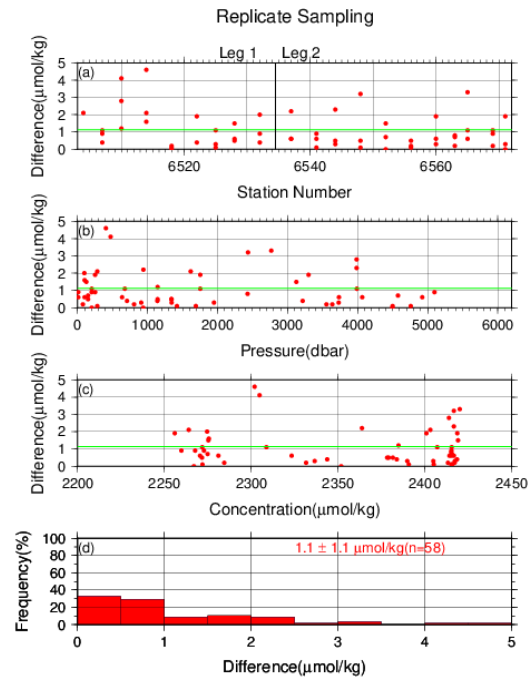


Figure C.7.4. Results of (left) replicate and (right) duplicate measurements during the cruise versus (a) station number, (b) pressure, and (c)  $A_T$  determined by apparatus A. The green lines denote the averages of the measurements. The bottom panels (d) show histograms of the measurements.



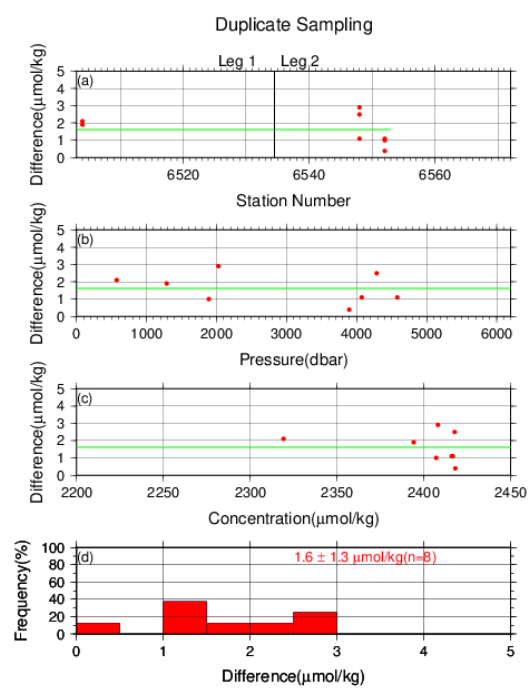


Figure C.7.5. Same as Figure C.7.4, but for apparatus B.

## (7.2) Measurements of CRM and working reference materials

The precision of the measurements was monitored by using the CRMs and working reference materials bottled in our laboratory (Appendix A2 in C.6). The measurements of the CRMs and working reference materials were the same those used to measure DIC (see (6.2) in C.6), except that the CRM measurement was repeated 3 times from the same bottle. Table C.7.5 summarizes the differences in the repeated measurements of the CRMs, the mean  $A_T$  of the CRM measurements, and the mean  $A_T$  of the working reference material measurements. Figures C.7.6–C.7.8 show detailed results.

Table C.7.5. Summary of difference and mean of  $A_T$  in the repeated measurements of CRM and the mean  $A_T$  of the working reference material. These data are based on good measurements. Unit is  $\mu\text{mol kg}^{-1}$ .

HCl Batches	CRM	Working reference material	
	Average magnitude of difference $\pm$ S.D.	Mean Ave. $\pm$ S.D.	Mean Ave. $\pm$ S.D.
A_1	0.7 $\pm$ 0.5 (N=12)	2219.3 $\pm$ 1.6 (N=12)	2292.5 $\pm$ 1.0 (N=6)
A_2	0.7 $\pm$ 0.6 (N=9)	2219.3 $\pm$ 1.4 (N=9)	2292.8 $\pm$ 1.1 (N=4)
A_3	0.9 $\pm$ 0.7 (N=10)	2219.3 $\pm$ 1.6 (N=10)	2292.4 $\pm$ 1.9 (N=5)
A_4	0.9 $\pm$ 0.7 (N=12)	2219.3 $\pm$ 1.4 (N=12)	2293.4 $\pm$ 1.4 (N=7)
B_1	2.2 $\pm$ 1.8 (N=10)	2219.3 $\pm$ 2.0 (N=10)	2291.2 $\pm$ 1.2 (N=5)
B_2	1.3 $\pm$ 1.1 (N=10)	2219.3 $\pm$ 1.3 (N=10)	2292.9 $\pm$ 2.7 (N=4)
B_3	0.8 $\pm$ 0.6 (N=10)	2219.3 $\pm$ 0.9 (N=10)	2291.9 $\pm$ 1.0 (N=5)
B_4	0.9 $\pm$ 0.7 (N=12)	2219.3 $\pm$ 0.9 (N=12)	2293.0 $\pm$ 1.9 (N=6)

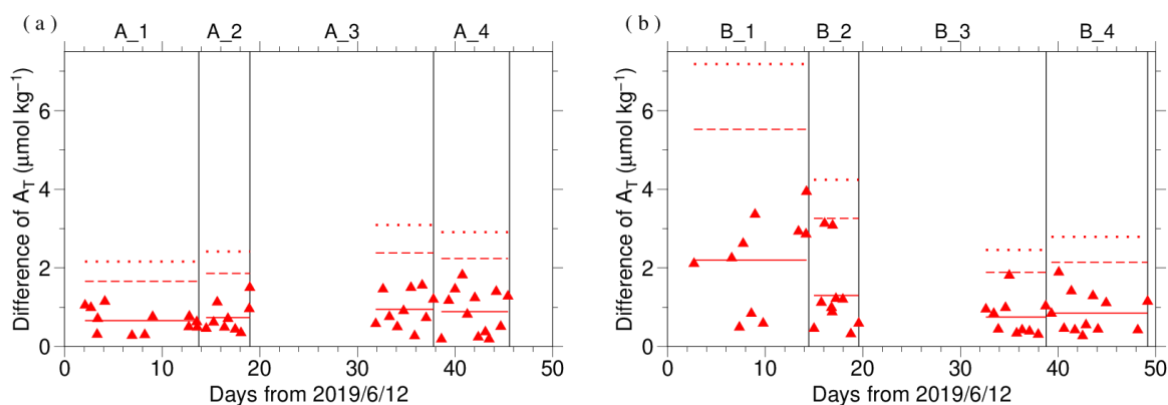


Figure C.7.6. The absolute difference ( $R$ ) of  $A_T$  in repeated measurements of CRM determined by apparatus (a) A and (b) B. The solid line indicates the average of  $R$  (). The dashed and dotted lines denote the upper warning limit (2.512) and upper control limit (3.267), respectively (see Dickson et al., 2007).

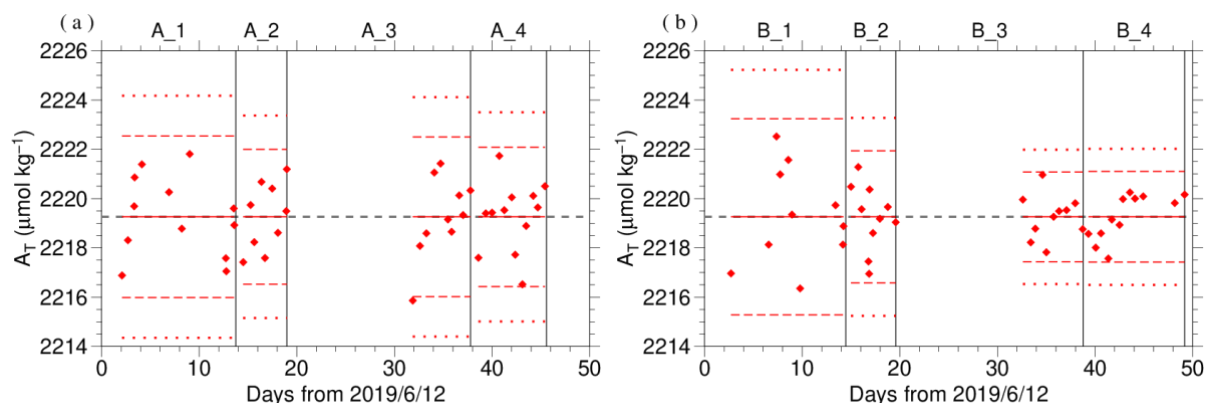


Figure C.7.7. The mean  $A_T$  of measurements of CRM. The panels show the results for apparatus (a) A and (b) B. The solid line indicates the mean of the measurements. The dashed and dotted lines denote the upper/lower warning limit (mean  $\pm$  2S.D.) and the upper/lower control limit (mean  $\pm$  3S.D.), respectively. The gray dashed line denotes certified  $A_T$  of CRM. The labels at the top of the graph and vertical lines have the same meaning as in Figure C.7.3.

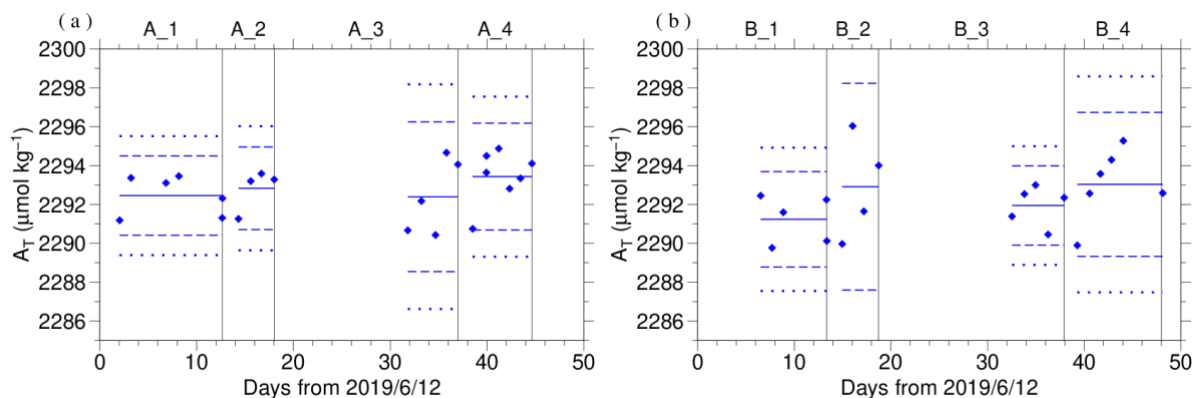


Figure C.7.8. Calculated  $A_T$  of working reference material measured by apparatus (a) A and

(b) B. The solid, dashed and dotted lines have the same meaning as in Figure C.7.7. The labels at the top of the graph and vertical lines have the same meaning as in Figure C.7.3.

### (7.3) Comparisons with other CRM batches

At every few stations, other CRM batches (175 and 182) were measured to provide comparisons with batch 179 to confirm the determination of  $A_T$  in our measurements. For these CRM measurements,  $A_T$  was calculated from  $HCl_A$  determined from batch 179 measurement. Figures C.7.9 show the differences between the calculated and certified  $A_T$ .

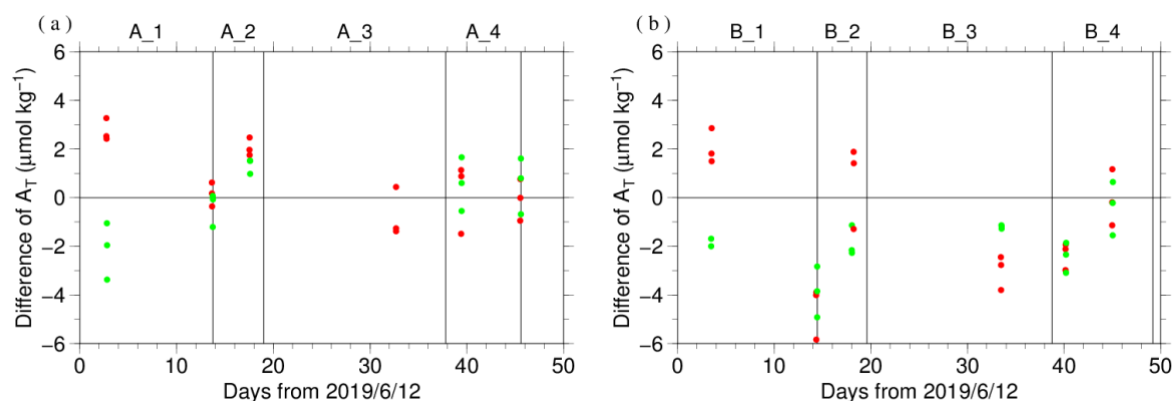


Figure C.7.9. The differences between the calculated  $A_T$  from batch 179 measurements and the certified  $A_T$ . The panels show the results for apparatus (a) A and (b) B. The labels at the top of the graph and vertical lines have the same meaning as in Figure C.7.3. Colors indicate CRM batches; red: 175 and green: 182.

### (7.4) Quality control flag assignment

A quality control flag value was assigned to the TA measurements (Table C.7.6) using the code defined in the IOCCP Report No.14 (Swift, 2010).

Table C.7.6. Summary of assigned quality control flags.

Flag	Definition	Number of samples
2	Good	1318
3	Questionable	5
4	Bad (Faulty)	3
5	Not reported	0
6	Replicate measurements	115
Total number of samples		1441

## Appendix

### A1. Methods

#### (A1.1) Measurement

The unit for TA measurements in the coupled DIC/TA analyzer consists of sample treatment unit with a calibrated sample pipette and an open titration cell that are water-jacketed and connected to a thermostated water bath (25 °C), an auto syringe connected to reagent bottle of titrant stored at 25 °C, and a double-beam spectrophotometric system with two CCD image sensor spectrometers combined with a high power Xenon lamp. The mixture of 0.05 N HCl and 40  $\mu\text{mol L}^{-1}$  BCG in 0.65 M NaCl solution was used as reagent to automatically titrate the sample as follows:

- (a) A portion of sample seawater was delivered into the sample pipette (approx. 42 mL) following sample delivery into the DIC unit for a measurement. After the temperature in the pipette was recorded, the sample was transferred into a cylindrical quartz cell.
- (b) An absorption spectrum of sample seawater in the visible light domain was then measured, and the absorbances were recorded at wavelengths of 444 nm, 509 nm, 616 nm, and 730 nm as well as the temperature in the cell.
- (c) The titrant that contains HCl was added to the sample seawater by the auto syringe so that pH of sample seawater altered in the range between 3.85 and 4.05.
- (d) While the acidified sample was being stirred, the evolved CO<sub>2</sub> was purged with the stream of purified N<sub>2</sub> bubbled into the sample at approx. 200 mL min<sup>-1</sup> for 5 minutes.
- (e) After the bubbled sample steadied down for 1 minute, the absorbance of BCG in the sample was measured in the same way as described in (b), and pH (in total hydrogen ion scale, pH<sub>T</sub>) of the acidified seawater was precisely determined spectrophotometrically.

#### A2. HCl reagents recipes

0.05 N HCl and 40  $\mu\text{mol L}^{-1}$  BCG in 0.65 M NaCl solution

Dissolve 0.30 g of BCG and 190 g of NaCl in roughly 1.5 L of deionized water (DW) in a 5 L flask, and slowly add 200 mL concentrated HCl. After the powders completely dissolved, dilute with DW to a final volume of 5 L.

## References

- Breland II, J. A. and R. H. Byrne (1993), Spectrophotometric procedures for determination of sea water alkalinity using bromocresol green, *Deep-Sea Res. I*, 470, 629–641.
- Dickson, A. G., C. L. Sabine, and J. R. Christian (Eds.) (2007), Guide to best practices for ocean CO<sub>2</sub> measurements. PICES Special Publication 3, 191 pp.
- DOE (1994), Handbook of methods for the analysis of the various parameters of the carbon dioxide system in sea water; version 2. *A. G. Dickson and C. Goyet (eds), ORNL/CDIAC-74.*
- Yao, W. and R. H. Byrne (1998), Simplified seawater alkalinity analysis: Use of linear array spectrometers. *Deep-Sea Res. I*, 45, 1383–1392.
- Swift, J. H. (2010): Reference-quality water sample data, Notes on acquisition, record keeping, and evaluation. *IOCCP Report No.14, ICPO Pub. 134, 2010 ver.1.*



## 8. pH

30 September 2023

### (21) Personnel

OKA Takahiro

INAMI Haruna (Leg 1)

USHIO Nobuyasu (Leg 1)

AKIEDA Chikako (Leg 2)

TANIZAKI Chiho (Leg 2)

### (22) Station occupied

A total of 40 stations (Leg 1: 18, Leg 2: 22) were occupied for pH. Station location and sampling layers of them are shown in Figures C.8.1 and C.8.2, respectively.

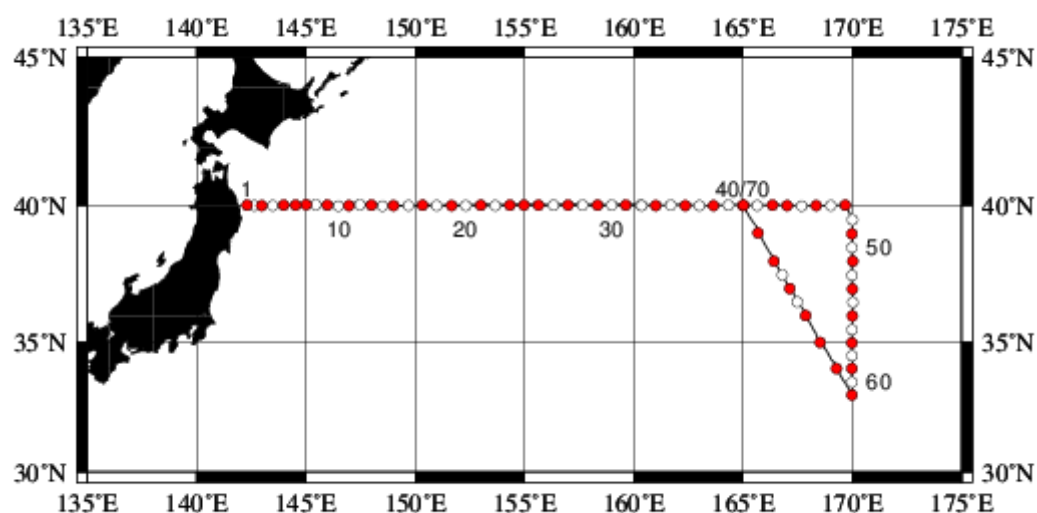


Figure C.8.1. Location of observation stations of pH. Closed and open circles indicate sampling and no-sampling stations, respectively.

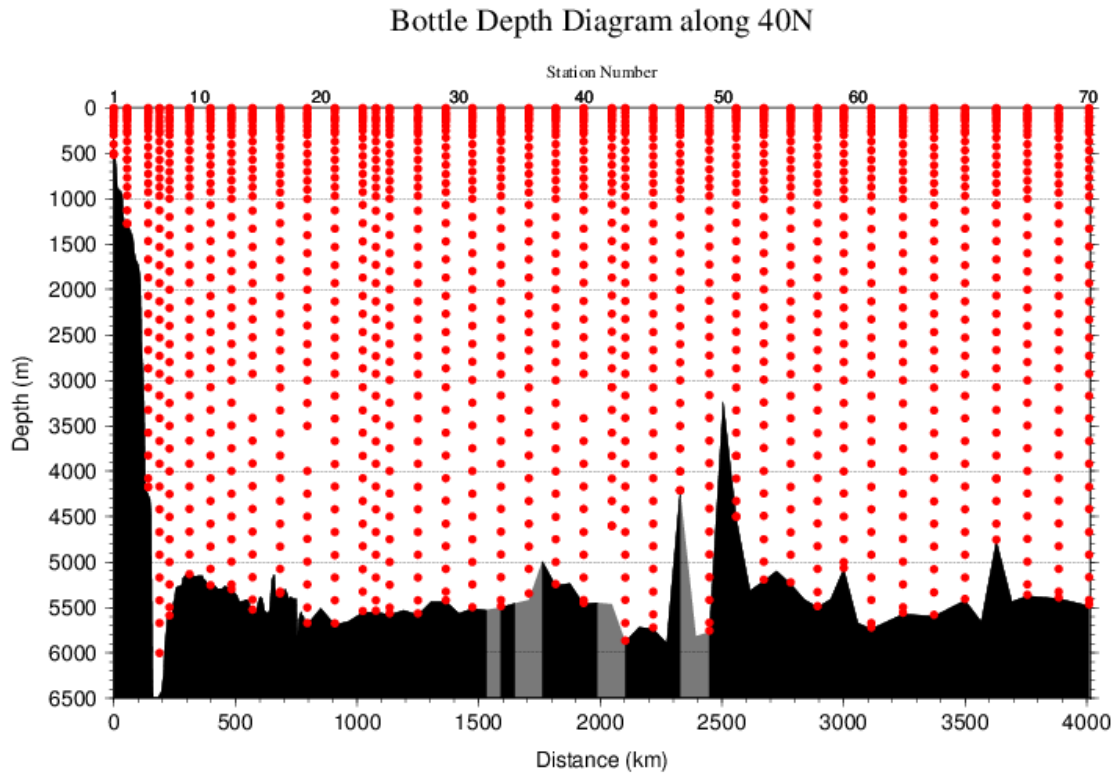


Figure C.8.2. Distance-depth distribution of sampling layers of pH.

### (23) Instrument

The measurement of pH was carried out with a pH analyzer (Nihon ANS Co. Ltd, Japan).

### (24) Sampling and measurement

Methods of seawater sampling, poisoning, spectrophotometric measurements using the indicator dye *m*-cresol purple (hereafter *m*CP) and calculation of  $\text{pH}_T$  (on the total hydrogen ion scale; Appendix A1) were based on Saito et al. (2008). The  $\text{pH}_T$  is calculated from absorbance ratio ( $R$ ) with the following equations,

$$\cdot \quad (\text{C8.1})$$

$$(\text{C8.2})$$

where  $\text{p}K_2$  is the acid dissociation constant of *m*CP,

$$\cdot \quad (\text{C8.3})$$

$$(293 \text{ K} \leq T \leq 303 \text{ K}, 30 \leq S \leq 37).$$

and in equation (C8.2) are absorbance of seawater itself and dye plus seawater, respectively, at wavelength  $\lambda$  (nm). The value of  $\text{p}K_2$  in equation (C8.3) is expressed as a function of temperature  $T$  (in Kelvin) and salinity  $S$  (in psu). Finally,  $\text{pH}_T$  is reported as the value at temperature of 25 °C. Details are shown in Appendix A1.

## (25) pH perturbation caused by addition of *m*-cresol purple solution

The *m*CP solution using as indicator dye was prepared in our laboratory (Appendix A2) and was subdivided into some bottles (*m*CP batches) that attached to the apparatus. The injection of *m*CP solution perturbs the sample  $\text{pH}_T$  slightly because the acid-base equilibrium of the seawater is disrupted by the addition of the dye acid-base pair (Dickson et al., 2007).

Before applying  $R$  to the equation (C8.1), the measured  $R$  in the sample was corrected to that value expected to be unperturbed by the addition of the dye (Dickson et al., 2007; Clayton and Byrne, 1993). The magnitude of the perturbation ( $\Delta R$ ) was calculated empirically from that by the second addition of the dye and absorbance ratio measurement as follows:

$$\Delta R = R_2 - R_1, \quad (\text{C8.4})$$

where  $R_1$  and  $R_2$  are the absorbance ratio after the initial addition of dye solution in the sample measurement and after the second addition in the experimental measurement, respectively. Because the value of  $\Delta R$  depends on the  $\text{pH}_T$  of sample, we expressed  $\Delta R$  as a quadratic function of  $R_1$  based on experimental  $\Delta R$  measurement obtained at this cruise as follows:

$$\Delta R = C_0 + C_1 R_1 + C_2 R_1^2 \quad (\text{C8.5})$$

In each measurement for a station,  $\Delta R$  was measured for about 10 samples from various depths to obtain wide range of  $R_1$  and experimental  $\Delta R$  data. For each *m*CP batch bottle, coefficients ( $C_0$ ,  $C_1$  and  $C_2$ ) were calculated by equation (C8.5), and  $\Delta R$  was evaluated for each  $R_1$ . The coefficients for each *m*CP batch are showed in Table C.8.1. The plots and function curves are illustrated in Figure C.8.3.

Table C.8.1. Summary of coefficients;  $C_2$ ,  $C_1$  and  $C_0$  in .

Stations	<i>m</i> CP batch	$C_2$	$C_1$	$C_0$
1–31	1	–5.44069E–03	–7.31606E–03	1.20463E–02
34–57	2	–6.72893E–03	–6.32867E–03	1.23599E–02
59–70	3	–3.77665E–03	–1.23313E–02	1.53307E–02

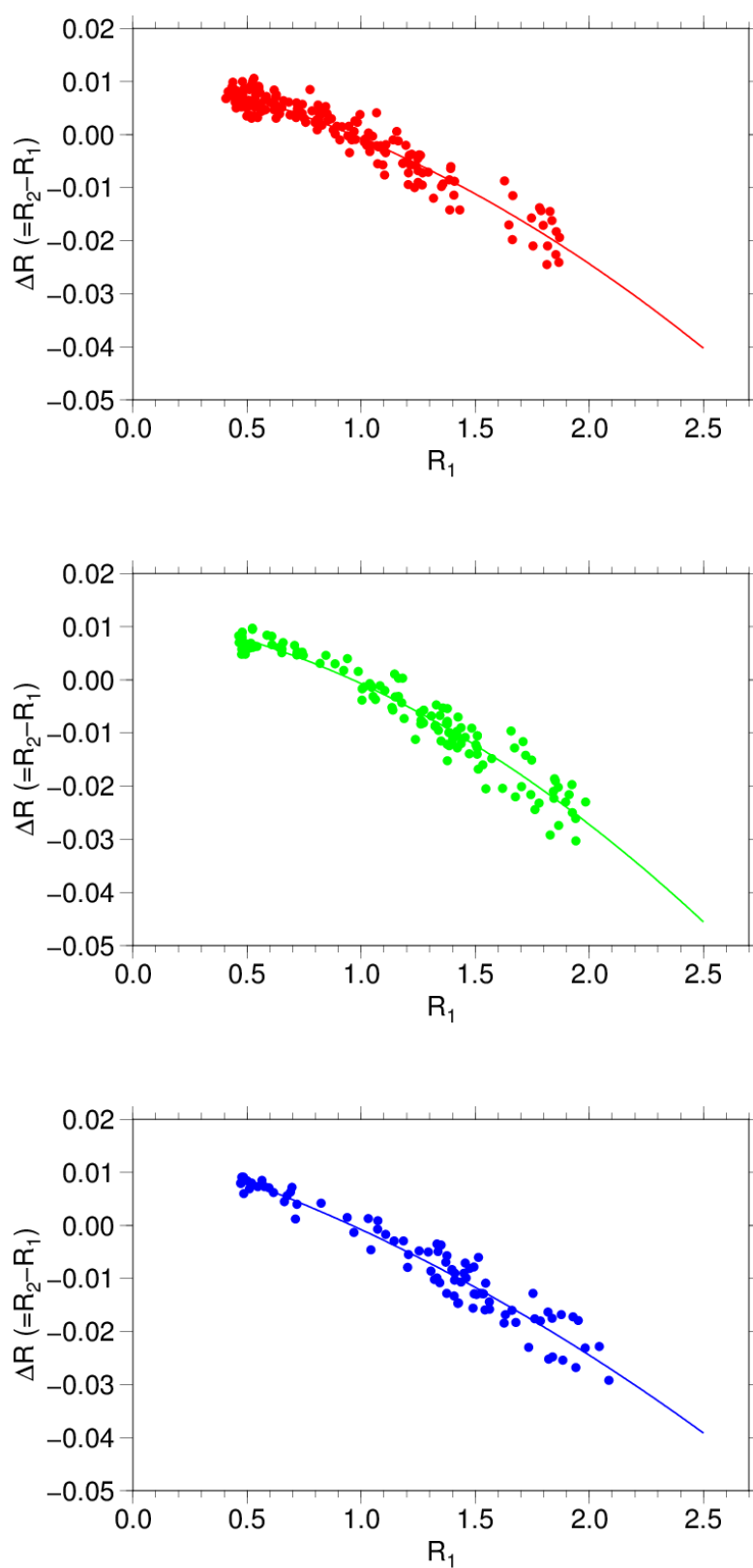


Figure C.8.3. The function curve of the  $\Delta R (= R_2 - R_1)$  vs  $R_1$  for (top) first, (middle) second and (bottom) third  $mCP$  batch of solution shown in Table C.8.1.

## (26) Quality Control

### (6.1) Replicate and duplicate analyses

We took replicate (pair of water samples taken from a single Niskin bottle) and duplicate (pair of water samples taken from different Niskin bottles closed at the same depth) samples for  $\text{pH}_T$  determination throughout the cruise. Table C.8.2 summarizes the results of the measurements. Figure C.8.4 shows details of the results. The calculation of the standard deviation from the difference of sets of measurements was based on a procedure (SOP 23) in DOE (1994).

Table C.8.2. Summary of replicate and duplicate measurements of  $\text{pH}_T$ .

Measurement	Average magnitude of difference $\pm$ S.D.
Replicate	$0.0016 \pm 0.0015$ (N=116)
Duplicate	$0.0019 \pm 0.0018$ (N=16)

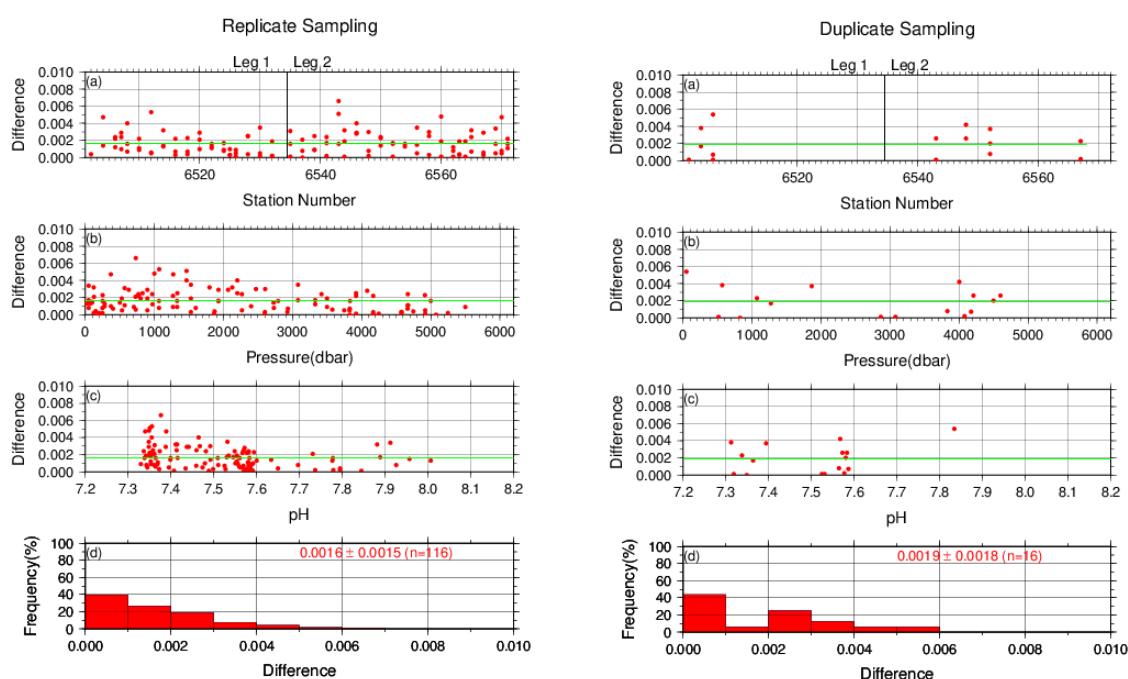


Figure C.8.4. Results of (left) replicate and (right) duplicate measurements during the cruise versus (a) station number, (b) pressure and (c)  $\text{pH}_T$ . The green lines denote the averages of the measurements. The bottom panels (d) show histograms of the measurements.

### (6.2) Measurements of CRM and working reference materials

The precision of the measurements was monitored by using the CRMs and working reference materials bottled in our laboratory (Appendix A2 in C.6). Although the  $\text{pH}_T$  value of the CRM was not assigned, it could be calculated from certified parameters of DIC and TA ([https://www.ncei.noaa.gov/access/ocean-carbon-acidification-data-system/oceans/Dickson\\_CRM/batches.html](https://www.ncei.noaa.gov/access/ocean-carbon-acidification-data-system/oceans/Dickson_CRM/batches.html)) based on the chemical equilibrium of the carbonate system (Lueker et al.,

2000). The  $pH_T$  of the CRM (batch 182) was calculated to be 7.8665. Working reference material measurements were carried out first at every station. If the results of the measurements were confirmed to be good, measurements on seawater samples were begun. CRM (batch 182) measurements were done at every few (about 3) stations. The measurement for seawater sample and working reference material was made once for a single bottle, and that for CRM was made twice. Table C.8.3 summarizes the means of difference of  $pH_T$  between two measurements and  $pH_T$  values for a CRM bottle and the means of the  $pH_T$  value for a working reference material for each  $mCP$  batch. Figures C.8.5–C.8.7 show detailed results.

Table C.8.3. Summary of difference and means of the  $pH_T$  values for two measurements for a CRM bottle, and mean of  $pH_T$  for a working reference material, which was calculated with data with good measurements.

<i>mCP</i> Batches	CRM	Working reference material	
	Magnitude of difference	Mean	Mean
	Ave. $\pm$ S.D.	Ave. $\pm$ S.D.	Ave. $\pm$ S.D.
1	0.0019 $\pm$ 0.0015 (N=7)	7.8600 $\pm$ 0.0017 (N=7)	7.9321 $\pm$ 0.0016 (N=18)
2	0.0013 $\pm$ 0.0011 (N=5)	7.8592 $\pm$ 0.0008 (N=5)	7.9330 $\pm$ 0.0022 (N=13)
3	0.0016 $\pm$ 0.0013 (N=3)	7.8587 $\pm$ 0.0005 (N=3)	7.9310 $\pm$ 0.0013 (N=11)

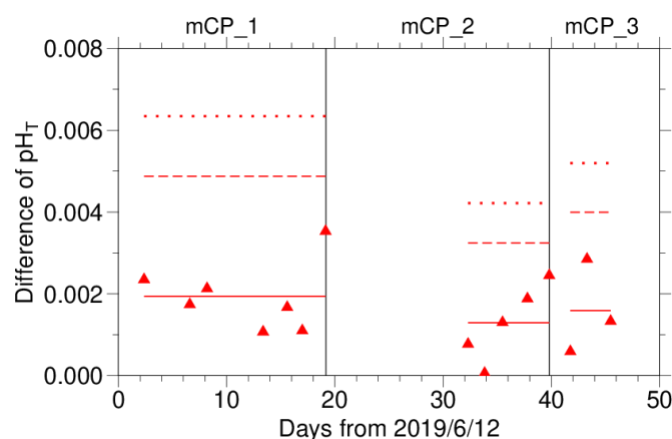


Figure C.8.5. The absolute difference ( $R$ ) of  $pH_T$  between two measurements of a CRM bottle. The  $mCP$  batch names are shown above the graph, and vertical lines denote the day  $mCP$  batches were changed. The solid, dashed and dotted lines denote the average range ( $\bar{R}$ ), upper warning limit (2.512) and upper control limit (3.267) for each  $mCP$  batch bottle, respectively (see Dickson et al., 2007).

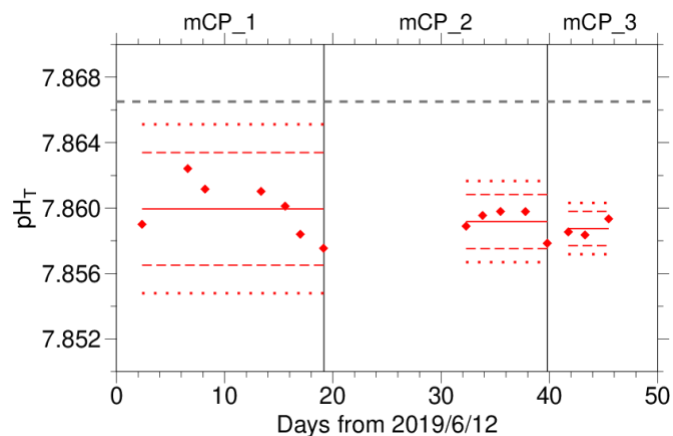


Figure C.8.6. The mean of  $\text{pH}_T$  values between two measurements of a CRM bottle. The *mCP* batch names are shown above the graph, and vertical lines denote the day when the *mCP* batch was changed. The solid, dashed, and dotted lines denote the mean of measurements, upper/lower warning limit (mean  $\pm$  2S.D.), and upper/lower control limit (mean  $\pm$  3S.D.) for each *mCP* batch bottle, respectively (see Dickson et al., 2007). The gray dashed line denotes  $\text{pH}_T$  of CRM calculated from certified parameters.

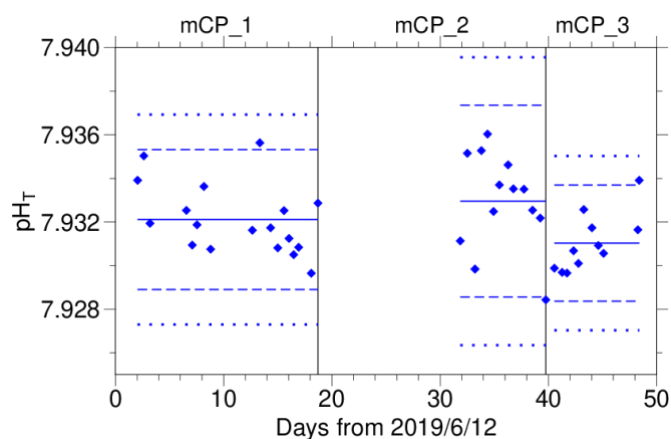


Figure C.8.7. Same as C.8.6, but for working reference material.

### (6.3) Quality control flag assignment

A quality control flag value was assigned to the pH measurements (Table C.8.4) using the code defined in the IOCCP Report No.14 (Swift, 2010).

Table C.8.4. Summary of assigned quality control flags.

Flag	Definition	Number of samples
2	Good	1321
3	Questionable	2
4	Bad (Faulty)	2
5	Not reported	1
6	Replicate measurements	115
Total number of samples		1441

### (6.4) Comparison at cross-stations during the cruise

There was a cross-station during the cruise located at 40°N/165°E. At stations of Stn.40 and Stn.70, hydrocast sampling for pH<sub>T</sub> was conducted two times at interval of 11 days. These profiles are shown in Figure C.8.8.

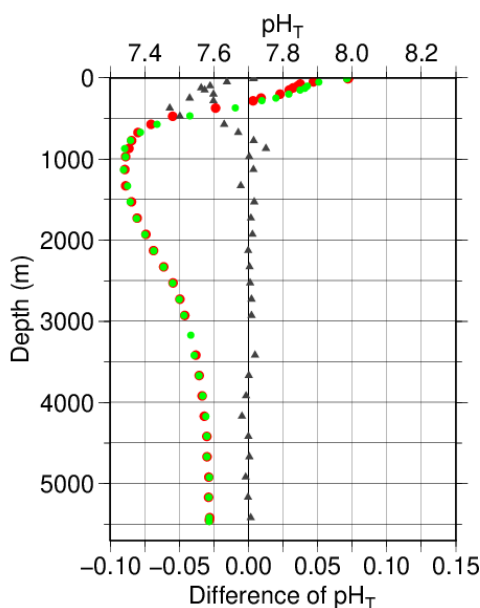


Figure C.8.8. Comparison of pH<sub>T</sub> observed at same location in different legs of this cruise: 40°N/165°E (stations 40 and 70). The red and green circles denote station 40 and station 70, respectively. Triangles denote the difference in pH<sub>T</sub> measured at same depth in different legs.

### (6.5) Comparison at cross-stations of WHP cruises

We compared pH<sub>T</sub> data of this cruise and other WHP cruises by JMA and Japan Agency for



Marine-Earth Science and Technology (JAMSTEC) at cross points. Summary of the comparisons are shown in Figure C.8.9(a) for cross point with WHP-P10 line (around 40°N/145°E) and Figure C.8.9(b) for cross point with WHP-P13 line (around 40°N/165°E). Data of other cruises are downloaded from the CCHDO web site (<https://cchdo.ucsd.edu>).

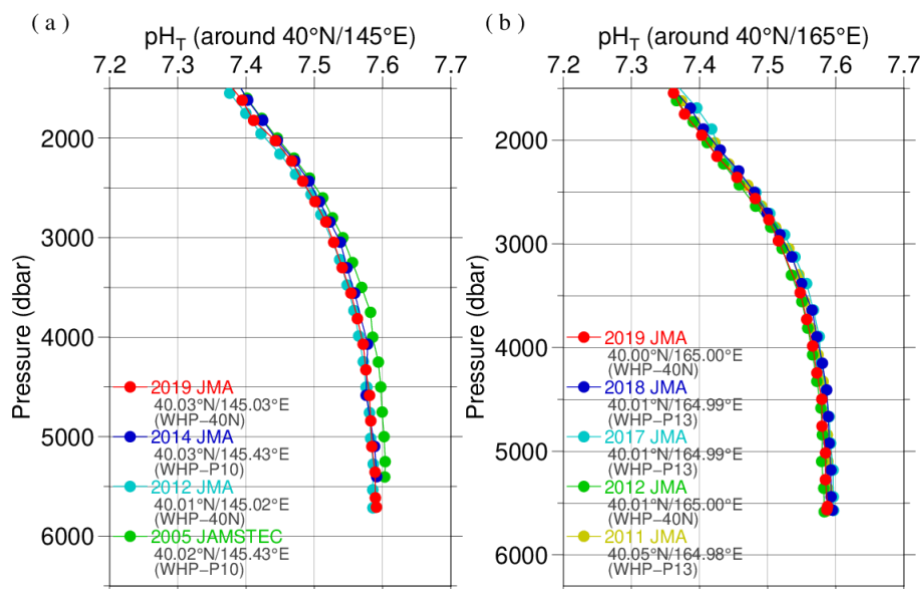


Figure C.8.9. Comparison of pH<sub>T</sub> profiles at (a) 40°N/145°E (cross point with WHP-P10 line) and (b) 40°N/165°E (cross point with WHP-P13 line). Circles and triangles denote good and questionable values, respectively. The red ones show this cruise.

## Appendix

### A1. Methods

#### (A1.1) Seawater sampling

Seawater samples were collected from 10-liters Niskin bottles mounted on CTD-system and a stainless steel bucket for the surface. Samples for pH were transferred to Schott Duran® glass bottles using sample drawing tubes. Bottles were filled smoothly from the bottom after overflowing double a volume while taking care of not entraining any bubbles, and lid temporarily with ground glass stoppers.

After all sampling finished, 2 mL of sample is removed from each bottle to make a headspace to allow thermal expansion. Although the procedure is differed from Standard Operating Procedure (SOP) described in PICES Special Publication 3, SOP-2 (Dickson, 2007), poisoned with 0.2 mL of saturated HgCl<sub>2</sub> solution to prevent change in pH<sub>T</sub> caused by biological activity. Finally, samples were sealed with ground glass stoppers lubricated with Apiezon® grease (L).

#### (A1.2) Measurement

Custom-made pH analyzer (2009 model; Nihon ANS) was prepared and operated in the cruise. The analyzer comprised of a sample dispensing unit, a pre-treatment unit combined with an automated syringe, and two (sample and reference) spectrophotometers combined with a high power xenon light source. Spectrophotometric cell was made of quartz tube that has figure of “U”. This cell was covered with stainless bellows tube to keep the external surface dry and for total light to reflect in the tube. The temperature of the cell was regulated to  $25.0 \pm 0.1$  °C by means of immersing the cell into the thermostat bath, where the both ends of bellows tube located above the water surface of the bath. Spectrophotometer, cell and light source were connected with optical fiber.

The analysis procedure was as follows:

- a) Seawater was ejected from a sample loop.
- b) A portion of sample was introduced into a sample loop including spectrophotometric cell. The spectrophotometric cell was flushed two times with sample in order to remove air bubbles.
- c) An absorption spectrum of seawater in the visible light range was measured. Absorbance at wavelengths of 434 nm, 488 nm, 578 nm and 730 nm as well as cell temperature were recorded. To eject air bubbles from the cell, the sample was moved four times and the absorbance was recorded at each stop.
- d) 10 µl of indicator *m*CP was injected to the loop.
- e) Circulating 2 minutes 40 seconds through the loop tube, seawater sample and indicator dye was mixed together.
- f) Absorbance of *m*CP plus seawater was measured in the same way described above (c).

### (A1.3) Calculation

In order to state clearly the scale of pH, we mention “pH<sub>T</sub>” that is defined by equation (C8.A1.3.1),

$$\text{(C8.A1.3.1)}$$

where  $[H^+]_T$  denotes the concentration of hydrogen ion expressed in the total hydrogen ion scale. , where  $[H^+]_F$  is the concentration of free hydrogen ion,  $[SO_4]_T$  is the total concentration of sulphate ion and  $K_a$  is acid dissociation constant of hydrogen sulphate ion (Dickson, 1990).  $C^0$  is the standard value of concentration (1 mole per kilogram of seawater, mol kg<sup>-1</sup>). The pH<sub>T</sub> was reported as the value at temperature of 25 °C in “total hydrogen ion scale”.

pH<sub>T</sub> was calculated from the measured absorbance ( $A$ ) based on the following equations (C8.A1.3.2) and (C8.A1.3.3), which are the same as (C8.1) and (C8.2), respectively.

$$\cdot \quad \text{(C8.A1.3.2)}$$

$$\text{(C8.A1.3.3)}$$

where  $pK_2$  is the acid dissociation constant of  $mCP$ .  $[I^{2-}] / [HI^-]$  is the ratio of  $mCP$  base form ( $I^{2-}$ ) concentration over acid form ( $HI^-$ ) concentration which is calculated from the corrected absorbance ratio ( $R$ ) shown in the section 8(5) and the ratios of extinction coefficients (Clayton and Byrne, 1993). and in equation (C8.A1.3.3) are absorbance of seawater itself and dye plus seawater, respectively, at wavelength  $\lambda$  (nm). The value of  $pK_2$  ( $K^0 = 1 \text{ mol kg}^{-1}$ ) had also been expressed as a function of temperature  $T$  (in Kelvin) and salinity  $S$  (in psu) by Clayton and Byrne (1993), but the calculated value has been subsequently corrected by 0.0047 on the basis of a reported pH<sub>T</sub> value accounting for “tris” buffer (DelValls and Dickson, 1998):

$$\therefore \quad \text{(C8.A1.3.4)}$$
$$(293 \text{ K} \leq T \leq 303 \text{ K}, 30 \leq S \leq 37)$$

Finally, pH<sub>T</sub> determined at a temperature  $t$  (pH<sub>T</sub>( $t$ ), with  $t$  in °C) was corrected to the pH<sub>T</sub> at 25.00 °C (pH<sub>T</sub>(25)) with the following equation (Saito et al., 2008).

$$\dots \quad \text{(C8.A1.3.5)}$$

### A2. pH indicator

Indicator *m*-cresol purple ( $mCP$ ) solution

Add 0.67 g  $mCP$  to 500 mL deionized water (DW) in a borosilicate glass flask. Pour DW

slowly into flask to weight of 1 kg (*m*CP + DW), and mix well to dissolve *m*CP. Regulate the pH (free hydrogen ion scale) of indicator solution to  $7.9 \pm 0.1$  by small amount of diluted NaOH solution (approx.  $0.25 \text{ mol L}^{-1}$ ) if the pH was out of the range. The pH of indicator solution was monitored using glass electrode pH meter. The reagent had not been refining.

## References

- Clayton T.D. and R.H. Byrne 1993. Spectrophotometric seawater pH measurements: total hydrogen ion concentration scale calibration of m-cresol purple and at-sea results. *Deep-Sea Res. I*, **40**, 2115–2129.
- DelValls, T. A and A. G. Dickson, 1998. The pH of buffers based on 2-amino-2-hydroxymethyl-1,3-propanediol ('tris') in synthetic sea water. *Deep-Sea Res. I*, **45**, 1541-1554.
- Dickson, A.G. 1990. Standard potential of the reaction:  $\text{AgCl(s)} + 1/2 \text{H}_2(\text{g}) = \text{Ag(s)} + \text{HCl(aq)}$ , and the standard acidity constant of the ion  $\text{HSO}_4^-$  in synthetic sea water from 273.15 to 318.15 K. *J. Chem. Thermodynamics*, **22**, 113–127.
- Dickson, A.G., Sabine, C.L. and Christian, J.R. (Eds.) 2007. Guide to best practices for ocean  $\text{CO}_2$  measurements. *PICES Special Publication 3*, 191 pp.
- Lueker, T.J, A.G. Dickson and C.D. Keeling, 2000. Ocean  $p\text{CO}_2$  calculated from dissolved inorganic carbon, alkalinity, and equations for  $K_1$  and  $K_2$ : validation based on laboratory measurements of  $\text{CO}_2$  in gas and seawater at equilibrium. *Marine Chem.*, **70**, 105-119.
- Saito, S., M. Ishii, T. Midorikawa and H.Y. Inoue 2008. Precise Spectrophotometric Measurement of Seawater  $\text{pH}_\text{T}$  with an Automated Apparatus using a Flow Cell in a Closed Circuit. *Technical Reports of Meteorological Research Institute*, **57**, 1–28.
- Swift, J. H. (2010): Reference-quality water sample data, Notes on acquisition, record keeping, and evaluation. *IOCCP Report No.14, ICPO Pub. 134, 2010 ver.1*